

TU-479
March, 1995

Ph.D thesis

Effects of the Gravitino on the Inflationary Universe

Takeo Moroi

Department of Physics, Tohoku University, Sendai 980-77, Japan

Contents

1	Introduction	1
1.1	Overview	1
1.2	Organization of this thesis	3
2	Motivations of supersymmetry	5
2.1	Hierarchy problem in the standard model	5
2.2	Supersymmetric extension of the standard model	6
3	Review of supergravity	12
3.1	Heuristic approach to supergravity lagrangian	12
3.2	Minimal supergravity model	14
3.3	General supergravity lagrangian	17
3.4	Super-Higgs mechanism	22
3.5	Super-trace formula in supergravity	24
3.6	Model with Polonyi's superpotential	26
3.7	Mass of a scalar field in the hidden sector	30
4	Feynman rules for the gravitino	32
4.1	Four-component notation for fermions	32
4.2	Wave function for massive gravitino	33
4.3	Quantization of free massive gravitino field	36
4.4	Interactions of the gravitino	40
4.5	Effective lagrangian for light gravitino	42
5	Phenomenology of the gravitino : overview	49
5.1	Collider experiments with the gravitino	49
5.2	Cosmology	50
5.3	The Polonyi problem	51
6	Cosmology with unstable gravitino	54
6.1	Gravitino production in the early universe	54
6.2	Radiative decay of the gravitino	57
6.3	BBN with high energy photon injection	58

6.4	BBN with high energy neutrino injection	66
6.5	Discussion about hadron injection	70
6.6	Other constraints	71
7	Cosmology with stable gravitino	74
7.1	Constraints from the mass density of the universe	74
7.2	Constraint from BBN	77
7.3	Remarks	78
8	Conclusions and discussion	80
8.1	Summary of conclusions	80
8.2	Discussion	81
A	Notations	86
A.1	Conventions	86
A.2	Two component notation	86
A.3	Four component notation	87
B	Photon spectrum	89
B.1	Boltzmann equations	89
B.2	Spectrum with high energy photon injection	94
B.3	Spectrum with high energy neutrino injection	100
C	Big-bang nucleosynthesis	111
C.1	Theoretical framework	111
C.2	Numerical results	115
C.3	Observations	117

Chapter 1

Introduction

1.1 Overview

When we think of new physics beyond the standard model, supersymmetric (SUSY) extension [1] of the standard model is one of the most attractive candidates. Cancellation of quadratic divergences in SUSY models naturally explains the stability of the electroweak scale against radiative corrections [2, 3]. Furthermore, if we assume the particle contents of the minimal SUSY standard model (MSSM), the three gauge coupling constants in the standard model meet at $\sim 10^{16}\text{GeV}$ [4, 5], which strongly supports grand unified theory (GUT) based on SUSY [6, 7].

In spite of these strong motivations, no direct evidence of SUSY (especially superpartners) has been discovered yet. Therefore, the SUSY is broken in nature, if it exists. Although many efforts have been made to understand the origin of the SUSY breaking, no convincing scenario of SUSY breaking has found yet. Nowadays, many people expect the existence of *local* SUSY (*i.e.* supergravity) [8] and try to find a mechanism to break SUSY spontaneously in the framework. In the broken phase of the supergravity, super-Higgs effect occurs and gravitino, which is the superpartner of graviton, acquires mass by absorbing the Nambu-Goldstone fermion associated with SUSY breaking. In this case, the gravitino mass $m_{3/2}$ is expected to give us some informations about the SUSY breaking mechanism. For example, in models with the minimal kinetic term, the following (tree level) super-trace formula among the mass matrices \mathbf{M}_J^2 's holds;

$$\text{Str}\mathbf{M}^2 \equiv \sum_{\text{spin } J} (-1)^{2J} (2J+1) \text{tr}\mathbf{M}_J^2 \simeq 2(n_\phi - 1)m_{3/2}^2, \quad (1.1)$$

where n_ϕ is the number of the chiral multiplets in the spontaneously broken local SUSY model. In this case, all the SUSY breaking masses of squarks and sleptons are equal to the gravitino mass at the Planck scale. Meanwhile in models with “no-scale like” Kähler potential [9, 10], SUSY breaking masses for sfermions vanish at the gravitational scale and are induced by radiative corrections, and hence the gravitino mass is not directly related to the scale of the SUSY breaking in the observable sector (which contains ordinary particles

in the standard model and their superpartners). In order to understand the physics of the SUSY breaking, it is significant to clarify the property of the gravitino. But contrary to our theoretical interests, we have no hope to see the gravitino in collider experiments since its interaction is extremely weak.

On the contrary, cosmological arguments provide us some informations about the gravitino. In general, cosmology severely constrains properties of exotic particles. Let us review the constraints derived from cosmology.

- The first is on the mass density of the exotic particle during the big-bang nucleosynthesis. If it is too large, it speeds up the expansion rate of the universe during that epoch and results in too many ${}^4\text{He}$.
- The second is on the entropy production by the decay of the exotic particle. If the decay of the exotic particle releases a large amount of entropy, the baryon-to-photon ratio may become much well below what is observed today.
- The third arises from the effects of the decay products on the big-bang nucleosynthesis. If the photon or some charged particle is produced by the decay of the exotic particle after the big-bang nucleosynthesis has started, energetic photons induced by the decay products may destruct light nuclei (D, ${}^3\text{He}$, ${}^4\text{He}$) and destroy the great success of the big-bang nucleosynthesis.
- Furthermore, one can obtain the fourth constraints by considering the cosmic microwave background distortion by the exotic particle with lifetime larger than $\sim 10^{10}\text{sec}$.
- If exotic particle is stable, its present mass density provides us a fifth constraint.

In fact, the most severe constraints on models based on supergravity are derived from the light element photo-dissociation and the present mass density of the universe.

Following the above arguments, we can obtain stringent constraints on the gravitino mass in the standard big-bang cosmology. If the gravitino is unstable, it may decay after the big-bang nucleosynthesis and releases tremendous amount of entropy, which may conflict with the big-bang nucleosynthesis scenario. As Weinberg first pointed out [11], the gravitino mass should be larger than $\sim 10\text{TeV}$ so that the gravitino can decay before the big-bang nucleosynthesis starts. Furthermore in SUSY models with R -parity invariance, unstable gravitino produces heavy stable particle (*i.e.* the lightest superparticle) in its decay processes, which results in unacceptably high mass density of the present universe [12]. In order to reduce the number density of the lightest superparticle through pair annihilation processes, gravitinos should decay when the temperature of the universe is higher than $(1 - 10)\text{GeV}$. This requires that the gravitino mass should be larger than $(10^6 - 10^7)\text{GeV}$, which seems to be disfavored from the naturalness point of view. In the case of stable gravitino, the gravitino mass larger than $\sim 1\text{keV}$ is excluded since the present mass density of the gravitino exceeds the critical

density of the present universe [13]. The above constraints on the gravitino mass seem to be very stringent especially for models with the minimal Kähler potential, since in such models the gravitino mass is expected to give the scale of the SUSY breaking in observable sector.

In the inflationary universe [14], however, situation changes [15]. In this case, the initial abundance of the gravitino is diluted during the inflation, and hence the number density of the gravitino becomes much less than that in the case of the standard big-bang cosmology. But even in the inflationary universe, the gravitino may cause the cosmological problems mentioned above since secondary gravitinos are produced through scattering processes off the background radiations or decay processes of superparticles. As we will see later, number density of the secondary gravitinos is approximately proportional to the reheating temperature after the inflation and hence the upperbound on the reheating temperature is derived.

In this thesis, we study details on the gravitino production in early universe and on its effects in the inflationary universe. Compared with the previous works, we have made an essential improvement on the following points.

- Gravitino production cross sections are calculated by using full relevant terms in the local SUSY lagrangian.
- High energy photon spectrum induced by the gravitino decay is obtained by solving the Boltzmann equations numerically.
- Time evolutions of the light nuclei (D, ^3He , ^4He) with non-standard energetic photons are calculated by modifying Kawano's computer code.

In our analysis, we assume that the light elements are synthesized through the (almost) standard scenario of the big-bang nucleosynthesis (with baryon-to-photon ratio $10^{-9} - 10^{-10}$), and take the reheating temperature as a free parameter.

1.2 Organization of this thesis

The outline of this thesis is as follows. The former half of this thesis is devoted to the review of related topics, especially that of the gravitino properties. In Chapter 2, we review the motivation of SUSY. In Chapter 3, the gravitino field which is the gauge field associated with local SUSY transformation is introduced. Furthermore, lagrangian based on local SUSY is also shown in Chapter 3 and the super-trace formula in that framework is derived. Conventions used in Chapter 3 (and in other chapters) are shown in Appendix A. In Chapter 4, we quantize a massive gravitino field and derive Feynman rules for gravitino.

In the latter half of this thesis, we study the cosmology with the gravitino in detail. Overview of phenomenology with the gravitino is given in Chapter 5. In Chapter 6, effects of unstable gravitino in the inflationary cosmology are analyzed in detail. In deriving constraints, we first derive photon spectrum induced by the decay of the gravitino. The procedure to obtain the photon spectrum is given in Appendix B. Then, we calculate the

time evolution of light nuclei with the obtained high energy photon spectrum, and we derive constraints on the reheating temperature and on the gravitino mass. In our analysis, we assume the standard big-bang nucleosynthesis scenario which is reviewed in Appendix C. The case of stable gravitino is discussed in Chapter 7. Chapter 8 is devoted to discussions.

Chapter 2

Motivations of supersymmetry

2.1 Hierarchy problem in the standard model

For particle physicists, symmetries in nature are significant guiding principles. Especially, interactions of elementary particles (like quarks and leptons) can be understood by using the concept of the local gauge symmetry. Strong interaction is expected to originate to $SU(3)_C$ gauge group, and its theoretical predictions (like three gluon vertex and asymptotic free nature of its gauge coupling constant) have been confirmed experimentally. Meanwhile, results of recent electroweak precision measurements are in good agreements with the predictions of the spontaneously broken $SU(2)_L \times U(1)_Y$ gauge theory. Accompanied by theoretical and experimental successes, the standard model, based on the $SU(3)_C \times SU(2)_L \times U(1)_Y$ gauge group, is regarded as the established one which describes particle interactions below the energy scale $\sim 100\text{GeV}$.

But once we look up high energy scale, one unpleasant problem, which is called hierarchy problem, appears in the standard model. In the standard model, existence of the elementary scalar boson, *i.e.* Higgs boson, is assumed in order to cause a spontaneous breaking of the gauge symmetry $SU(2)_L \times U(1)_Y \rightarrow U(1)_{em}$. This is the origin of the hierarchy problem. As one can easily see, radiative corrections to the Higgs boson mass squared δm_H^2 are quadratically divergent. Therefore, if one assumes the existence of the cut-off scale of the standard model Λ_{CUT} at which the parameters in the standard model are set by a more fundamental theory, $\delta m_H^2 \sim O(\alpha \Lambda_{CUT}^2)$ where α represents the coupling factor. The relation between the bare mass squared $m_{H,B}^2$ and the renormalized one $m_{H,R}^2$ is written in the following way;

$$m_{H,R}^2 = m_{H,B}^2 + \delta m_H^2. \quad (2.1)$$

In order to give the electroweak scale correctly, the renormalized mass squared $m_{H,R}^2$ should be $O((100\text{GeV})^2)$. On the other hand, if we assume a larger value of Λ_{CUT} , δm_H^2 increases quadratically and a fine tuning of $m_{H,B}^2$ is needed so that the renormalized mass squared $m_{H,R}^2$ remains $O((100\text{GeV})^2)$. For example, if we assume the cut-off scale of the standard model to be at the Planck scale $\sim 10^{19}\text{GeV}$, both $m_{H,B}^2$ and δm_H^2 are $O((10^{19}\text{GeV})^2)$ for α

$\sim O(1)$, and they should be chosen as

$$m_{H,B}^2 + \delta m_H^2 \sim O((10^{19}\text{GeV})^2) - O((10^{19}\text{GeV})^2) \sim O((100\text{GeV})^2). \quad (2.2)$$

This is a terrific fine tuning. Therefore, if one assume that the cut-off scale of the standard model is much larger than the electroweak scale, we have to accept an unbelievable fine tuning of Higgs boson mass. This is the hierarchy problem. In fact, this problem stems from the fact that there is no symmetry which stabilizes the electroweak scale [16, 17]. In order to solve this problem, we hope that some new physics (in other words, some new symmetry) in which quadratic divergences do not exist at all, appears at a energy scale $O(100\text{GeV} - 1\text{TeV})$ and solve this difficulty.

2.2 Supersymmetric extension of the standard model

One of the most attractive solution to the hierarchy problem is SUSY [1]. SUSY is a symmetry which transforms bosons into fermions and vice versa. Therefore, in SUSY models the number of bosonic degrees of freedom is equal to that of fermionic ones. As we will see later, quadratic divergence of the Higgs (and other) boson masses are canceled out between the contributions from boson and fermion loops.

Experimentally, however, we have not found any superpartners of the observed particles. This fact indicates that SUSY is broken in nature, if it exists. In order to solve the hierarchy problem, the SUSY must be broken softly [18] so that quadratic divergences do not exist at all. Usually, such a softly broken global SUSY model is regarded as a low energy effective theory of the spontaneously broken local SUSY model. We will comment on this point in the next chapter and here, we consider a phenomenologically acceptable (softly broken) SUSY model.

When we extend the standard model to the supersymmetric one, we usually add “superpartners” for the ordinary particles existed in the standard model. In Table 2.1, we show the particles in the minimal SUSY standard model (MSSM) and their gauge quantum numbers. Along with the existence of the superpartners, one big difference between the standard model and the SUSY one is the number of Higgs doublets, *i.e.* the MSSM requires two Higgs doublets (see Table 2.1). In the SUSY standard model, Higgs bosons are accompanied by their fermionic superpartners which have the same gauge quantum numbers as the Higgs bosons. In this case, anomaly cancellation is not guaranteed if both of H_1 and H_2 are not included. Furthermore, in order to give fermion masses to up-type quarks as well as down-type quarks and leptons from Yukawa couplings of Higgs bosons, at least two chiral superfields H_1 and H_2 are needed. Mainly from the above two reasons, two Higgs doublets with representation $(\mathbf{1}, \mathbf{2}, -1/2)$ and $(\mathbf{1}, \mathbf{2}, 1/2)$ are introduced into the MSSM.

Next, we will see the lagrangian of the MSSM. As a first step, we comment on R -parity. If we assume a particle content of the MSSM shown in Table 2.1, we can write down

Gauge sector		
Representation	Boson ($R = +1$)	Fermion ($R = -1$)
$(\mathbf{8}, \mathbf{1}, 0)$	G_μ	\tilde{g}
$(\mathbf{1}, \mathbf{3}, 0)$	W_μ	\tilde{w}
$(\mathbf{1}, \mathbf{1}, 0)$	B_μ	\tilde{b}

Higgs sector		
Representation	Boson ($R = +1$)	Fermion ($R = -1$)
$(\mathbf{1}, \mathbf{2}, -1/2)$	H_1	χ_{H_1}
$(\mathbf{1}, \mathbf{2}, 1/2)$	H_2	χ_{H_2}

Quark / lepton sector		
Representation	Boson ($R = -1$)	Fermion ($R = +1$)
$(\mathbf{3}, \mathbf{2}, 1/6)$	\tilde{q}_i	q_i
$(\mathbf{3}^*, \mathbf{1}, -2/3)$	\tilde{u}_i^c	u_i^c
$(\mathbf{3}^*, \mathbf{1}, 1/3)$	\tilde{d}_i^c	d_i^c
$(\mathbf{1}, \mathbf{2}, -1/2)$	\tilde{l}_i	l_i
$(\mathbf{1}, \mathbf{2}, 1)$	\tilde{e}_i^c	e_i^c

Table 2.1: Particle content of the minimal SUSY standard model. Index i is the generation index which runs from 1 to 3. For each particles, representation of the $SU(3)_C \times SU(2)_L \times U(1)_Y$ gauge group is also shown.

interactions which violate baryon- or lepton-number conservations. For example, interactions such as $u^c d^c \tilde{d}^c$ or $d^c q \tilde{l}$ cannot be forbidden by gauge invariance or renormalizability. But phenomenologically, strength of these interactions is severely constrained since they may induce unwantedly high rate of nucleon decay and neutron-anti-neutron oscillation, and they wash out baryon number in the early universe [19]. Rather than assuming extremely small coupling constants for them, we usually forbid these dangerous terms by introducing a discrete symmetry, that is called R -parity. R -parity assigns $+1$ for ordinary particles in the standard model and -1 for their superpartners. One can see that if we require the invariance under the R -parity, baryon- and lepton-numbers are conserved under the restriction of renormalizability. In this thesis, we adopt the R -invariance below. Notice that R -invariance also guarantees the stability of the lightest R -odd particle, *i.e.* the lightest superparticle (LSP).

Assuming the R -invariance, the superpotential of the MSSM is given by

$$\begin{aligned}
W_{\text{MSSM}} = & y_{ij}^{(u)} u_i^c q_j H_2 + y_{ij}^{(d)} d_i^c q_j H_1 + y_{ij}^{(e)} e_i^c l_j H_1 \\
& + \mu_H H_1 H_2,
\end{aligned} \tag{2.3}$$

where i and j are generation indices, and we have omitted the group indices for simplicity.

Here, $y^{(u)}$, $y^{(d)}$ and $y^{(e)}$ are the Yukawa coupling constants of the up-, down- and lepton-sector, respectively.

Since the SUSY should be broken in nature, SUSY breaking terms are also necessary in lagrangian. In order not to induce quadratic divergences, SUSY should be broken softly. In general, soft SUSY breaking terms are gaugino mass terms, scalar mass terms and trilinear coupling terms for scalar bosons of same chirality [18]. In the MSSM, SUSY breaking terms are given by

$$\begin{aligned}\mathcal{L}_{\text{soft}} = & -m_{\tilde{q}ij}^2 \tilde{q}_i^* \tilde{q}_j - m_{\tilde{u}ij}^2 \tilde{u}_i^{c*} \tilde{u}_j^c - m_{\tilde{d}ij}^2 \tilde{d}_i^{c*} \tilde{d}_j^c - m_{\tilde{l}ij}^2 \tilde{l}_i^* \tilde{l}_j - m_{\tilde{e}ij}^2 \tilde{e}_i^{c*} \tilde{e}_j^c \\ & - \left(A_{ij}^{(u)} \tilde{u}_i^c \tilde{q}_j H_2 + A_{ij}^{(d)} \tilde{d}_i^c \tilde{q}_j H_1 + A_{ij}^{(e)} \tilde{e}_i^c \tilde{l}_j H_1 + h.c. \right) \\ & - m_{H_1}^2 |H_1|^2 - m_{H_2}^2 |H_2|^2 - \left(m_3^2 H_1 H_2 + h.c. \right) \\ & - \left(m_{G3} \tilde{g} \tilde{g} + m_{G2} \tilde{w} \tilde{w} + m_{G1} \tilde{b} \tilde{b} + h.c. \right),\end{aligned}\tag{2.4}$$

where $m_{\tilde{q}}^2 - m_{\tilde{e}}^2$ are the squark and slepton masses, and $m_{G3} - m_{G1}$ the gauge fermion masses. In the next chapter, we will see that these SUSY breaking parameters can be obtained in a low energy effective theory of local SUSY models.

As mentioned before, quadratic divergence of the two point functions of scalar bosons disappears in SUSY models. At the one loop level, this can be easily seen. For example, we will see the cancellation in the mass of H_2 . Feynman diagrams which give quadratically divergent radiative corrections to the H_2 mass are shown in Fig. 2.1. Each of them are quadratically divergent;

$$\delta m_{H_2}^2 \Big|_{\text{CB}} \simeq \frac{1}{8\pi^2} y_{ij}^{(u)} y_{ij}^{(u)*} \Lambda_{\text{CUT}}^2 + \dots,\tag{2.5}$$

$$\delta m_{H_2}^2 \Big|_{\text{CF}} \simeq -\frac{1}{8\pi^2} y_{ij}^{(u)} y_{ij}^{(u)*} \Lambda_{\text{CUT}}^2 + \dots,\tag{2.6}$$

$$\delta m_{H_2}^2 \Big|_{\text{GB}} \simeq \frac{1}{4\pi^2} \left(\frac{1}{2} g_2^2 + \frac{1}{4} g_1^2 \right) \Lambda_{\text{CUT}}^2 + \dots,\tag{2.7}$$

$$\delta m_{H_2}^2 \Big|_{\text{GF}} \simeq -\frac{1}{4\pi^2} \left(\frac{1}{2} g_2^2 + \frac{1}{4} g_1^2 \right) \Lambda_{\text{CUT}}^2 + \dots,\tag{2.8}$$

where CF (CB, GB, GF) represents the contribution from chiral fermion (chiral boson, gauge boson, gauge fermion), \dots the terms which do not contain quadratic divergences and Λ_{CUT} the cut-off. These quadratic divergences, however, cancel out between boson and fermion loops. Quadratic divergences in other scalar masses also disappear in the same way, and hence the hierarchy problem can be solved by extending the standard model to the supersymmetric one.

In the MSSM, other interesting new physics, *i.e.* the grand unified theory (GUT) [20], is suggested from the renormalization group analysis [4, 5]. As mentioned before, SUSY extension of the standard model increases the number of particles, which changes the renormalization group equation of the gauge coupling constants. In Fig. 2.2, we show the renor-

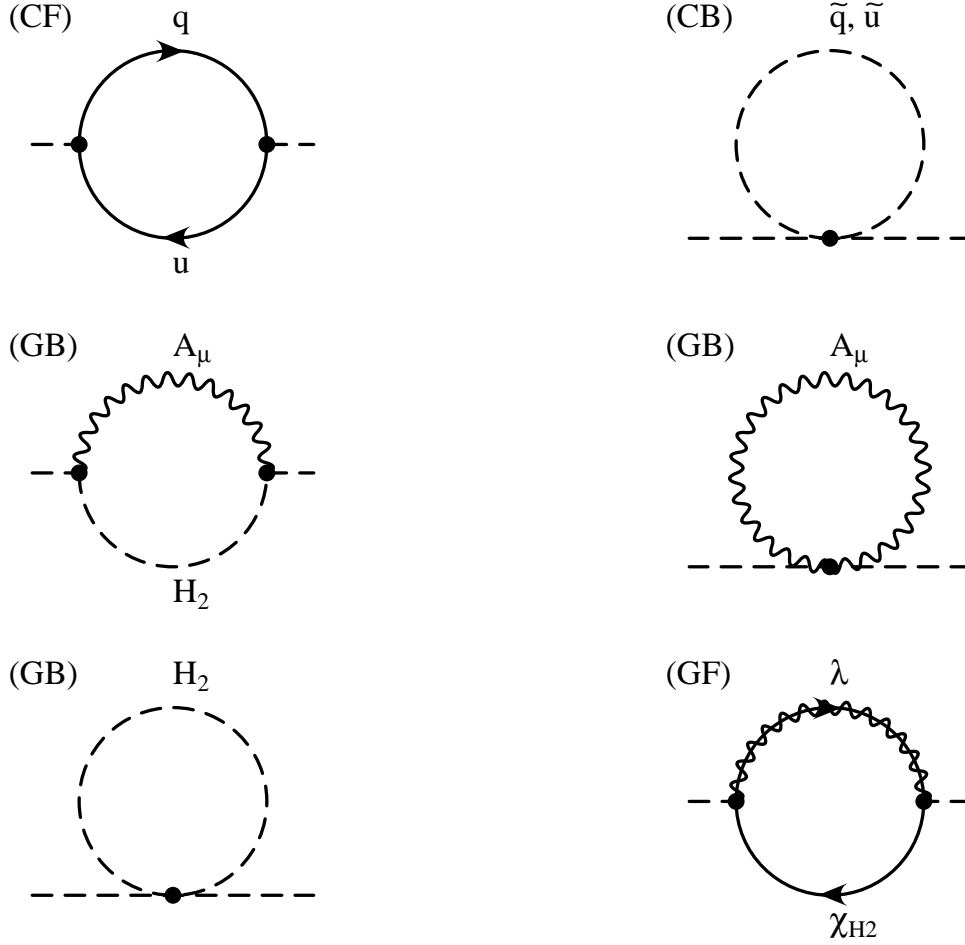


Figure 2.1: Quadratically divergent Feynman diagrams for the H_2 mass. Diagram with CF (CB, GB, GF) is the contribution from chiral fermion (chiral boson, gauge boson, gauge fermion) loop. Dashed lines in external lines represent H_2 . Notice that the diagram with H_2 loop (lower-left) originates to the gauge D -term, and hence we classify it as the contribution of gauge boson.

malization group flow of $SU(3)_C$, $SU(2)_L$ and $U(1)_Y$ gauge coupling constants in the MSSM case and in the standard model case. In the MSSM case, three gauge coupling constants meet at the energy scale $\sim 10^{16}\text{GeV}$ which may be identified with the GUT scale, while in the standard model case, the renormalization group flow of the gauge coupling constants conflicts with the gauge coupling unification.

Another indirect evidence of SUSY GUT is the bottom-tau mass ratio [21, 22, 23]. In $SU(5)$ or $SO(10)$ GUT, Yukawa coupling constants of down- and lepton-sectors to the Higgs boson are also expected to be unified at the GUT scale, and hence we can get a relation between the bottom- and tau-Yukawa coupling constants at the electroweak scale. By using this relation, the mass of the bottom quark is obtained once the tau-lepton mass ($\simeq 1.777\text{GeV}$ [24]) is fixed. In Fig. 2.3, we show the predicted bottom-quark mass as a function of $\tan\beta = \langle H_1 \rangle / \langle H_2 \rangle$. Notice that the maximal and minimal values for $\tan\beta$ are

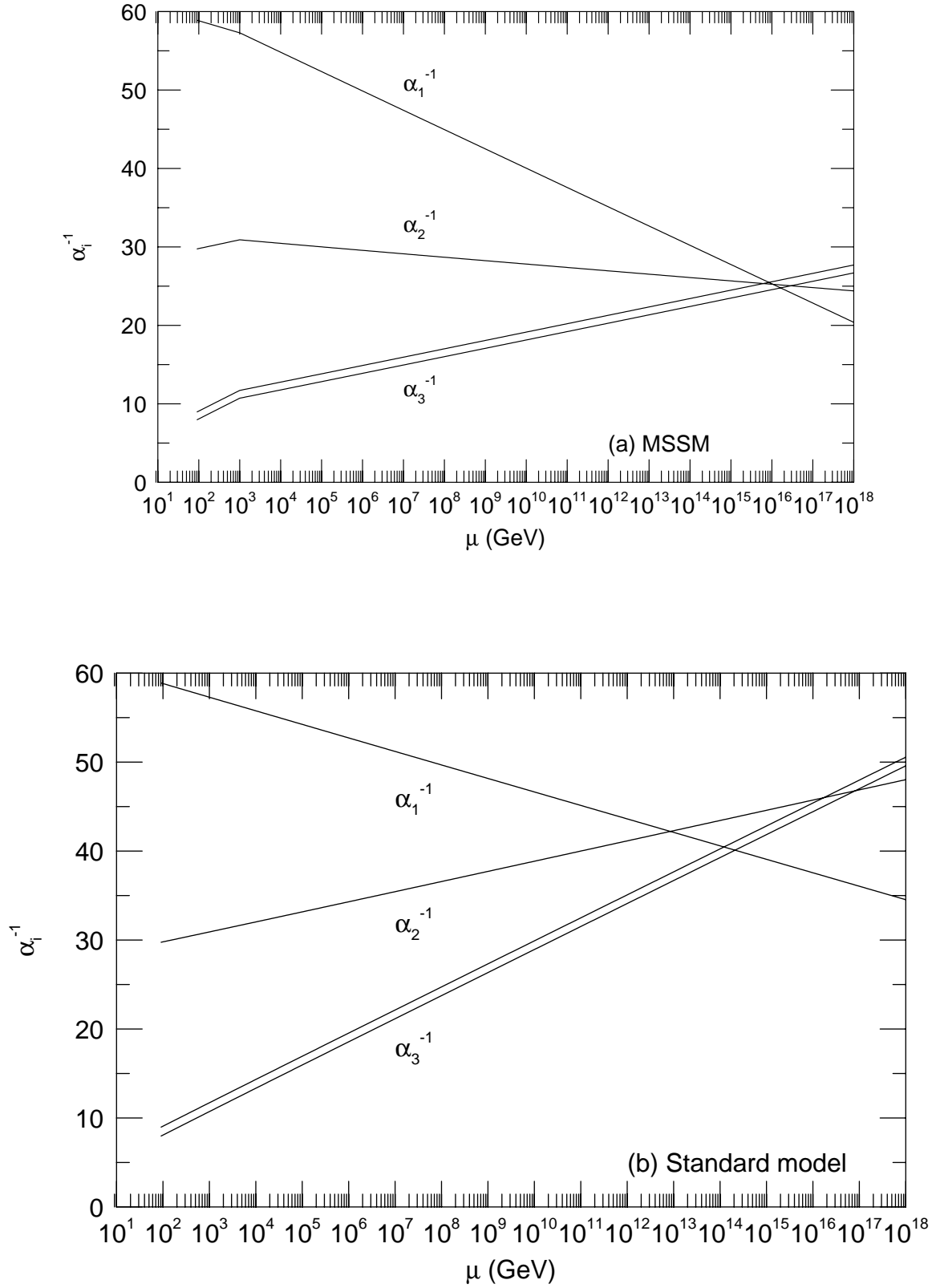


Figure 2.2: Renormalization group flow of the coupling constants of $SU(3)_C$, $SU(2)_L$ and $U(1)_Y$ gauge group for the case of (a) the MSSM, and (b) the standard model. Here, we use two loop renormalization group equations, and take the SUSY scale at 1TeV for the MSSM case.

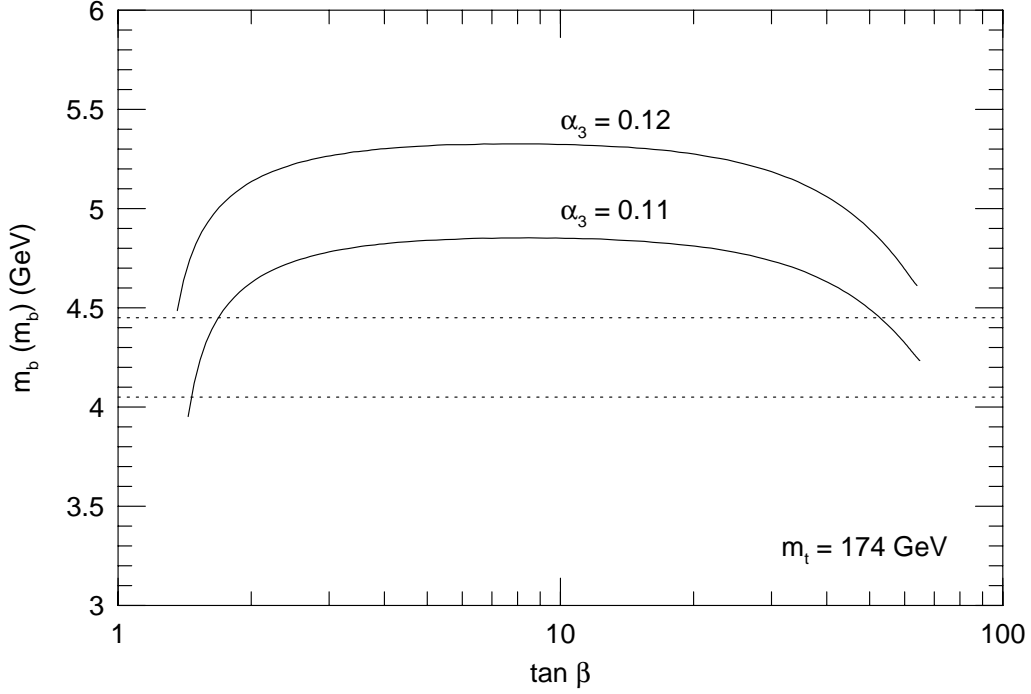


Figure 2.3: The predicted value of the running bottom-quark mass $m_b(m_b)$ is shown as a function of $\tan\beta$ for $\alpha_3(m_Z) = 0.11$ and 0.12 . Here, we take the (on-shell) top-quark mass at 174GeV .

determined so that all the Yukawa coupling constants do not blow up below the GUT scale. As one can see, SUSY GUT predicts the bottom-quark mass to be $(4 - 6)\text{GeV}$ which is close to that determined from experiments; $m_b(m_b) = (4.25 \pm 0.2)\text{GeV}$ [25] (where we have doubled the uncertainty), especially when $\tan\beta$ approaches its maximal or minimal value.

Contrary to those attractive features, no direct evidence of SUSY has been found, which certainly indicates that the SUSY is a (softly) broken symmetry. The physics of SUSY breaking is, however, still an open question and we have not understood it yet. Especially in the framework of global SUSY, it seems to be very much difficult to construct a phenomenologically favorable model. One of the reason is that there exists a mass formula in the global SUSY model;

$$\text{Str}\mathbf{M}^2 \equiv \sum_{J=0}^1 (-1)^J \text{tr}\mathbf{M}_J^2 = 0, \quad (2.9)$$

which prevents all the squarks and sleptons from having masses larger than those of quarks and leptons. To avoid this constraint, many people extend the global SUSY to the local one and consider the physics of SUSY breaking in the framework of supergravity. In the next chapter, we will investigate local SUSY model and see how the mass formula in global SUSY models (2.9) is modified.

Chapter 3

Review of supergravity

In this chapter, we will introduce a lagrangian which is invariant under the local SUSY transformation, and derive super-trace formula in that framework. Conventions used in this chapter are essentially equal to those used in ref.[26] except that we use the metric (in flat space-time) as $g_{\mu\nu} \simeq \text{diag}(1, -1, -1, -1)$. For our convention, see also Appendix A.

3.1 Heuristic approach to supergravity lagrangian

Compared with the global SUSY, one of the characteristics of the local one is the existence of a gauge field associated with the local SUSY, which is called gravitino. As in the case of ordinary gauge theories, the gravitino couples to a Noether current of SUSY and maintains the invariance under the local SUSY transformation. In this section, we will briefly review the role of the gravitino in the local SUSY theory by using the simplest model, which is the Wess-Zumino model [1] without interactions.

Let us begin with the global case. In this case, total lagrangian contains only two terms, one is the kinetic term of a massless complex scalar boson ϕ and the other is that of a massless chiral fermion χ ;

$$\mathcal{L}_{\text{WZ}} = \partial^\mu \phi \partial_\mu \phi^* + i \bar{\chi} \bar{\sigma}^\mu \partial_\mu \chi. \quad (3.1)$$

Up to total derivative, this lagrangian is invariant under the following global SUSY transformation,

$$\delta \phi = \sqrt{2} \xi \chi, \quad (3.2)$$

$$\delta \chi = -i \sqrt{2} \sigma^\mu \bar{\xi} (\partial_\mu \phi), \quad (3.3)$$

where ξ is the infinitesimal Grassmann-odd parameter.

If ξ has space-time dependence, lagrangian (3.1) is not invariant but extra terms which

are proportional to $\partial\xi$ or $\partial\bar{\xi}$ appear with the supertransformation (3.2) and (3.3);

$$\begin{aligned}\delta\mathcal{L}_{\text{WZ}} &= \sqrt{2} \left\{ (\partial_\mu\xi)\sigma^\nu\bar{\sigma}^\mu\chi(\partial_\nu\phi^*) + \bar{\chi}\bar{\sigma}^\mu\sigma^\nu(\partial_\mu\bar{\xi})(\partial_\nu\phi) \right\} + (\text{total derivative}) \\ &\equiv i(\partial_\mu\xi)J^\mu + h.c. + (\text{total derivative}).\end{aligned}\quad (3.4)$$

where

$$J^\mu \equiv -i\sqrt{2}\sigma^\nu\bar{\sigma}^\mu\chi(\partial_\nu\phi^*). \quad (3.5)$$

Notice that J^μ is the Noether current of SUSY, which is called supercurrent. In order to keep invariance, we introduce a gauge field ψ_μ . As in the cases of ordinary gauge theories, the gauge field ψ_μ couples to the supercurrent in the following way;

$$\mathcal{L}_{\psi J} = -\frac{i}{2}G_S\psi_\mu J^\mu + h.c. , \quad (3.6)$$

where G_S is the ‘‘coupling constant’’ which we will determine later. Since the charge of SUSY has a Grassmann-odd nature with spin index, the gauge field ψ_μ associated with SUSY is a spin $\frac{3}{2}$ fermion. Varying eq.(3.6), one obtains

$$\delta\mathcal{L}_{\psi J} = -\frac{i}{2}G_S \{(\delta\psi_\mu)J^\mu + \psi_\mu(\delta J^\mu)\} + h.c. \quad (3.7)$$

Therefore, if ψ_μ transforms as

$$\delta\psi_\mu \sim \frac{2}{G_S}\partial_\mu\xi, \quad (3.8)$$

the first term in eq.(3.7) cancels out the contribution from eq.(3.4).

Next, we will consider the second term in eq.(3.7). Supertransformation of the supercurrent (3.5) gives energy-momentum tensor $T_\mu{}^\nu$ of the chiral multiplet (ϕ, χ) ;

$$\begin{aligned}\{\bar{Q}_{\dot{\alpha}}, J_\alpha^\mu\} &= -2\sigma_{\alpha\dot{\alpha}}^\nu T_\nu{}^\mu + (\text{total derivative}), \\ \{Q^\alpha, \bar{J}^{\mu\dot{\alpha}}\} &= -2\bar{\sigma}^{\nu\dot{\alpha}\alpha} T_\nu{}^\mu + (\text{total derivative}),\end{aligned}\quad (3.9)$$

where Q and \bar{Q} are the generators of the SUSY transformation, and hence the second term in eq.(3.7) becomes

$$-\frac{i}{2}G_S \{\psi_\mu(\delta J^\mu)\} + h.c. = \frac{i}{2}G_S \left\{ \psi_\mu\sigma_\nu\bar{\xi} + \psi_\nu\sigma_\mu\bar{\xi} + \bar{\psi}_\mu\bar{\sigma}_\nu\xi + \bar{\psi}_\nu\bar{\sigma}_\mu\xi \right\} T^{\mu\nu}. \quad (3.10)$$

In order to cancel out these terms, we rewrite the lagrangian (3.1) by explicitly expressing the metric tensor $g_{\mu\nu}$;

$$\mathcal{L}_{\text{WZ}} \rightarrow \sqrt{-g}g_{\mu\nu} (\partial^\mu\phi\partial^\nu\phi^* + i\bar{\chi}\bar{\sigma}^\mu\partial^\nu\chi), \quad (3.11)$$

where $g \equiv \det g_{\mu\nu}$, and use the fact that the metric is the gauge field associated with the energy-momentum tensor (which is the Noether current of the space-time translation), that is, the energy-momentum tensor $T_\mu{}^\nu$ is obtained if one varies lagrangian by $g_{\mu\nu}$;

$$\frac{\partial \mathcal{L}}{\partial g_{\mu\nu}} \sim 2T^{\mu\nu}. \quad (3.12)$$

Then, the metric tensor $g_{\mu\nu}$ (*i.e.* graviton) can be regarded as a superpartner of the gravitino field ψ_μ , and its transformation law is determined so that the local SUSY invariance is maintained;

$$\delta g_{\mu\nu} \frac{\delta \mathcal{L}_{\text{WZ}}}{\delta g_{\mu\nu}} \sim -\frac{i}{2} G_S \left\{ \psi^\mu \sigma^\nu \bar{\xi} + \psi^\nu \sigma^\mu \bar{\xi} + \bar{\psi}^\mu \bar{\sigma}^\nu \xi + \bar{\psi}^\nu \bar{\sigma}^\mu \xi \right\} T_{\mu\nu}. \quad (3.13)$$

Combining eq.(3.12) with eq.(3.13), one can obtain the transformation law of the metric tensor;

$$\delta g_{\mu\nu} \sim -iG_S \left(\psi_\mu \sigma_\nu \bar{\xi} + \psi_\nu \sigma_\mu \bar{\xi} + \bar{\psi}_\mu \bar{\sigma}_\nu \xi + \bar{\psi}_\nu \bar{\sigma}_\mu \xi \right). \quad (3.14)$$

In the following arguments, in fact, it is more convenient to use the vierbein $e_\mu{}^a$ rather than the metric tensor $g_{\mu\nu} = \eta_{ab} e_\mu{}^a e_\nu{}^b$, where $\eta_{ab} = \text{diag}(1, -1, -1, -1)$ is the metric tensor in flat space-time. In supergravity models, transformation law of the vierbein $e_\mu{}^a$ is defined as

$$\delta e_\mu{}^a = -iG_S \left(\xi \sigma^a \bar{\psi}_\mu + \bar{\xi} \bar{\sigma}^a \psi_\mu \right), \quad (3.15)$$

with $G_S = M^{-1}$. This transformation law gives eq.(3.14). Under the local SUSY transformation, the vierbein $e_\mu{}^a$ and the gravitino ψ_μ (and some other auxiliary fields) make up a multiplet, which we call a supergravity multiplet.

As we have seen, if we extend the global SUSY to the local one, the metric tensor $g_{\mu\nu}$ automatically comes into the theory, and hence we must consider gravity. This is the reason why the local SUSY is sometimes called supergravity.

3.2 Minimal supergravity model

In the previous section, we have introduced the gravitino field ψ_μ in order to keep the local SUSY invariance. As we have seen, the gravitino field couples to the supercurrent, but the strength G_S of the coupling between the gravitino and the supercurrent has not been determined yet. In order to determine the coupling strength G_S , we must see the invariance of the kinetic terms of $e_\mu{}^a$ and ψ_μ under the local SUSY transformation.

In this section, we will explicitly investigate the local SUSY invariance of the minimal supergravity model which contains only the graviton $e_\mu{}^a$ and the gravitino field ψ_μ . As a

result, we will see the coupling strength G_S should be equal to the inverse of the gravitational scale.

The lagrangian of the minimal supergravity model is given by

$$\mathcal{L}_{\text{MSG}} = \mathcal{L}_{\text{EH}} + \mathcal{L}_{\text{RS}}, \quad (3.16)$$

where \mathcal{L}_{EH} is the usual Einstein-Hilbert lagrangian, and \mathcal{L}_{RS} is the Rarita-Schwinger lagrangian which is essentially the kinetic term of the spin $\frac{3}{2}$ gravitino field. The Einstein-Hilbert lagrangian is given by

$$\mathcal{L}_{\text{EH}} = -\frac{M^2}{2}eR, \quad (3.17)$$

with

$$R \equiv e_a{}^\mu e_b{}^\nu \left(\partial_\mu \omega_\nu{}^{ab} - \partial_\nu \omega_\mu{}^{ab} - \omega_\mu{}^{ac} \omega_{\nu c}{}^b + \omega_\nu{}^{ac} \omega_{\mu c}{}^b \right), \quad (3.18)$$

where $\omega_\mu{}^{ab}$ denotes the spin connection and $e \equiv \det e_a{}^\mu$. On the other hand, the Rarita-Schwinger lagrangian can be written as

$$\mathcal{L}_{\text{RS}} = e \epsilon^{\mu\nu\rho\sigma} \bar{\psi}_\mu \bar{\sigma}_\nu \tilde{\mathcal{D}}_\rho \psi_\sigma, \quad (3.19)$$

where $\epsilon^{\mu\nu\rho\sigma}$ is the totally anti-symmetric tensor ($\epsilon_{0123} = -1$ in flat space-time) and the covariant derivative of the gravitino field is given by

$$\tilde{\mathcal{D}}_\mu \psi_\nu \equiv \partial_\mu \psi_\nu + \frac{1}{2} \omega_\mu{}^{ab} \sigma_{ab} \psi_\nu. \quad (3.20)$$

In the following, we will see the invariance of the minimal supergravity lagrangian (3.16) under the local SUSY transformation;

$$\delta e_\mu{}^a = -iG_S \left(\xi \sigma^a \bar{\psi}_\mu + \bar{\xi} \bar{\sigma}^a \psi_\mu \right), \quad (3.21)$$

$$\delta \psi_\mu = \frac{2}{G_S} \tilde{\mathcal{D}}_\mu \xi \equiv \frac{2}{G_S} \left(\partial_\mu \xi + \frac{1}{2} \omega_\mu{}^{ab} \sigma_{ab} \xi \right), \quad (3.22)$$

where parameter G_S will be determined so that the local SUSY invariance is maintained (see eq.(3.8) and eq.(3.15)).

Before checking the invariance of the minimal supergravity lagrangian (3.16), we will comment on the spin connection $\omega_\mu{}^{ab}$. As we will see below, $\omega_\mu{}^{ab}$ is represented as a function of the vierbein $e_\mu{}^a$ and the gravitino ψ_μ by solving its field equation;

$$\frac{\delta \mathcal{L}_{\text{MSG}}}{\delta \omega_\mu{}^{ab}} = \frac{\partial \mathcal{L}_{\text{MSG}}}{\partial \omega_\mu{}^{ab}} - \partial_\nu \frac{\partial \mathcal{L}_{\text{MSG}}}{\partial (\partial_\nu \omega_\mu{}^{ab})} = 0, \quad (3.23)$$

and hence ω_μ^{ab} is regarded as an auxiliary field. From eq.(3.23), one can obtain

$$M^2 \left\{ \left(\partial_\mu e_\nu^a + \omega_\mu^{ab} e_{\nu b} \right) - \left(\partial_\nu e_\mu^a + \omega_\nu^{ab} e_{\mu b} \right) \right\} = -\frac{i}{2} \left(\bar{\psi}_\mu \bar{\sigma}^a \psi_\nu - \bar{\psi}_\nu \bar{\sigma}^a \psi_\mu \right). \quad (3.24)$$

By solving this equation, explicit form of the spin connection is given by

$$\begin{aligned} \omega_{\mu\rho\sigma} &\equiv e_{\rho a} e_{\sigma b} \omega_\mu^{ab} \\ &= \frac{1}{2} \{ e_{\sigma a} (\partial_\mu e_\rho^a - \partial_\rho e_\mu^a) + e_{\rho a} (\partial_\sigma e_\mu^a - \partial_\mu e_\sigma^a) - e_{\mu a} (\partial_\rho e_\sigma^a - \partial_\sigma e_\rho^a) \} \\ &\quad - \frac{i}{4M^2} e_{\sigma a} (\psi_\rho \sigma^a \bar{\psi}_\mu - \psi_\mu \sigma^a \bar{\psi}_\rho) - \frac{i}{4M^2} e_{\rho a} (\psi_\mu \sigma^a \bar{\psi}_\sigma - \psi_\sigma \sigma^a \bar{\psi}_\mu) \\ &\quad + \frac{i}{4M^2} e_{\mu a} (\psi_\sigma \sigma^a \bar{\psi}_\rho - \psi_\rho \sigma^a \bar{\psi}_\sigma). \end{aligned} \quad (3.25)$$

Now let us see the invariance of the lagrangian (3.16). With the help of chain rule, variation of the total lagrangian is given by

$$\begin{aligned} \delta \mathcal{L}_{\text{MSG}} &= \delta e_\mu^a \left. \frac{\delta \mathcal{L}_{\text{MSG}}}{\delta e_\mu^a} \right|_{\psi, \omega} + \delta \psi_\mu \left. \frac{\delta \mathcal{L}_{\text{MSG}}}{\delta \psi_\mu} \right|_{e, \omega} \\ &\quad + \left(\delta e_\mu^a \frac{\delta \omega_\mu^{ab}}{\delta e_\mu^a} + \delta \psi_\mu \frac{\delta \omega_\mu^{ab}}{\delta \psi_\mu} \right) \left. \frac{\delta \mathcal{L}_{\text{MSG}}}{\delta \omega_\mu^{ab}} \right|_{e, \psi}, \end{aligned} \quad (3.26)$$

where we have used the fact that the spin connection ω_μ^{ab} is a function of the vierbein e_μ^a and the gravitino ψ_μ . The important point is that the last two terms in eq.(3.26) which are proportional to $(\delta \mathcal{L}_{\text{MSG}}/\delta \omega)$ vanish since the spin connection obeys its field equation $(\delta \mathcal{L}_{\text{MSG}}/\delta \omega) = 0$. Therefore, we only have to vary e_μ^a and ψ_μ (with ω_μ^{ab} fixed) in order to obtain $\delta \mathcal{L}_{\text{MSG}}$. (We denote this operation Δ .)

Variation of the Einstein-Hilbert lagrangian \mathcal{L}_{EH} gives the Einstein tensor multiplied by δe_μ^a ;

$$\begin{aligned} \Delta \mathcal{L}_{\text{EH}} &\equiv \delta e_\mu^a \left. \frac{\delta \mathcal{L}_{\text{EH}}}{\delta e_\mu^a} \right|_{\psi, \omega} + \delta \psi_\mu \left. \frac{\delta \mathcal{L}_{\text{EH}}}{\delta \psi_\mu} \right|_{e, \omega} \\ &= i G_S M^2 e \left(R_a^\mu - \frac{1}{2} e_a^\mu R \right) \bar{\psi}_\mu \sigma^a \xi + h.c., \end{aligned} \quad (3.27)$$

with

$$R_\mu^a \equiv e_b^\nu \left(\partial_\mu \omega_\nu^{ab} - \partial_\nu \omega_\mu^{ab} - \omega_\mu^{ac} \omega_{\nu c}^b + \omega_\nu^{ac} \omega_{\mu c}^b \right). \quad (3.28)$$

On the other hand, after some straightforward calculations, $\Delta \mathcal{L}_{\text{RS}}$ becomes the following form;

$$\Delta \mathcal{L}_{\text{RS}} \equiv \delta e_\mu^a \left. \frac{\delta \mathcal{L}_{\text{RS}}}{\delta e_\mu^a} \right|_{\psi, \omega} + \delta \psi_\mu \left. \frac{\delta \mathcal{L}_{\text{RS}}}{\delta \psi_\mu} \right|_{e, \omega}$$

$$\begin{aligned}
&= \left\{ -\frac{i}{G_S} M^2 e \left(R_a{}^\mu - \frac{1}{2} e_a{}^\mu R \right) \bar{\psi}_\mu \bar{\sigma}^a \xi + h.c. \right\} \\
&\quad - e \epsilon^{\mu\nu\rho\sigma} \left\{ \frac{2}{G_S} \left(\partial_\mu e_\nu{}^a + \omega_\mu{}^{ab} e_{\nu b} \right) + i G_S \left(\bar{\psi}_\mu \bar{\sigma}^a \psi_\nu \right) \right\} \bar{\xi} \bar{\sigma}_a \tilde{D}_\rho \psi_\sigma. \quad (3.29)
\end{aligned}$$

By setting $G_S = M^{-1}$, the first line in eq.(3.29) is equal to $-\Delta\mathcal{L}_{\text{EH}}$, the second line vanishes due to eq.(3.24), and hence $\delta\mathcal{L}_{\text{MSG}}$ vanishes;

$$\delta\mathcal{L}_{\text{MSG}} = \Delta\mathcal{L}_{\text{EH}} + \Delta\mathcal{L}_{\text{RS}} = 0. \quad (3.30)$$

This is the end of the proof of the invariance. We have seen the invariance of the minimal supergravity lagrangian (3.16) under the local SUSY transformation (3.21) and (3.22) with $G_S = M^{-1}$.

This fact suggests that the coupling strength G_S between the gravitino field ψ_μ and the supercurrent J_μ is not a free parameter but a model independent constant which is determined by the requirement that the kinetic term of the supergravity multiplet $(\psi_\mu, e_\mu{}^a)$ is invariant under the local SUSY transformation. In the next section, we can see that general supergravity lagrangian contains interaction terms between the gravitino field ψ_μ and the supercurrent J_μ with definite coupling strength (*i.e.* $G_S = M^{-1}$);

$$\mathcal{L}_{\psi J} = -\frac{i}{2M} \psi_\mu J^\mu + h.c. \quad (3.31)$$

As we will see in the following chapters, such interaction terms become very important in investigating phenomenology with the gravitino.

3.3 General supergravity lagrangian

In this section, we will extend the minimal supergravity model to general one. Derivation of the general supergravity lagrangian is given in elsewhere [8, 26], but it is very much complicated task. Therefore, we only give a final form here by following ref.[26]. In this section, we use the $M = 1$ unit for simplicity.

The general supergravity lagrangian is essentially characterized by three functions; Kähler potential $K(\phi, \phi^*)$, superpotential $W(\phi)$, and kinetic function $f(\phi)$ for vector multiplets. Notice that the Kähler potential $K(\phi, \phi^*)$ is a function of scalar fields ϕ and ϕ^* , while the superpotential $W(\phi)$ and the kinetic function $f(\phi)$ depend scalar fields with definite chirality.

By using these functions, the general form of the supergravity lagrangian, which contains scalar field ϕ , chiral fermion χ , gauge boson A_μ , and gauge fermion λ as well as the vierbein $e_\mu{}^a$ and the gravitino ψ_μ can be written as

$$\begin{aligned}
\mathcal{L}_{\text{SUGRA}} &= -\frac{1}{2} e R + e g_{ij}{}^* \tilde{D}_\mu \phi^i \tilde{D}^\mu \phi^{*j} - \frac{1}{2} e g^2 D_{(a)} D^{(a)} \\
&\quad + i e g_{ij}{}^* \bar{\chi}^j \bar{\sigma}^\mu \tilde{D}_\mu \chi^i + e \epsilon^{\mu\nu\rho\sigma} \bar{\psi}_\mu \bar{\sigma}_\nu \tilde{D}_\rho \psi_\sigma
\end{aligned}$$

$$\begin{aligned}
& -\frac{1}{4}e f_{(ab)}^R F_{\mu\nu}^{(a)} F^{\mu\nu(b)} + \frac{1}{8}e \epsilon^{\mu\nu\rho\sigma} f_{(ab)}^I F_{\mu\nu}^{(a)} F_{\rho\sigma}^{(b)} \\
& + \frac{i}{2}e \left[\lambda_{(a)} \sigma^\mu \tilde{D}_\mu \bar{\lambda}^{(a)} + \bar{\lambda}_{(a)} \bar{\sigma}^\mu \tilde{D}_\mu \lambda^{(a)} \right] - \frac{1}{2} f_{(ab)}^I \tilde{D}_\mu \left[e \lambda^{(a)} \sigma^\mu \bar{\lambda}^{(b)} \right] \\
& + \sqrt{2} e g g_{ij^*} X_{(a)}^{*j} \chi^i \lambda^{(a)} + \sqrt{2} e g g_{ij^*} X_{(a)}^i \bar{\chi}^j \bar{\lambda}^{(a)} \\
& - \frac{i}{4} \sqrt{2} e g \partial_i f_{(ab)} D^{(a)} \chi^i \lambda^{(b)} + \frac{i}{4} \sqrt{2} e g \partial_{i^*} f_{(ab)}^* D^{(a)} \bar{\chi}^i \bar{\lambda}^{(b)} \\
& - \frac{1}{4} \sqrt{2} e \partial_i f_{(ab)} \chi^i \sigma^{\mu\nu} \lambda^{(a)} F_{\mu\nu}^{(b)} - \frac{1}{4} \sqrt{2} e \partial_{i^*} f_{(ab)}^* \bar{\chi}^i \bar{\sigma}^{\mu\nu} \bar{\lambda}^{(a)} F_{\mu\nu}^{(b)} \\
& + \frac{1}{2} e g D_{(a)} \psi_\mu \sigma^\mu \bar{\lambda}^{(a)} - \frac{1}{2} e g D_{(a)} \bar{\psi}_\mu \bar{\sigma}^\mu \lambda^{(a)} \\
& - \frac{1}{2} \sqrt{2} e g_{ij^*} \tilde{D}_\nu \phi^{*j} \chi^i \sigma^\mu \bar{\sigma}^\nu \psi_\mu - \frac{1}{2} \sqrt{2} e g_{ij^*} \tilde{D}_\nu \phi^i \bar{\chi}^j \bar{\sigma}^\mu \sigma^\nu \bar{\psi}_\mu \\
& - \frac{i}{4} e \left[\psi_\mu \sigma^{\nu\rho} \sigma^\mu \bar{\lambda}_{(a)} + \bar{\psi}_\mu \bar{\sigma}^{\nu\rho} \bar{\sigma}^\mu \lambda_{(a)} \right] \left[F_{\nu\rho}^{(a)} + \hat{F}_{\nu\rho}^{(a)} \right] \\
& + \frac{1}{4} e g_{ij^*} \left[i \epsilon^{\mu\nu\rho\sigma} \psi_\mu \sigma_\nu \bar{\psi}_\rho + \psi_\mu \sigma^\sigma \bar{\psi}^\mu \right] \chi^i \sigma_\sigma \bar{\chi}^i \\
& - \frac{1}{8} e \left[g_{ij^*} g_{kl^*} - 2 R_{ij^* kl^*} \right] \chi^i \chi^k \bar{\chi}^j \bar{\chi}^l \\
& + \frac{1}{16} e \left[2 g_{ij^*} f_{(ab)}^R + f^{R(cd)-1} \partial_i f_{(bc)} \partial_{j^*} f_{(ad)}^* \right] \bar{\chi}^j \bar{\sigma}^\mu \chi^i \bar{\lambda}^{(a)} \bar{\sigma}_\mu \lambda^{(b)} \\
& + \frac{1}{8} e \nabla_i \partial_j f_{(ab)} \chi^i \chi^j \lambda^{(a)} \lambda^{(b)} + \frac{1}{8} e \nabla_{i^*} \partial_{j^*} f_{(ab)}^* \bar{\chi}^i \bar{\chi}^j \bar{\lambda}^{(a)} \bar{\lambda}^{(b)} \\
& + \frac{1}{16} e f^{R(cd)-1} \partial_i f_{(ac)} \partial_j f_{(bd)} \chi^i \lambda^{(a)} \chi^j \lambda^{(b)} \\
& + \frac{1}{16} e f^{R(cd)-1} \partial_{i^*} f_{(ac)}^* \partial_{j^*} f_{(bd)}^* \bar{\chi}^i \bar{\lambda}^{(a)} \bar{\chi}^j \bar{\lambda}^{(b)} \\
& - \frac{1}{16} e g^{ij^*} \partial_i f_{(ab)} \partial_{j^*} f_{(cd)}^* \lambda^{(a)} \lambda^{(b)} \bar{\lambda}^{(c)} \bar{\lambda}^{(d)} \\
& + \frac{3}{16} e \lambda_{(a)} \sigma^\mu \bar{\lambda}^{(a)} \lambda_{(b)} \sigma_\mu \bar{\lambda}^{(b)} \\
& + \frac{i}{4} \sqrt{2} e \partial_i f_{(ab)} \left[\chi^i \sigma^{\mu\nu} \lambda^{(a)} \psi_\mu \sigma_\nu \bar{\lambda}^{(b)} - \frac{1}{4} \bar{\psi}_\mu \bar{\sigma}^\mu \chi^i \lambda^{(a)} \lambda^{(b)} \right] \\
& + \frac{i}{4} \sqrt{2} e \partial_{i^*} f_{(ab)}^* \left[\bar{\chi}^i \bar{\sigma}^{\mu\nu} \bar{\lambda}^{(a)} \bar{\psi}_\mu \bar{\sigma}_\nu \lambda^{(b)} - \frac{1}{4} \psi_\mu \sigma^\mu \bar{\chi}^i \bar{\lambda}^{(a)} \bar{\lambda}^{(b)} \right] \\
& - e e^{K/2} \left\{ W^* \psi_\mu \sigma^{\mu\nu} \psi_\nu + W \bar{\psi}_\mu \bar{\sigma}^{\mu\nu} \bar{\psi}_\nu \right\} \\
& + \frac{i}{2} \sqrt{2} e e^{K/2} \left\{ D_i W \chi^i \sigma^\mu \bar{\psi}_\mu + D_{i^*} W^* \bar{\chi}^i \bar{\sigma}^\mu \psi_\mu \right\} \\
& - \frac{1}{2} e e^{K/2} \left\{ \mathcal{D}_i D_j W \chi^i \chi^j + \mathcal{D}_{i^*} D_{j^*} W^* \bar{\chi}^i \bar{\chi}^j \right\} \\
& + \frac{1}{4} e e^{K/2} g^{ij^*} \left\{ D_{j^*} W^* \partial_i f_{(ab)} \lambda^{(a)} \lambda^{(b)} + D_i W \partial_{j^*} f_{(ab)}^* \bar{\lambda}^{(a)} \bar{\lambda}^{(b)} \right\} \\
& - e e^K \left[g^{ij^*} (D_i W) (D_{j^*} W^*) - 3 W^* W \right], \tag{3.32}
\end{aligned}$$

where $f^R \equiv \text{Re} f$ and $f^I \equiv \text{Im} f$. Indices i, j, \dots represent species of chiral multiplets, and $(a), (b), \dots$ are indices for adjoint representation of gauge group (with gauge coupling constant

g and structure constant f^{abc}) which are raised and lowered with $f_{(ab)}^R$ and its inverse. Notice that the Kähler potential K and the superpotential W in the total lagrangian (3.32) can be arranged into the following form;

$$G \equiv K + \ln(W^*W). \quad (3.33)$$

Covariant derivatives are defined as

$$\tilde{\mathcal{D}}_\mu \phi^i \equiv \partial_\mu \phi^i - g A_\mu^{(a)} X_{(a)}^i, \quad (3.34)$$

$$\begin{aligned} \tilde{\mathcal{D}}_\mu \chi^i &\equiv \partial_\mu \chi^i + \frac{1}{2} \omega_\mu^{ab} \sigma_{ab} \chi^i + \Gamma_{jk}^i \tilde{\mathcal{D}}_\mu \phi^j \chi^k - g A_\mu^{(a)} \frac{\partial X_{(a)}^i}{\partial \phi^j} \chi^j \\ &\quad - \frac{1}{4} (K_j \tilde{\mathcal{D}}_\mu \phi^j - K_{j^*} \tilde{\mathcal{D}}_\mu \phi^{*j}) \chi^i - \frac{i}{2} g A_\mu^{(a)} \text{Im} F_{(a)} \chi^i, \end{aligned} \quad (3.35)$$

$$\begin{aligned} \tilde{\mathcal{D}}_\mu \lambda^{(a)} &\equiv \partial_\mu \lambda^{(a)} + \frac{1}{2} \omega_\mu^{ab} \sigma_{ab} \lambda^{(a)} - g f^{abc} A_\mu^{(b)} \lambda^{(c)} \\ &\quad + \frac{1}{4} (K_j \tilde{\mathcal{D}}_\mu \phi^j - K_{j^*} \tilde{\mathcal{D}}_\mu \phi^{*j}) \lambda^{(a)} + \frac{i}{2} g A_\mu^{(b)} \text{Im} F_{(b)} \lambda^{(a)}, \end{aligned} \quad (3.36)$$

$$\begin{aligned} \tilde{\mathcal{D}}_\mu \psi_\nu &\equiv \partial_\mu \psi_\nu + \frac{1}{2} \omega_\mu^{ab} \sigma_{ab} \psi_\nu \\ &\quad + \frac{1}{4} (K_j \tilde{\mathcal{D}}_\mu \phi^j - K_{j^*} \tilde{\mathcal{D}}_\mu \phi^{*j}) \psi_\nu + \frac{i}{2} g A_\mu^{(b)} \text{Im} F_{(b)} \psi_\nu. \end{aligned} \quad (3.37)$$

$F_{\mu\nu}^{(a)}$ is the field strength tensor for the gauge boson $A_\mu^{(a)}$, and $\hat{F}_{\mu\nu}^{(a)}$ is defined as

$$\hat{F}_{\mu\nu}^{(a)} \equiv F_{\mu\nu}^{(a)} - \frac{i}{2} \left(\psi_\mu \sigma_\nu \bar{\lambda}^{(a)} + \bar{\psi}_\mu \bar{\sigma}_\nu \lambda^{(a)} + \psi_\nu \sigma_\mu \bar{\lambda}^{(a)} + \bar{\psi}_\nu \bar{\sigma}_\mu \lambda^{(a)} \right). \quad (3.38)$$

Differentiation by the scalar field ϕ^i is symbolically represented by the index i ;

$$(\cdots)_i \equiv \partial_i(\cdots) \equiv \frac{\partial(\cdots)}{\partial \phi^i}, \quad (\cdots)_{i^*} \equiv \partial_{i^*}(\cdots) \equiv \frac{\partial(\cdots)}{\partial \phi^{*i}}. \quad (3.39)$$

With the help of eq.(3.39), “derivatives” of the superpotential are defined as

$$D_i W \equiv W_i + K_i W, \quad (3.40)$$

$$\mathcal{D}_i \mathcal{D}_j W \equiv W_{ij} + K_{ij} W + K_i \mathcal{D}_j W + K_j \mathcal{D}_i W - K_i K_j W - \Gamma_{ij}^k \mathcal{D}_k W. \quad (3.41)$$

“Metric of the Kähler manifold” g_{ij^*} is defined by varying the Kähler potential K by the scalar fields ϕ^i and ϕ^{*j} ;

$$g_{ij^*} \equiv \frac{\partial^2 K}{\partial \phi^i \partial \phi^{*j}}, \quad (3.42)$$

and g^{ij*} is its inverse,

$$g_{ij*}g^{ik*} = \delta_{j*}^{k*}, \quad g_{ij*}g^{kj*} = \delta_i^k. \quad (3.43)$$

From this metric, “connection” Γ_{ij}^k and “curvature” R_{ij*kl*} is given by

$$\Gamma_{ij}^k \equiv g^{kl*} \frac{\partial}{\partial \phi^i} g_{jl*}, \quad (3.44)$$

$$R_{ij*kl*} \equiv \frac{\partial}{\partial \phi^i} \frac{\partial}{\partial \phi^{j*}} g_{kl*} - g^{mn*} \left(\frac{\partial}{\partial \phi^{j*}} g_{ml*} \right) \left(\frac{\partial}{\partial \phi^i} g_{kn*} \right). \quad (3.45)$$

By using the connection given in eq.(3.44), “covariant derivative” ∇_i is defined as

$$\nabla_i V_j \equiv \frac{\partial}{\partial \phi^i} V_j - \Gamma_{ij}^k V_k. \quad (3.46)$$

(Here, V_i is a function of scalar fields with index i .)

Next, we will comment on $X^{(a)i}$ and $D^{(a)}$. $X^{(a)i}(\phi)$ is the Killing vector associated with Kähler metric g_{ij*} . That is, with the field transformation

$$\phi^i \rightarrow \phi^{i'} = \phi^i + X^{(a)i}(\phi)\epsilon, \quad (3.47)$$

$$\phi^{i*} \rightarrow \phi^{i'*} = \phi^{i*} + X^{*(a)i}(\phi^*)\epsilon, \quad (3.48)$$

(where ϵ is a infinitesimal parameter), the Lie derivative $\delta_X^{(L)}$ of g_{ij*} vanishes;

$$\begin{aligned} \delta_X^{(L)} g_{\tilde{i}\tilde{j}} &\equiv X^{(a)\tilde{k}} \frac{\partial}{\partial \phi^{\tilde{k}}} g_{\tilde{i}\tilde{j}} + g_{\tilde{i}\tilde{k}} \frac{\partial}{\partial \phi^{\tilde{j}}} X^{(a)\tilde{k}} + g_{\tilde{j}\tilde{k}} \frac{\partial}{\partial \phi^{\tilde{i}}} X^{(a)\tilde{k}} \\ &= \nabla_{\tilde{i}} X_{\tilde{j}}^{(a)} + \nabla_{\tilde{j}} X_{\tilde{i}}^{(a)} \\ &= 0, \end{aligned} \quad (3.49)$$

where $X_{\tilde{i}}^{(a)} \equiv g_{\tilde{i}\tilde{j}} X^{(a)\tilde{j}}$, and the index \tilde{i} represents both i and i^* . From the above equation, we obtain two equations for the Killing vectors $X^{(a)i}(\phi)$ and $X^{*(a)i}(\phi^*)$;

$$\nabla_i X_j^{(a)} + \nabla_j X_i^{(a)} = 0, \quad (3.50)$$

$$\nabla_i X_{j*}^{(a)} + \nabla_{j*} X_i^{(a)} = 0. \quad (3.51)$$

The former equation is automatically satisfied, while the latter allows one to write down the Killing vectors $X^{(a)i}(\phi)$ and $X^{*(a)i}(\phi^*)$ as derivatives of some function $D^{(a)}$ (which is called Killing potential);

$$X^{(a)i}(\phi) = -ig^{ij*} \frac{\partial}{\partial \phi^{j*}} D^{(a)}, \quad (3.52)$$

$$X^{*(a)i}(\phi^*) = ig^{ij*} \frac{\partial}{\partial \phi^i} D^{(a)}. \quad (3.53)$$

By solving eq.(3.51), eq.(3.52) and eq.(3.53), the Killing vectors $X^{(a)i}(\phi)$, $X^{*(a)i}(\phi^*)$, and the Killing potential $D^{(a)}$ can be obtained. $F^{(a)}$, which is a analytic function of ϕ^i , is defined as

$$F^{(a)} \equiv -ig^{ij*} \frac{\partial D^{(a)}}{\partial \phi^{*j}} \frac{\partial K}{\partial \phi^i} + iD^{(a)}. \quad (3.54)$$

For example for the minimal Kähler potential $K^{min} = \phi^i \phi^{*i}$, the Killing vectors and the Killing potential take the following forms;

$$X^{(a)i}(\phi) = -iT_{ij}^a \phi^j, \quad (3.55)$$

$$X^{*(a)i}(\phi^*) = i\phi^{*j} T_{ji}^a, \quad (3.56)$$

$$D^{(a)} = \phi^{*i} T_{ij}^a \phi^j, \quad (3.57)$$

where T_{ij}^a is a generator of gauged Lie group.

For the local SUSY transformation, variations of each component field are given by

$$\delta e_\mu^a = -i \left(\xi \sigma^a \bar{\psi}_\mu + \bar{\xi} \bar{\sigma}^a \psi_\mu \right), \quad (3.58)$$

$$\delta \phi^i = \sqrt{2} \xi \chi^i, \quad (3.59)$$

$$\begin{aligned} \delta \chi^i &= i\sqrt{2} \sigma^\mu \left(\tilde{\mathcal{D}}_\mu \phi^i - \frac{1}{\sqrt{2}} \psi_\mu \chi^i \right) - \Gamma_{jk}^i \delta \phi^j \chi^k \\ &\quad + \frac{1}{4} \left(K_j \delta \phi^j - K_{j*} \delta \phi^{j*} \right) \chi^i - \sqrt{2} F^i \xi \\ &\quad + \frac{1}{2\sqrt{2}} \xi g^{ij*} \partial_{j*} f_{(ab)}^* \bar{\lambda}^{(a)} \bar{\lambda}^{(b)}, \end{aligned} \quad (3.60)$$

$$\delta A_\mu^{(a)} = i \left(\xi \sigma_\mu \bar{\lambda}^{(a)} + \bar{\xi} \bar{\sigma}_\mu \lambda^{(a)} \right), \quad (3.61)$$

$$\begin{aligned} \delta \lambda^{(a)} &= \hat{F}_{\mu\nu}^{(a)} \sigma^{\mu\nu} \xi - \frac{1}{4} \left(K_j \delta \phi^j - K_{j*} \delta \phi^{j*} \right) \lambda^{(a)} - ig D^{(a)} \xi \\ &\quad + \frac{1}{2\sqrt{2}} \xi f^{R(ab)-1} \partial_i f_{(bc)} \chi^i \lambda^{(c)} - \frac{1}{2\sqrt{2}} \xi f^{R(ab)-1} \partial_{i*} f_{(bc)}^* \bar{\chi}^i \bar{\lambda}^{(c)}, \end{aligned} \quad (3.62)$$

$$\begin{aligned} \delta \psi_\mu &= 2\tilde{\mathcal{D}}_\mu \xi - \frac{i}{2} \sigma_{\mu\nu} \xi g_{ij*} \chi^i \sigma^\nu \bar{\chi}^j + \frac{i}{2} (e_\mu^a e_{\nu a} + \sigma_{\mu\nu}) \xi \lambda_{(a)} \sigma^\nu \bar{\lambda}^{(a)} \\ &\quad - \frac{1}{4} \left(K_j \delta \phi^j - K_{j*} \delta \phi^{j*} \right) \psi_\mu + ie^{K/2} W \sigma_\mu \bar{\xi}. \end{aligned} \quad (3.63)$$

with

$$F^i \equiv e^{K/2} g^{ij*} D_{j*} W^*. \quad (3.64)$$

Notice that F^i given in eq.(3.64) corresponds to the auxiliary field in chiral multiplet in the global SUSY case. (Do not confuse F^i with $F^{(a)}$ defined in eq.(3.54).)

As mentioned in the previous section, the total lagrangian (3.32) contains interaction terms between the gravitino field ψ_μ and the supercurrent J_μ in the form of eq.(3.31). For a later convenience, we note the interaction terms here;

$$\begin{aligned}\mathcal{L}_{\psi J} = & -\frac{1}{\sqrt{2}M}eg_{ij*}\tilde{D}_\nu\phi^{*j}\chi^i\sigma^\mu\bar{\sigma}^\nu\psi_\mu - \frac{1}{\sqrt{2}M}eg_{ij*}\tilde{D}_\nu\phi^i\bar{\chi}^j\bar{\sigma}^\mu\sigma^\nu\bar{\psi}_\mu \\ & -\frac{i}{2M}e\left(\psi_\mu\sigma^{\nu\rho}\sigma^\mu\bar{\lambda}_{(a)} + \bar{\psi}_\mu\bar{\sigma}^{\nu\rho}\bar{\sigma}^\mu\lambda_{(a)}\right)F_{\nu\rho}^{(a)},\end{aligned}\quad (3.65)$$

where we have explicitly written down the M -dependence.

3.4 Super-Higgs mechanism

With the general supergravity lagrangian (3.32), we now can investigate the super-Higgs mechanism [8] which is closely related to the spontaneous breaking of the local SUSY. If the global SUSY is broken spontaneously, massless Nambu-Goldstone fermion which is called goldstino appears, while in spontaneously broken local SUSY models, this goldstino component is absorbed by the gravitino through the super-Higgs mechanism. In this section, we will discuss this mechanism in more detail. (As in the previous section, we take $M = 1$ unit in this and the next sections.)

We will begin by considering the SUSY breaking in supergravity. In global SUSY models, a spontaneous breaking occurs if some auxiliary field, which is obtained by the SUSY transformation of some chiral fermion χ or gauge fermion λ , receives non-vanishing vacuum-expectation values. In the local SUSY case, we also use $\delta\chi$ and $\delta\lambda$ as order parameters of the SUSY breaking from the reasons mentioned below. As one can see in eq.(3.60) and eq.(3.62), the local SUSY transformations of spin $\frac{1}{2}$ fermions contain terms which are similar to the auxiliary fields obtained in the global case. Assuming (local) Lorentz invariance of the ground state and no fermion-fermion condensation (like gaugino-gaugino condensation), $\langle\delta\chi\rangle \neq 0$ and $\langle\delta\lambda\rangle \neq 0$ reduce to the following conditions;

$$\langle\delta\chi^i\rangle = -\sqrt{2}\langle F^i\rangle\xi \neq 0, \quad (3.66)$$

$$\langle\delta\lambda^{(a)}\rangle = -ig\langle D^{(a)}\rangle\xi \neq 0. \quad (3.67)$$

As we will see later, if $\delta\chi$ or $\delta\lambda$ has non-vanishing vacuum-expectation value, the gravitino, which is the gauge field associated with the local SUSY, absorbs a massless eigenstate of fermion mass matrix and acquires a non-vanishing mass (which is called super-Higgs mechanism). Furthermore, the vacuum-expectation value of F^i or $D^{(a)}$ may provide a mass splitting of bosonic and fermionic states (*i.e.* $\text{Str}\mathbf{M}^2 \neq 0$, see the next section). These phenomena indicate a spontaneous breaking of SUSY and hence in this thesis, we regard $\delta\chi$ and $\delta\lambda$ as order parameters of SUSY even in local SUSY case.

Before investigating detail of the fermion mass matrix, we give some comments. The

first comment is on kinetic terms of chiral and vector multiplets. In supergravity lagrangian (3.32), these kinetic terms are characterized by the Kähler potential K and the kinetic function f , respectively. The kinetic terms are properly normalized if $g_{ij^*} \equiv K_{ij^*} = \delta_{ij^*} + \dots$, and $f_{(ab)} = \delta_{ab} + \dots$, where \dots represents the higher order terms which produce interactions of higher dimensions. For simplicity, we ignore these higher order terms and use the minimal Kähler potential K^{min} and the minimal kinetic function f^{min} ;

$$K^{min} = \sum_i \phi^i \phi^{*i}, \quad f_{(ab)}^{min} = \delta_{ab}. \quad (3.68)$$

Another comment is on the cosmological constant. Since we are interested in field theories in the Minkowski space-time, we require the cosmological constant to vanish. In the supergravity models, the vanishing cosmological constant is obtained if the following condition is satisfied;

$$e^K \{ (D_i W) (D_{i^*} W^*) - 3W^* W \} + \frac{1}{2} g^2 D^{(a)} D^{(a)} = 0. \quad (3.69)$$

If $e^{K/2} D_i W$ or $D^{(a)}$ has a non-vanishing vacuum-expectation value, the superpotential W should have a non-vanishing vacuum-expectation value in order to satisfy the condition (3.69). As we will see later, the gravitino mass is given by $e^{K/2} W$, and hence the condition for the vanishing cosmological constant (3.69) requires non-vanishing gravitino mass.

Now, let us discuss the super-Higgs mechanism. We first write down the quadratic part of the fermion terms without derivative in the lagrangian (3.32) by using G defined in eq.(3.33);

$$\begin{aligned} \mathcal{L}_F^{(2)} = & -e^{G/2} \left(\psi_\mu \sigma^{\mu\nu} \psi_\nu + \bar{\psi}_\mu \bar{\sigma}^{\mu\nu} \bar{\psi}_\nu \right) \\ & + \frac{1}{2} g D^{(a)} \psi_\mu \sigma^\mu \bar{\chi}^{(a)} - \frac{1}{2} g D^{(a)} \bar{\psi}_\mu \bar{\sigma}^\mu \chi^{(a)} \\ & - e^{G/2} \left(\frac{i}{\sqrt{2}} G_i \chi^i \sigma^\mu \bar{\psi}_\mu + \frac{i}{\sqrt{2}} G_{i^*} \bar{\chi}^i \bar{\sigma}^\mu \psi_\mu \right) \\ & - e^{G/2} \left\{ \frac{1}{2} (G_{ij} + G_i G_j) \chi^i \chi^j + \frac{1}{2} (G_{i^* j^*} + G_{i^*} G_{j^*}) \bar{\chi}^i \bar{\chi}^j \right\} \\ & + \sqrt{2} g \left(-i D_i^{(a)} \chi^i \lambda^{(a)} + i D_{i^*}^{(a)} \bar{\chi}^i \bar{\lambda}^{(a)} \right). \end{aligned} \quad (3.70)$$

Notice that if $e^{K/2} D_i W$ or $D^{(a)}$ has a non-vanishing vacuum-expectation value, the gravitino field ψ_μ mixes with spin $\frac{1}{2}$ fermion χ or λ . These mixing terms can be eliminated by a shift of the gravitino field ψ_μ ;

$$\begin{aligned} \mathcal{L}_F^{(2)} = & -e^{G/2} \left(\psi_\mu + \frac{1}{3} \bar{\eta} \bar{\sigma}_\mu \right) \sigma^{\mu\nu} \left(\psi_\nu - \frac{1}{3} \sigma_\nu \bar{\eta} \right) \\ & - e^{G/2} \left(\frac{1}{2} G_{i^* j^*} + \frac{1}{6} G_{i^*} G_{j^*} \right) \bar{\chi}^i \bar{\chi}^j \\ & - \frac{1}{6} e^{-G/2} g^2 D^{(a)} D^{(b)} \bar{\chi}^i \bar{\chi}^j \end{aligned}$$

$$+i \left(\sqrt{2}gD_{i^*}^{(a)} - \frac{\sqrt{2}}{3}gG_{i^*}D^{(a)} \right) \bar{\chi}^i \bar{\lambda}^{(a)} + h.c. , \quad (3.71)$$

with

$$\bar{\eta} \equiv \frac{i}{\sqrt{2}}G_{i^*}\bar{\chi}^i + \frac{1}{2}e^{-G/2}gD^{(a)}\bar{\lambda}^{(a)}. \quad (3.72)$$

From the above lagrangian, we can read off the gravitino mass $m_{3/2}$ as¹

$$m_{3/2} = e^{G/2} \equiv |e^{K/2}W|. \quad (3.73)$$

On the other hand, masses of the spin $\frac{1}{2}$ fermions $(\chi^i, \lambda^{(a)})$ can be obtained from the following mass matrix

$$\begin{pmatrix} m_{ij}^{(1/2)} & m_{ib}^{(1/2)} \\ m_{ja}^{(1/2)} & m_{ab}^{(1/2)} \end{pmatrix}, \quad (3.74)$$

whose each components are given by

$$m_{ij}^{(1/2)} \equiv e^{G/2} \left(G_{ij} + \frac{1}{3}G_i G_j \right), \quad (3.75)$$

$$m_{ab}^{(1/2)} \equiv \frac{1}{3}e^{-G/2}g^2 D^{(a)} D^{(b)}, \quad (3.76)$$

$$m_{ia}^{(1/2)} \equiv i\sqrt{2} \left(-gD_i^{(a)} + \frac{1}{3}gG_i D^{(a)} \right). \quad (3.77)$$

One can easily check that the fermionic field η defined in eq.(3.72) is a massless eigenstate of the mass matrix (3.74) and hence it is a goldstino component. Therefore, the gravitino field ψ_μ absorbs the goldstino component η and acquires a non-vanishing mass $m_{3/2} = e^{G/2}$.

3.5 Super-trace formula in supergravity

Having seen the structure of the mass matrix of fermionic sector in the previous section, we will next investigate mass differences between bosonic and fermionic states. For this purpose, we use the super-trace of the mass-squared matrices

$$\text{Str}\mathbf{M}^2 \equiv \sum_{J=0}^{3/2} (-1)^J \text{tr}\mathbf{M}_J^2, \quad (3.78)$$

since it represents some information on the mass splitting of bosons and fermions.

First, let us consider trace of the scalar mass matrix. In deriving masses of scalar bosons (and other fields), we expand the scalar potential V at a stationary point in scalar field.

¹For simplicity, in the following arguments in this and the next sections, we omit the bracket $\langle \hat{\mathcal{O}} \rangle$ which represents the vacuum-expectation value of $\hat{\mathcal{O}}$.

From the supergravity lagrangian (3.32), scalar potential V is given by

$$V(\phi, \phi^*) = e^G (G_i G_{i^*} - 3) + \frac{1}{2} g^2 D^{(a)} D^{(a)}. \quad (3.79)$$

Stationary condition can be written as

$$\begin{aligned} 0 &= \frac{\partial V}{\partial \phi^j} \\ &= G_j e^G (G_i G_{i^*} - 3) + e^G (G_{ij} G_{i^*} + G_i G_{i^* j}) + g^2 D^{(a)} D_j^{(a)}. \end{aligned} \quad (3.80)$$

Multiplying this equation by G_{j^*} , and using the identity $D_j^{(a)} G_{j^*} = D^{(a)}$, one can obtain

$$e^G G_j G_{j^*} (G_i G_{i^*} - 3) + e^G (G_{ij} G_{i^*} G_{j^*} + G_i G_{i^*}) + g^2 D^{(a)} D^{(a)} = 0. \quad (3.81)$$

Furthermore, we demand the cosmological constant to vanish at the stationary point. The condition for vanishing cosmological constant has been derived in eq.(3.69), which becomes

$$e^G (G_i G_{i^*} - 3) + \frac{1}{2} g^2 D^{(a)} D^{(a)} = 0. \quad (3.82)$$

The mass-squared matrix for scalar fields can be obtained from the second derivative of the scalar potential V . Especially, its diagonal part is given by

$$\begin{aligned} \frac{\partial^2 V}{\partial \phi^j \partial \phi^{*k}} &= e^G \left\{ G_j G_{k^*} (G_i G_{i^*} - 3) + \delta_{jk^*} (G_i G_{i^*} - 3) + G_{ij} G_{i^* k^*} \right. \\ &\quad \left. + G_j (G_{k^*} + G_i G_{i^* k^*}) + G_{k^*} (G_{ij} G_{i^*} + G_j) + \delta_{jk^*} \right\} \\ &\quad + g^2 (D_j^{(a)} D_{k^*}^{(a)} + D^{(a)} D_{jk^*}^{(a)}). \end{aligned} \quad (3.83)$$

With the stationary condition (3.81) and the condition for vanishing cosmological constant (3.82), the trace of the scalar mass matrix \mathbf{M}_0^2 can be obtained as

$$\begin{aligned} \text{tr} \mathbf{M}_0^2 &= 2 \frac{\partial^2 V}{\partial \phi^j \partial \phi^{*j}} \\ &= (-n_\phi - 1) g^2 D^{(a)} D^{(a)} - \frac{1}{2} e^{-G} (g^2 D^{(a)} D^{(a)})^2 \\ &\quad + 2e^G (G_{ij} G_{i^* j^*} + n_\phi) + 2g^2 (D_i^{(a)} D_{i^*}^{(a)} + D^{(a)} D_{ii^*}^{(a)}), \end{aligned} \quad (3.84)$$

where $n_\phi \equiv \sum_i g_{ii^*}$ is the number of chiral multiplets.

Next, we will consider the mass matrix for vector bosons. Mass terms of vector bosons come from the covariant derivatives of scalar fields;

$$\frac{1}{2} m_A^{2(ab)} A_\mu^{(a)} A^{(b)\mu} = g^2 \phi^i T_{ij}^a T_{jk}^b \phi^k A_\mu^{(a)} A^{(b)\mu}. \quad (3.85)$$

From the above equation, one can easily read off the mass-squared matrix for vector bosons, and its trace is given by

$$\begin{aligned}\text{tr}\mathbf{M}_1^2 &= 3 \times 2g^2 \phi^{*i} T_{ij}^a T_{jk}^a \phi^k \\ &= 6g^2 D_i^{(a)} D_{i^*}^{(a)},\end{aligned}\tag{3.86}$$

where the Killing potential $D^{(a)}$ for the case of the minimal Kähler potential is given in eq.(3.57). Notice that the prefactor 3 in the right-hand side of eq.(3.86) corresponds to the number of polarization of a massive vector boson.

The mass matrix of fermionic sector has been derived in the previous section, and we can easily obtain the trace of it. Masses of spin $\frac{1}{2}$ fermions are obtained from the matrix (3.74), and the trace of the spin $\frac{1}{2}$ fermion mass-squared matrix is given by

$$\begin{aligned}\text{tr}\mathbf{M}_{1/2}^2 &= 2 \times \left(\sum_{ij} |m_{ij}^{(1/2)}|^2 + \sum_{ab} |m_{ab}^{(1/2)}|^2 + 2 \sum_{ia} |m_{ia}^{(1/2)}|^2 \right) \\ &= 2e^G (G_{ij} G_{i^*j^*} - 1) - 2g^2 D^{(a)} D^{(a)} \\ &\quad - \frac{1}{2} e^{-G} (g^2 D^{(a)} D^{(a)})^2 + 8g^2 D_i^{(a)} D_{i^*}^{(a)}.\end{aligned}\tag{3.87}$$

In supergravity, spin $\frac{3}{2}$ particle is only the gravitino, and the trace of its mass matrix is given by

$$\text{tr}\mathbf{M}_{3/2}^2 = 4e^G = 4m_{3/2}^2.\tag{3.88}$$

Combining eq.(3.84), eq.(3.86), eq.(3.87) and eq.(3.88), the super-trace of the mass-squared matrices are given by

$$\text{Str}\mathbf{M}^2 = 2(n_\phi - 1)m_{3/2}^2 - (n_\phi - 1)g^2 D^{(a)} D^{(a)} + 2g^2 D^{(a)} D_{ii^*}^{(a)}.\tag{3.89}$$

In SUSY models with $e^{K/2} D_i W \neq 0$ and $D^{(a)} = 0$ (*i.e.* if the SUSY is broken by the F -term condensation), the SUSY breaking is characterized by gravitino mass $m_{3/2}$, and scalar particles are expected to become heavier than their superparticles. This is phenomenologically favorable. In the next section, we will see an example for such models.

3.6 Model with Polonyi's superpotential

In constructing a phenomenologically acceptable model based on supergravity, we mostly consider a model which contains two sectors; a so-called hidden sector responsible for the spontaneous breaking of SUSY, and an observable sector which contains ordinary particles such as quarks, leptons, Higgses, gauge fields, and their superpartners. The strength of interactions between the hidden and the observable sectors are at the same order of gravitational

one, and hence these two sectors couple very weakly for each other. In this section, we will investigate a simple model for the hidden sector proposed by Polonyi [27]. As we will see below, this model is simple but very suggestive.

We first discuss the hidden sector. The simplest hidden sector, proposed by Polonyi, contains only one chiral multiplet (ϕ_P, χ_P) , which takes the following superpotential W_P ;

$$W_P = \mu^2 (\phi_P + \omega), \quad (3.90)$$

where μ and ω are the free parameters which we will determine by the phenomenological requirements. For the Kähler potential for the Polonyi field ϕ_P , we use the minimum one, *i.e.* $K = \phi_P^* \phi_P$. In this model, the order parameter of SUSY breaking is given by

$$F_P = \mu^2 \left\{ \frac{\phi_P^*}{M^2} (\phi_P + \omega) + 1 \right\} e^{\phi_P \phi_P^* / 2M^2}. \quad (3.91)$$

For the case $|\omega| < 2M$, solution to the equation $F_P = 0$ does not exist, and the SUSY is expected to be spontaneously broken. The scalar potential for the Polonyi field ϕ_P is obtained as

$$V(\phi_P) = \mu^4 \left\{ \left| \frac{1}{M^2} \phi_P^* (\phi_P + \omega) + 1 \right|^2 - \frac{3}{M^2} |\phi_P + \omega|^2 \right\} e^{\phi_P \phi_P^* / M^2}. \quad (3.92)$$

The minimum of this potential is given by the solution to the following equation;

$$\begin{aligned} 0 &= \frac{\partial V}{\partial \phi_P} \\ &= \frac{\mu^4}{M^2} \left[(\phi_P + \omega) \left\{ \frac{1}{M^2} \phi_P^* (\phi_P + \omega) + 1 \right\} \right. \\ &\quad \left. + \phi_P \left\{ \frac{1}{M^2} \phi_P (\phi_P^* + \omega) + 1 \right\} - 3(\phi_P^* + \omega) \right] e^{\phi_P \phi_P^* / M^2} \\ &\quad + \frac{\mu^4}{M^2} \left\{ \left| \frac{1}{M^2} \phi_P^* (\phi_P + \omega) + 1 \right|^2 - \frac{3}{M^2} |\phi_P + \omega|^2 \right\} \phi_P^* e^{\phi_P \phi_P^* / M^2}. \end{aligned} \quad (3.93)$$

Furthermore, since we are interested in field theories in flat space-time, we demand the cosmological constant to vanish at the potential minimum;

$$\langle V \rangle = \left\langle \mu^4 \left\{ \left| \frac{1}{M^2} \phi_P^* (\phi_P + \omega) + 1 \right|^2 - \frac{3}{M^2} |\phi_P + \omega|^2 \right\} e^{\phi_P \phi_P^* / M^2} \right\rangle = 0. \quad (3.94)$$

The parameter ω is chosen so that eq.(3.93) and eq.(3.94) have a solution simultaneously. Then ω is determined to be $\omega = \pm(2 - \sqrt{3})M$.² Hereafter, we use the branch $\omega = (2 - \sqrt{3})M$.

²In fact, even for $\omega = \pm(2 + \sqrt{3})M$, eq.(3.93) and eq.(3.94) have a solution simultaneously. In this case, however, the solution does not correspond to the absolute minimum of the potential V and the potential at the true minimum becomes negative. Therefore, we do not consider this case.

By solving eq.(3.93), vacuum-expectation value of the Polonyi field ϕ_P is given by

$$\langle \phi_P \rangle = (\sqrt{3} - 1) M, \quad (3.95)$$

and one can obtain the vacuum-expectation value of the superpotential W_P and the order parameter F_P ;

$$\langle W_P \rangle = \mu^2 M, \quad (3.96)$$

$$\langle F_P \rangle = \sqrt{3} e^{2-\sqrt{3}} \mu^2. \quad (3.97)$$

From the vacuum-expectation value of W_P , the gravitino acquires a non-vanishing mass

$$m_{3/2} = e^{2-\sqrt{3}} \frac{\mu^2}{M}. \quad (3.98)$$

Notice that for the given gravitino mass $m_{3/2}$, the scale of the condensation of F_P (which is the same order of μ^2) is determined; $\langle F_P \rangle \sim O(m_{3/2} M)$.

The mass eigenvalues $m_{\phi_{P1}}$ and $m_{\phi_{P2}}$ for the scalar fields are obtained by expanding Polonyi field ϕ_P around its vacuum-expectation value;

$$\phi_P = (\sqrt{3} - 1) M + \frac{1}{\sqrt{2}} (\phi_{P1} + i \phi_{P2}). \quad (3.99)$$

Substitute this to the potential (3.92), the masses are given by

$$m_{\phi_{P1}}^2 = 2\sqrt{3} m_{3/2}^2, \quad m_{\phi_{P2}}^2 = (4 - 2\sqrt{3}) m_{3/2}^2, \quad (3.100)$$

while the superpartner of ϕ_P is a goldstino and absorbed in the gravitino.

Now, let us consider the coupling between hidden and observable sectors. The hidden sector couples to the observable sector if we introduce a superpotential W_{obs} for the observable sector;

$$W = W_P + W_{\text{obs}}(\phi_{\text{obs}}), \quad (3.101)$$

where we denote the particles in the observable sector by ϕ_{obs} . Assuming the minimal Kähler potential for ϕ_{obs} , the scalar potential is given by

$$\begin{aligned} V(\phi_P, \phi_{\text{obs}}) &= \exp \left(\frac{|\phi_P|^2 + \sum_i |\phi_{\text{obs}}^i|^2}{M^2} \right) \\ &\times \left(\left| \frac{\phi_P^*}{M^2} W + \frac{\partial W_P}{\partial \phi_P} \right|^2 + \sum_i \left| \frac{\phi_{\text{obs}}^{i*}}{M^2} W + \frac{\partial W_{\text{obs}}}{\partial \phi_{\text{obs}}^i} \right|^2 - \frac{3}{M^2} |W|^2 \right). \end{aligned} \quad (3.102)$$

In the potential (3.102), all interactions between the hidden and the observable sectors are

suppressed by powers of M^{-1} .

In order to derive a low energy effective theory for the observable sector, we take a limit $M \rightarrow \infty$ with gravitino mass $m_{3/2} = \langle e^{K/2M^2} W/M^2 \rangle$ fixed. (This is sometimes called flat limit.) Then, one can obtain a potential for the observable sector;

$$V(\phi_{\text{obs}}) \simeq \sum_i \left| \frac{\partial \tilde{W}_{\text{obs}}}{\partial \phi_{\text{obs}}^i} \right|^2 + m_{3/2}^2 \sum_i |\phi_{\text{obs}}^i|^2 + m_{3/2} \left[\sum_i \phi_{\text{obs}}^i \frac{\partial \tilde{W}_{\text{obs}}}{\partial \phi_{\text{obs}}^i} + \{b^*(a+b) - 3\} \tilde{W}_{\text{obs}} + h.c. \right], \quad (3.103)$$

where

$$\tilde{W}_{\text{obs}} \equiv \langle e^{K/2M^2} \rangle W_{\text{obs}}, \quad (3.104)$$

$$a^* \equiv \left\langle \frac{(\partial W_P / \partial \phi_P) M}{W_P} \right\rangle = 1, \quad (3.105)$$

$$b \equiv \left\langle \frac{\phi_P}{M} \right\rangle = \sqrt{3} - 1. \quad (3.106)$$

The above potential is nothing but a potential for the softly broken (global) SUSY. The first term in eq.(3.106) is a scalar potential in a global supersymmetric model, while the rest can be regarded as soft SUSY breaking terms for scalar bosons. Especially, in this model all the scalars in the observable sector receive an universal SUSY breaking mass which is fixed by gravitino mass $m_{3/2}$.

In order to keep the masses of squarks and sleptons at $O(100\text{GeV} - 1\text{TeV})$ so that the hierarchy problem is solved, the gravitino mass $m_{3/2}$ is taken smaller than $O(1\text{TeV})$. From this phenomenological requirement, $\langle F_P \rangle$ is determined;

$$\langle F_P \rangle \sim (10^{11} - 10^{12})\text{GeV}, \quad (3.107)$$

provided $m_{3/2} \sim O(100\text{GeV} - 1\text{TeV})$.

Finally we will comment on gauge fermion mass. In a model with the minimal kinetic function for gauge multiplet; $f_{(ab)} = \delta_{(ab)}$, gauge fermion remains massless. To generate a non-vanishing gauge fermion mass term, we assume a non-minimal kinetic function; $(\partial f_{(ab)} / \partial \phi_P) \neq 0$. Then with a SUSY breaking in the hidden sector, gauge fermion acquires mass from the interaction in the total supergravity lagrangian (3.32);

$$\mathcal{L}_{\lambda\lambda} = \frac{1}{4} \left\langle F_P \frac{\partial f_{(ab)}}{\partial \phi_P} \right\rangle \lambda^{(a)} \lambda^{(b)} + h.c. \quad (3.108)$$

The simplest example for the non-minimal kinetic function is

$$f_{(ab)} = \delta_{(ab)} \left\{ 1 + \frac{\kappa}{M} (\phi_P - \langle \phi_P \rangle) \right\}, \quad (3.109)$$

where κ is a dimensionless coupling parameter. Then, the gauge fermion mass is given by $\kappa \langle F_P \rangle / 2M$, which is of the order of the gravitino mass $m_{3/2}$ for $\kappa \sim O(1)$.

3.7 Mass of a scalar field in the hidden sector

As we have seen in the previous section, masses of the Polonyi fields ϕ_{P1} and ϕ_{P2} are of the order of the gravitino mass $m_{3/2}$. In fact, this is not an accidental case, *i.e.* in supergravity there exists a scalar field with mass of order $m_{3/2}$ in a wide class of models with the following features.

- At the stationary point of the scalar potential V , cosmological the constant vanishes.
- SUSY is broken by a condensation of a F -term in the hidden sector. (In this case, the vacuum-expectation value of $\langle F \rangle$ is $O(m_{3/2}M)$ so that the cosmological constant vanishes.)
- Cut-off scale of the model is of the order of the gravitational scale M .

As we will see below, a scalar boson with mass of order $m_{3/2}$ exists in a model with these conditions.

The existence of such a scalar field can be seen by using only simple order estimations. Assuming the cosmological constant to vanish, the condensation of F -terms are constrained as³

$$\langle F^i \rangle \lesssim O(\langle e^{G/2M^2} W / M \rangle) \sim O(m_{3/2}M) \quad (\text{for all } i). \quad (3.110)$$

Combining this condition with the stability condition $\langle \partial V / \partial \phi \rangle = 0$, we get [28, 29]

$$\langle M e^{G/2M^2} G_{ij} F^j \rangle \lesssim O(m_{3/2}^2 M), \quad (3.111)$$

where we have used that the cut-off scale of the model is of order M , *i.e.* $\langle G_{ijk^*} \rangle \lesssim M^{-1}$.

The mass squared matrix of the scalar fields are given by the second derivative of the scalar potential V . Especially, the diagonal part is given by

$$\begin{aligned} \left\langle \frac{\partial^2 V}{\partial \phi^i \partial \phi^{j*}} \right\rangle &= \langle M e^{G/2M^2} G_{ik} \rangle \langle g^{kl*} \rangle \langle M e^{G/2M^2} G_{l^*j^*} \rangle \\ &\quad - \left(\langle M e^{G/2M^2} G_{ik} \rangle \langle g^{kl*} K_{l^*j^*m} \rangle \langle F^m \rangle + h.c. \right) \\ &\quad + O(m_{3/2}^2). \end{aligned} \quad (3.112)$$

³In order to obtain a correct normalization of kinetic terms, we take $\langle G_{ij^*} \rangle = \delta_{ij^*}$.

Denoting the chiral multiplet which breaks SUSY (ϕ^X, χ^X, F^X) , the vacuum expectation value of F^X is given by $\langle F^X \rangle \sim O(m_{3/2}M)$. Then, constraint (3.111) leads to

$$\left\langle Me^{G/2M^2} G_{Xi} \right\rangle \lesssim O(m_{3/2}), \quad (3.113)$$

and hence

$$\left\langle \frac{\partial^2 V}{\partial \phi^X \partial \phi^{X*}} \right\rangle \lesssim O(m_{3/2}^2). \quad (3.114)$$

From the above, we can conclude that the mass-squared matrix of scalar fields has a eigenvalue of order $m_{3/2}^2$ or less. We should note here that such a scalar field may cause serious cosmological difficulty [30] (so-called Polonyi problem) which will be discussed in Chapter 5.

Chapter 4

Feynman rules for the gravitino

In the previous chapter, we have seen that the gravitino, which is the gauge field associated with local SUSY invariance, plays a crucial role in supergravity. In order to see physics of the gravitino, we must discuss a field theory for it.

In supergravity, however, there exist non-renormalizable interactions which are suppressed by M^{-1} (or its higher power), and hence we cannot calculate loop effects by using the full supergravity lagrangian given in the previous chapter. Furthermore, because of these non-renormalizable interactions, the Born-unitarity breaks down at high energy scales of order M . Therefore, we regard the supergravity as a low energy effective theory which is appropriate for energy scales much below the gravitational one, and only consider tree level processes.

In this chapter, we derive Feynman rules for the massive gravitino field by using the supergravity lagrangian (3.32). For this purpose, we first solve the field equation for massive Rarita-Schwinger field, and then we discuss the quantization of the free gravitino field. Hereafter, we only consider the nature of the gravitino in (nearly) flat space-time, and hence we restrict the background metric in that of flat space-time $g_{\mu\nu} = \text{diag}(1, -1, -1, -1)$.

4.1 Four-component notation for fermions

For our following arguments, it is more convenient to use a four-component spinor for a fermionic field rather than two-component one used in the previous chapter. Therefore, we briefly introduce it before quantizing the gravitino field. (For our notations and conventions, see Appendix A).

The four-component spinors ψ (in chiral representation) can be constructed from two component spinors ξ and η ;

$$\psi \sim \begin{pmatrix} \xi_\alpha \\ \bar{\eta}^{\dot{\alpha}} \end{pmatrix}, \quad \bar{\psi} \sim (\eta^\alpha, \bar{\xi}_{\dot{\alpha}}). \quad (4.1)$$

Corresponding to this, γ -matrix consists of 2×2 matrices σ^μ and $\bar{\sigma}^\mu$;

$$\gamma^\mu = \begin{pmatrix} 0 & \bar{\sigma}^\mu \\ \sigma^\mu & 0 \end{pmatrix}. \quad (4.2)$$

In the above representation, we define four-component spinors for the gravitino, $\psi_\mu^{(M)}$, gaugino, $\lambda^{(M)}$, and chiral fermion, $\chi_R^{(D)}$;

$$\psi_\mu^{(M)} \equiv \begin{pmatrix} \psi_\mu \\ \bar{\psi}_\mu \end{pmatrix}, \quad \bar{\psi}_\mu^{(M)} \equiv (\psi_\mu, \bar{\psi}_\mu), \quad (4.3)$$

$$\lambda^{(M)} \equiv \begin{pmatrix} \lambda \\ \bar{\lambda} \end{pmatrix}, \quad \bar{\lambda}^{(M)} \equiv (\lambda, \bar{\lambda}), \quad (4.4)$$

$$\chi_R^{(D)} \equiv \begin{pmatrix} \chi \\ 0 \end{pmatrix}, \quad \bar{\chi}_L^{(D)} \equiv (0, \bar{\chi}). \quad (4.5)$$

Notice that $\psi_\mu^{(M)}$ and $\lambda^{(M)}$ satisfies the Majorana condition

$$\psi_\mu^{(M)} = \psi_\mu^{(M)C} \equiv C \bar{\psi}_\mu^{(M)T}, \quad \lambda^{(M)} = \lambda^{(M)C} \equiv C \bar{\lambda}^{(M)T}, \quad (4.6)$$

where C is the charge conjugation matrix (see Appendix A), while $\chi_R^{(D)}$ is chiral fermion with a definite chirality;

$$\frac{1}{2}(1 + \gamma_5) \chi_R^{(D)} = \chi_R^{(D)}, \quad \frac{1}{2}(1 - \gamma_5) \chi_R^{(D)} = 0, \quad (4.7)$$

where $\gamma_5 \equiv i\gamma^0\gamma^1\gamma^2\gamma^3$.

4.2 Wave function for massive gravitino

We will start by discussing the wave function for massive gravitino. The lagrangian for the free gravitino field is given in the full supergravity lagrangian (3.32). In the four-component notation, it can be written as

$$\mathcal{L}_{\text{MRS}} = -\frac{1}{2}\epsilon^{\mu\nu\rho\sigma}\bar{\psi}_\mu\gamma_5\gamma_\nu\partial_\rho\psi_\sigma - \frac{1}{4}m_{3/2}\bar{\psi}_\mu[\gamma^\mu, \gamma^\nu]\psi_\nu, \quad (4.8)$$

where we have dropped the index (M) for the gravitino field, for simplicity. (Hereafter, we use only the four-component notation otherwise mentioned, and drop indices (M) and (D) in order to avoid complications due to too many indices.) By using the Majorana condition for the gravitino field; $\psi_\mu = C\bar{\psi}_\mu^T$, the lagrangian (4.8) becomes

$$\mathcal{L}_{\text{MRS}} = \frac{1}{2}\epsilon^{\mu\nu\rho\sigma}\psi_\mu^T C^\dagger \gamma_5 \gamma_\nu \partial_\rho \psi_\sigma + \frac{1}{4}m_{3/2}\psi_\mu^T C^\dagger [\gamma^\mu, \gamma^\nu] \psi_\nu. \quad (4.9)$$

This lagrangian is our starting point.

Varying the above lagrangian for ψ_μ , we can obtain the field equation for the free gravitino field;

$$\begin{aligned} 0 &= \left\{ \left(\frac{\partial}{\partial \psi_\mu} \right) - \partial_\nu \left(\frac{\partial}{\partial (\partial_\nu \psi_\mu)} \right) \right\} \mathcal{L}_{\text{MRS}} \\ &= \epsilon^{\mu\nu\rho\sigma} C^\dagger \gamma_5 \gamma_\nu \partial_\rho \psi_\sigma + \frac{1}{2} m_{3/2} C^\dagger [\gamma^\mu, \gamma^\nu] \psi_\nu. \end{aligned} \quad (4.10)$$

From this, the following two equations are derived;

$$m_{3/2} (\not{\partial} \gamma^\nu \psi_\nu - \gamma^\nu \not{\partial} \psi_\nu) = 0, \quad (4.11)$$

$$2i (\partial_\lambda \gamma^\mu \psi_\mu - \not{\partial} \psi_\lambda) + m_{3/2} (\gamma_\lambda \gamma^\mu \psi_\mu + 2\psi_\lambda) = 0. \quad (4.12)$$

Notice that the former (latter) equation can be obtained by operating $\partial_\mu (\gamma_\lambda \gamma_\mu)$ on eq.(4.10). For a later convenience, we derive one more equation by multiplying eq.(4.12) by γ^λ ;

$$i (\not{\partial} \gamma^\mu \psi_\mu - \gamma^\lambda \not{\partial} \psi_\lambda) + 3m_{3/2} \gamma^\mu \psi_\mu = 0. \quad (4.13)$$

For the *massive* gravitino ($m_{3/2} \neq 0$), eq.(4.11) – eq.(4.13) yields the following simple equations;

$$\gamma^\mu \psi_\mu = 0, \quad (4.14)$$

$$\partial^\mu \psi_\mu = 0, \quad (4.15)$$

$$(i \not{\partial} - m_{3/2}) \psi_\mu = 0. \quad (4.16)$$

The solutions to the above equations can be constructed by using the wave function u for spin $\frac{1}{2}$ field and the polarization vector ϵ_μ for spin 1 field. In solving the field equations for the gravitino field ψ_μ , it is convenient to consider the wave function $\tilde{\psi}_\mu$ in the momentum space, $\psi_\mu \sim e^{-ipx} \tilde{\psi}_\mu$. Then, the solution to eq.(4.14) – eq.(4.16) is given by [31]

$$\tilde{\psi}_\mu(\mathbf{p}, \lambda) = \sum_{s, m} \left\langle \left(\frac{1}{2}, \frac{s}{2} \right) (1, m) \mid \left(\frac{3}{2}, \lambda \right) \right\rangle u(\mathbf{p}, s) \epsilon_\mu(\mathbf{p}, m), \quad (4.17)$$

where $\langle (\frac{1}{2}, \frac{s}{2}) (1, m) \mid (\frac{3}{2}, \lambda) \rangle$ is the Clebsch-Gordan coefficient, whose value is shown in Table 4.1.

The wave function for spin $\frac{1}{2}$ field $u(\mathbf{p}, s)$ is the solution to the ordinary Dirac equation (in momentum space) with a definite helicity ($s = \pm 1$);

$$(\not{p} - m_{3/2}) u(\mathbf{p}, s) = 0, \quad (4.18)$$

$$(\mathbf{n} \boldsymbol{\Sigma}) u(\mathbf{p}, s) = s u(\mathbf{p}, s), \quad (4.19)$$

where $\mathbf{n} \boldsymbol{\Sigma}$ is the helicity operator (see Appendix A). The explicit form of $u(\mathbf{p}, s)$ in the Dirac

	$m = -1$	$m = 0$	$m = +1$
$s = -1$	1	$\sqrt{2/3}$	$\sqrt{1/3}$
$s = +1$	$\sqrt{1/3}$	$\sqrt{2/3}$	1

Table 4.1: Clebsch-Gordan coefficients for the case $\lambda = \frac{s}{2} + m$; $\langle (\frac{1}{2}, \frac{s}{2})(1, m) | (\frac{3}{2}, \frac{s}{2} + m) \rangle$. Notice that the coefficient with $\lambda \neq \frac{s}{2} + m$ vanishes.

representation is given in Appendix A, and we take the following normalization condition on $u(\mathbf{p}, s)$;

$$\bar{u}(\mathbf{p}, s)u(\mathbf{p}, s') = 2m_{3/2}\delta_{ss'}. \quad (4.20)$$

For the momentum vector $p^\mu = (E, |\mathbf{p}| \sin \theta \cos \phi, |\mathbf{p}| \sin \theta \sin \phi, |\mathbf{p}| \cos \theta)$ of a massive particle ($p_\mu p^\mu = m_{3/2}^2 \neq 0$), the polarization vectors take the following forms;

$$\epsilon_\mu(\mathbf{p}, 1) = \frac{1}{\sqrt{2}}(0, \cos \theta \cos \phi - i \sin \phi, \cos \theta \sin \phi + i \cos \phi, -\sin \theta), \quad (4.21)$$

$$\epsilon_\mu(\mathbf{p}, 0) = \frac{1}{m_{3/2}}(|\mathbf{p}|, -E \sin \theta \cos \phi, -E \sin \theta \sin \phi, -E \cos \theta), \quad (4.22)$$

$$\epsilon_\mu(\mathbf{p}, -1) = \frac{-1}{\sqrt{2}}(0, \cos \theta \cos \phi + i \sin \phi, \cos \theta \sin \phi - i \cos \phi, -\sin \theta), \quad (4.23)$$

which are normalized as

$$\epsilon_\mu^*(\mathbf{p}, m)\epsilon^\mu(\mathbf{p}, m') = -\delta_{mm'}. \quad (4.24)$$

Notice that the polarization vectors (4.21) – (4.23) satisfy the following condition;

$$p^\mu \epsilon_\mu(\mathbf{p}, m) = p^\mu \epsilon_\mu^*(\mathbf{p}, m) = 0. \quad (4.25)$$

By using eq.(4.18), eq.(4.19) and eq.(4.25), one can easily check that $\tilde{\psi}_\mu$ defined in eq.(4.17) obeys the following equations;

$$\gamma^\mu \tilde{\psi}_\mu(\mathbf{p}, \lambda) = 0, \quad (4.26)$$

$$p^\mu \tilde{\psi}_\mu(\mathbf{p}, \lambda) = 0, \quad (4.27)$$

$$(\not{p} - m_{3/2}) \tilde{\psi}_\mu(\mathbf{p}, \lambda) = 0, \quad (4.28)$$

and hence the wave function in the coordinate space $\psi_\mu \sim e^{-ipx} \tilde{\psi}_\mu$ satisfies eq.(4.14) – eq.(4.16).

The explicit form of $\tilde{\psi}_\mu(\mathbf{p}, \lambda)$ depends on representations of the γ -matrix, and we do not write it down because it is complicated but almost useless. Instead of that, we give

some useful identities for $\tilde{\psi}_\mu(\mathbf{p}, \lambda)$, which hold irrespective of the representation of γ -matrix. Normalization of $\tilde{\psi}_\mu(\mathbf{p}, \lambda)$ is fixed by eq.(4.20) and eq.(4.24);

$$\bar{\tilde{\psi}}_\mu(\mathbf{p}, \lambda) \tilde{\psi}^\mu(\mathbf{p}, \lambda') = -2m_{3/2} \delta_{\lambda\lambda'}. \quad (4.29)$$

Furthermore, one can obtain the following identity which will be useful in deriving the momentum operator given in eq.(4.54) for the gravitino field;

$$\bar{\tilde{\psi}}_\mu(\mathbf{p}, \lambda) \gamma_\nu \tilde{\psi}^\mu(\mathbf{p}, \lambda') = -2p_\nu \delta_{\lambda\lambda'}. \quad (4.30)$$

For the helicity sum of the gravitino field, the following formula exists;

$$\begin{aligned} P_{\mu\nu}(\mathbf{p}) &\equiv \sum_\lambda \tilde{\psi}_\nu(\mathbf{p}, \lambda) \bar{\tilde{\psi}}_\mu(\mathbf{p}, \lambda) \\ &= -(\not{p} - m_{3/2}) \\ &\quad \times \left\{ \left(g_{\mu\nu} - \frac{p_\mu p_\nu}{m_{3/2}^2} \right) - \frac{1}{3} \left(g_{\mu\sigma} - \frac{p_\mu p_\sigma}{m_{3/2}^2} \right) \left(g_{\nu\lambda} - \frac{p_\nu p_\lambda}{m_{3/2}^2} \right) \gamma^\sigma \gamma^\lambda \right\}. \end{aligned} \quad (4.31)$$

$P_{\mu\nu}(\mathbf{p})$ obeys the following equations which correspond to eq.(4.26) – eq.(4.28);

$$\gamma^\mu P_{\mu\nu}(\mathbf{p}) = P_{\mu\nu}(\mathbf{p}) \gamma^\nu = 0, \quad (4.32)$$

$$p^\mu P_{\mu\nu}(\mathbf{p}) = P_{\mu\nu}(\mathbf{p}) p^\nu = 0, \quad (4.33)$$

$$(\not{p} - m_{3/2}) P_{\mu\nu}(\mathbf{p}) = P_{\mu\nu}(\mathbf{p}) (\not{p} - m_{3/2}) = 0. \quad (4.34)$$

General solution to eq.(4.14) – eq.(4.16) can be expanded by the mode function given in eq.(4.17) and its charge conjugation;

$$\psi_\mu(x) = \int \frac{d^3\mathbf{p}}{(2\pi)^3 2p_0} \sum_\lambda \left\{ e^{i\mathbf{p}\mathbf{x}} \tilde{\psi}_\mu(\mathbf{p}, \lambda) a_{\mathbf{p}\lambda}(t) + e^{-i\mathbf{p}\mathbf{x}} \tilde{\psi}_\mu^C(\mathbf{p}, \lambda) a_{\mathbf{p}\lambda}^\dagger(t) \right\}, \quad (4.35)$$

where $p_0 \equiv \sqrt{|\mathbf{p}|^2 + m_{3/2}^2}$, and $a_{\mathbf{p}\lambda}(t)$ is the expansion coefficient whose time dependence is determined by the field equation (4.16); $a_{\mathbf{p}\lambda}(t) \sim e^{-ip_0 t}$. Notice that because of the Majorana nature of the gravitino field ψ_μ , the coefficient of the $\tilde{\psi}_\mu^C(\mathbf{p}, \lambda)$ -term in eq.(4.35) is not an independent variable, but it is to be $a_{\mathbf{p}\lambda}^\dagger(t)$. One can easily check that the gravitino field ψ_μ in eq.(4.35) satisfies the Majorana condition; $\psi_\mu = \psi_\mu^C$.

4.3 Quantization of free massive gravitino field

In order to obtain Feynman rules for the gravitino, we have to quantize first the free gravitino field. In this section, we discuss the canonical quantization of the free gravitino field. Since in this thesis, we only consider spontaneously broken local SUSY models in

which the gravitino acquires a non-vanishing mass term, we only deal with the case of the massive gravitino.

Constraints on the physical mode of the gravitino field are obtained in the previous section, and they are given in eq.(4.14) and (4.15). The mode expansion of the physical degrees of freedom is given in eq.(4.35), and as in the usual quantization procedure, we regard the coefficients $a_{\mathbf{p}\lambda}(t)$'s and $a_{\mathbf{p}\lambda}^\dagger(t)$'s as dynamical variables and derive commutation relations among them.

As a first step in the quantization procedure, we derive canonical momenta. Time derivatives of $a_{\mathbf{p}\lambda}(t)$ and $a_{\mathbf{p}\lambda}^\dagger(t)$, which we denote $\dot{a}_{\mathbf{p}\lambda}(t)$ and $\dot{a}_{\mathbf{p}\lambda}^\dagger(t)$, are present in the lagrangian as

$$\begin{aligned} L_{\text{MRS}} &\equiv \int d^3\mathbf{x} \mathcal{L}_{\text{MRS}} \\ &= \frac{1}{2}i \int \frac{d^3\mathbf{p}}{(2\pi)^3 2p_0} \sum_{\lambda} \left\{ a_{\mathbf{p}\lambda}^\dagger(t) \dot{a}_{\mathbf{p}\lambda}(t) + a_{\mathbf{p}\lambda}(t) \dot{a}_{\mathbf{p}\lambda}^\dagger(t) \right\} \\ &\quad + (\text{terms without } \dot{a}_{\mathbf{p}\lambda}, \dot{a}_{\mathbf{p}\lambda}^\dagger). \end{aligned} \quad (4.36)$$

Differentiating lagrangian (4.36) with respect to $\dot{a}_{\mathbf{p}\lambda}(t)$ or $\dot{a}_{\mathbf{p}\lambda}^\dagger(t)$, one can obtain canonical momenta $\Pi_{\mathbf{p}\lambda}$ and $\bar{\Pi}_{\mathbf{p}\lambda}$;

$$\Pi_{\mathbf{p}\lambda} \equiv \frac{\delta L_{\text{MRS}}}{\delta \dot{a}_{\mathbf{p}\lambda}} = i \frac{1}{2} \frac{1}{(2\pi)^3 2p_0} a_{\mathbf{p}\lambda}^\dagger(t), \quad (4.37)$$

$$\bar{\Pi}_{\mathbf{p}\lambda} \equiv \frac{\delta L_{\text{MRS}}}{\delta \dot{a}_{\mathbf{p}\lambda}^\dagger} = i \frac{1}{2} \frac{1}{(2\pi)^3 2p_0} a_{\mathbf{p}\lambda}(t). \quad (4.38)$$

Since $\dot{a}_{\mathbf{p}\lambda}(t)$ and $\dot{a}_{\mathbf{p}\lambda}^\dagger(t)$ cannot be expressed as functions of canonical momenta, eq.(4.37) and eq.(4.38) are regarded as primary constraints on this system;

$$\Phi_{\mathbf{p}\lambda} \equiv \Pi_{\mathbf{p}\lambda} - i \frac{1}{2} \frac{1}{(2\pi)^3 2p_0} a_{\mathbf{p}\lambda}^\dagger(t) = 0, \quad (4.39)$$

$$\bar{\Phi}_{\mathbf{p}\lambda} \equiv \bar{\Pi}_{\mathbf{p}\lambda} - i \frac{1}{2} \frac{1}{(2\pi)^3 2p_0} a_{\mathbf{p}\lambda}(t) = 0. \quad (4.40)$$

For this system, Poisson bracket $\{\cdots\}_{\text{P}}$ is defined as in the usual case;

$$\begin{aligned} \{F, G\}_{\text{P}} &\equiv \int d^3\mathbf{p} \sum_{\lambda} \left\{ \left(\frac{\delta F}{\delta a_{\mathbf{p}\lambda}} \right)_{\text{R}} \left(\frac{\delta G}{\delta \Pi_{\mathbf{p}\lambda}} \right)_{\text{L}} + \left(\frac{\delta F}{\delta a_{\mathbf{p}\lambda}^\dagger} \right)_{\text{R}} \left(\frac{\delta G}{\delta \bar{\Pi}_{\mathbf{p}\lambda}} \right)_{\text{L}} \right\} \\ &\quad + \int d^3\mathbf{p} \sum_{\lambda} \left\{ \left(\frac{\delta G}{\delta a_{\mathbf{p}\lambda}} \right)_{\text{R}} \left(\frac{\delta F}{\delta \Pi_{\mathbf{p}\lambda}} \right)_{\text{L}} + \left(\frac{\delta G}{\delta a_{\mathbf{p}\lambda}^\dagger} \right)_{\text{R}} \left(\frac{\delta F}{\delta \bar{\Pi}_{\mathbf{p}\lambda}} \right)_{\text{L}} \right\}, \end{aligned} \quad (4.41)$$

where the index L (R) represents left (right) derivative. Especially for the dynamical vari-

ables $a_{\mathbf{p}\lambda}(t)$, $a_{\mathbf{p}\lambda}^\dagger(t)$ and the canonical momenta $\Pi_{\mathbf{p}\lambda}$, $\bar{\Pi}_{\mathbf{p}\lambda}$, Poisson brackets are given as

$$\{a_{\mathbf{p}\lambda}(t), \Pi_{\mathbf{p}'\lambda'}\}_{\mathbf{p}} = \delta_{\lambda\lambda'}\delta(\mathbf{p} - \mathbf{p}'), \quad (4.42)$$

$$\{a_{\mathbf{p}\lambda}^\dagger(t), \bar{\Pi}_{\mathbf{p}'\lambda'}\}_{\mathbf{p}} = \delta_{\lambda\lambda'}\delta(\mathbf{p} - \mathbf{p}'), \quad (4.43)$$

and those for constraints $\Phi_{\mathbf{p}\lambda}$ and $\bar{\Phi}_{\mathbf{p}\lambda}$ can be obtained as

$$\begin{aligned} C(\mathbf{p}, \lambda; \mathbf{p}', \lambda') &\equiv \begin{pmatrix} \left\{ \Phi_{\mathbf{p}\lambda}, \Phi_{\mathbf{p}'\lambda'} \right\}_{\mathbf{p}} & \left\{ \Phi_{\mathbf{p}\lambda}, \bar{\Phi}_{\mathbf{p}'\lambda'} \right\}_{\mathbf{p}} \\ \left\{ \bar{\Phi}_{\mathbf{p}\lambda}, \Phi_{\mathbf{p}'\lambda'} \right\}_{\mathbf{p}} & \left\{ \bar{\Phi}_{\mathbf{p}\lambda}, \bar{\Phi}_{\mathbf{p}'\lambda'} \right\}_{\mathbf{p}} \end{pmatrix} \\ &= \frac{i}{(2\pi)^3 2p_0} \begin{pmatrix} 0 & \delta_{\lambda\lambda'}\delta(\mathbf{p} - \mathbf{p}') \\ \delta_{\lambda\lambda'}\delta(\mathbf{p} - \mathbf{p}') & 0 \end{pmatrix}. \end{aligned} \quad (4.44)$$

Notice that the above matrix $C(\mathbf{p}, \lambda; \mathbf{p}', \lambda')$ has its inverse, and hence time evolutions of the primary constraints (4.39) and (4.40) do not induce secondary ones.

In order to quantize this constrained system, we introduce Dirac bracket $\{\cdot\cdot\}_{\mathbf{D}}$;

$$\begin{aligned} \{F, G\}_{\mathbf{D}} &\equiv \{F, G\}_{\mathbf{p}} - \int d^3\mathbf{p} d^3\mathbf{p}' \sum_{\lambda\lambda'} \left\{ F, \tilde{\Phi}_{\mathbf{p}\lambda} \right\}_{\mathbf{p}} C^{-1}(\mathbf{p}, \lambda; \mathbf{p}', \lambda') \left\{ \tilde{\Phi}_{\mathbf{p}'\lambda'}, G \right\}_{\mathbf{p}'} \\ &= \{F, G\}_{\mathbf{p}} + (2\pi)^3 i \int d^3\mathbf{p} \sum_{\lambda} 2p_0 \{F, \Phi_{\mathbf{p}\lambda}\}_{\mathbf{p}} \{\bar{\Phi}_{\mathbf{p}\lambda}, G\}_{\mathbf{p}} \\ &\quad + (2\pi)^3 i \int d^3\mathbf{p} \sum_{\lambda} 2p_0 \{F, \bar{\Phi}_{\mathbf{p}\lambda}\}_{\mathbf{p}} \{\Phi_{\mathbf{p}\lambda}, G\}_{\mathbf{p}}, \end{aligned} \quad (4.45)$$

where $\tilde{\Phi}_{\mathbf{p}\lambda}$ represents both $\Phi_{\mathbf{p}\lambda}$ and $\bar{\Phi}_{\mathbf{p}\lambda}$, and F and G arbitrary variables. Then, this system is quantized by replacing the Dirac bracket by (anti-)commutator;

$$i\{F, G\}_{\mathbf{D}} \rightarrow [F, G] \equiv FG - (-1)^{|F||G|}GF, \quad (4.46)$$

where $|F| = 1$ if F is Grassmann-odd and $|F| = 0$ if F is Grassmann-even. Especially, commutation-relations among $a_{\mathbf{p}\lambda}(t)$ and $a_{\mathbf{p}\lambda}^\dagger(t)$ are obtained as

$$\{a_{\mathbf{p}\lambda}(t), a_{\mathbf{p}'\lambda'}^\dagger(t)\} = (2\pi)^3 2p_0 \delta_{\lambda\lambda'} \delta(\mathbf{p} - \mathbf{p}'), \quad (4.47)$$

$$\{a_{\mathbf{p}\lambda}(t), a_{\mathbf{p}'\lambda'}(t)\} = \{a_{\mathbf{p}\lambda}^\dagger(t), a_{\mathbf{p}'\lambda'}^\dagger(t)\} = 0. \quad (4.48)$$

As in the ordinary procedure, we can get a hamiltonian for this system;

$$\begin{aligned} H &= \int d^3\mathbf{p} \sum_{\lambda} \left(\Pi_{\mathbf{p}\lambda} a_{\mathbf{p}\lambda} + \bar{\Pi}_{\mathbf{p}\lambda} a_{\mathbf{p}\lambda}^\dagger \right) - \int d^3\mathbf{x} \mathcal{L}_{\text{MRS}} \\ &= \int d^3\mathbf{x} \left(\frac{i}{2} \bar{\psi}_\mu \gamma^i \partial_i \psi^\mu - \frac{1}{2} m_{3/2} \bar{\psi}_\mu \psi^\mu \right) \\ &= \int \frac{d^3\mathbf{p}}{(2\pi)^3 2p_0} \sum_{\lambda} p_0 a_{\mathbf{p}\lambda}^\dagger(t) a_{\mathbf{p}\lambda}(t). \end{aligned} \quad (4.49)$$

By using this hamiltonian, equations of motion for $a_{\mathbf{p}\lambda}(t)$ and $a_{\mathbf{p}\lambda}^\dagger(t)$ are derived;

$$i\frac{d}{dt}a_{\mathbf{p}\lambda}(t) = [a_{\mathbf{p}\lambda}(t), H] = p_0 a_{\mathbf{p}\lambda}(t), \quad (4.50)$$

$$i\frac{d}{dt}a_{\mathbf{p}\lambda}^\dagger(t) = [a_{\mathbf{p}\lambda}^\dagger(t), H] = -p_0 a_{\mathbf{p}\lambda}^\dagger(t), \quad (4.51)$$

and these equations can be easily solved;

$$a_{\mathbf{p}\lambda}(t) = a_{\mathbf{p}\lambda} e^{-ip_0 t}, \quad a_{\mathbf{p}\lambda}^\dagger(t) = a_{\mathbf{p}\lambda}^\dagger e^{ip_0 t}, \quad (4.52)$$

where we denote $a_{\mathbf{p}\lambda}(t=0)$ and $a_{\mathbf{p}\lambda}^\dagger(t=0)$ as $a_{\mathbf{p}\lambda}$ and $a_{\mathbf{p}\lambda}^\dagger$.

Then, by using $a_{\mathbf{p}\lambda}$ and $a_{\mathbf{p}\lambda}^\dagger$, the field operator ψ_μ can be expanded as

$$\psi_\mu = \int \frac{d^3\mathbf{p}}{(2\pi)^3 2p_0} \sum_\lambda \left\{ e^{-ipx} \tilde{\psi}_\mu(\mathbf{p}, \lambda) a_{\mathbf{p}\lambda} + e^{ipx} \tilde{\psi}_\mu^C(\mathbf{p}, \lambda) a_{\mathbf{p}\lambda}^\dagger \right\}. \quad (4.53)$$

Furthermore, the momentum operator P_μ for the gravitino field is given by

$$P_\mu = \int \frac{d^3\mathbf{p}}{(2\pi)^3 2p_0} \sum_\lambda p_\mu a_{\mathbf{p}\lambda}^\dagger a_{\mathbf{p}\lambda}. \quad (4.54)$$

Fock space for the gravitino field is constructed by operating the creation operator $a_{\mathbf{p}\lambda}^\dagger$ on vacuum state $|0\rangle$ which satisfies the condition $a_{\mathbf{p}\lambda}|0\rangle = 0$. Especially, one particle state of the gravitino with momentum p and helicity λ is defined as

$$|p, \lambda\rangle \equiv a_{\mathbf{p}\lambda}^\dagger |0\rangle. \quad (4.55)$$

As one can see, this state satisfies the following relations;

$$\langle p, \lambda | p', \lambda' \rangle = (2\pi)^3 2p_0 \delta_{\lambda\lambda'} \delta(\mathbf{p} - \mathbf{p}'), \quad (4.56)$$

$$P_\mu |p, \lambda\rangle = p_\mu |p, \lambda\rangle, \quad (4.57)$$

where P_μ is the momentum operator defined in eq.(4.54). Notice that the normalization condition (4.56) on the one particle state (4.55) is Lorentz invariant since $p_0 \delta(\mathbf{p} - \mathbf{p}')$ is a Lorentz invariant variable.

From the above arguments, we obtain Feynman rules for the external gravitinos; for the gravitino with momentum p and helicity λ in initial the state, we should assign $\tilde{\psi}_\mu(\mathbf{p}, \lambda)$ or $\tilde{\psi}_\mu^C(\mathbf{p}, \lambda)$, and that in the final state, $\tilde{\psi}_\mu(\mathbf{p}, \lambda)$ or $\tilde{\psi}_\mu^C(\mathbf{p}, \lambda)$.

4.4 Interactions of the gravitino

In the previous section, we have quantized the massive free gravitino field, and obtained Feynman rules for the gravitino in external line. Our next purpose is to discuss the Feynman rules for the interactions of the gravitino field. Many interaction terms concerning the gravitino field ψ_μ exist in the full supergravity lagrangian (3.32), but most of them are irrelevant for our present purpose. This fact arises from the following two reasons.

- Since we are considering the processes with the energy scale much below the gravitational one; $\sqrt{s} \ll M$, contributions of the Feynman diagrams with higher dimensional operators are suppressed by factor $\sim \sqrt{s}/M \ll 1$ (or its higher power). As we will see later, the dimension of relevant operators is always five, and interaction terms with the dimension higher than six are not important for us.
- In our analysis in Chapter 6 and Chapter 7, gravitinos only appear at external lines in the Feynman diagram. Then, interaction terms which contain $\gamma^\mu \psi_\mu$ or $\bar{\psi}_\mu \gamma^\mu$ are not necessary since they vanish due to eq.(4.26).

In the following arguments, we take only the relevant interaction terms into account and ignore contributions from other terms.

The most important interaction terms come from the coupling between the gravitino field and the supercurrent, which is given in eq.(3.65). In the four-component notation (and in the flat space-time), these terms are written as

$$\begin{aligned} \mathcal{L}_{\psi J} = & -\frac{1}{\sqrt{2}M} \tilde{\mathcal{D}}_\nu \phi^{*i} \bar{\psi}_\mu \gamma^\nu \gamma^\mu \chi_R^i - \frac{1}{\sqrt{2}M} \tilde{\mathcal{D}}_\nu \phi^i \bar{\chi}_L^i \gamma^\mu \gamma^\nu \psi_\mu \\ & - \frac{i}{8M} \bar{\psi}_\mu [\gamma^\nu, \gamma^\rho] \gamma^\mu \lambda^{(a)} F_{\nu\rho}^{(a)}. \end{aligned} \quad (4.58)$$

From this, we construct Feynman rules for the interaction of the gravitino field ψ_μ with matter fields ϕ , χ , A_μ and λ . In Fig. 4.1, we show the Feynman rules derived from the lagrangian (4.58). In the following analysis, we use these rules and ignore other higher dimensional interactions.

As a simple example of applications of these Feynman rules, we calculate the decay rates of the gravitino. The dominant decay modes of the gravitino are $\psi_\mu \rightarrow \lambda + A_\mu$ and $\psi_\mu \rightarrow \phi^i + \bar{\chi}^i$ (and $\psi_\mu \rightarrow \phi^{i*} + \chi^i$) if these processes are kinematically allowed. Feynman diagrams for these processes are shown in Fig. 4.2.

For the process $\psi_\mu \rightarrow \lambda + A_\mu$, the invariant amplitude can be obtained as

$$\mathcal{M}(\psi_\mu \rightarrow \lambda + A_\nu) = \frac{i}{M} q_\rho \epsilon_{\nu} \bar{\lambda} (g^{\mu\rho} \gamma^\nu - g^{\mu\nu} \gamma^\rho) \tilde{\psi}_\mu. \quad (4.59)$$

By using the mode sum for $\tilde{\psi}_\mu$ given in eq.(4.31), eq.(4.59) becomes

$$\begin{aligned} \overline{|\mathcal{M}(\psi_\mu \rightarrow \lambda + A_\nu)|^2} &\equiv \frac{1}{4} \sum_{\lambda sm} |\mathcal{M}(\psi_\mu \rightarrow \lambda + A_\nu)|^2 \\ &= \frac{m_{3/2}^4}{2M^2} \left\{ 1 - \left(\frac{m_\lambda}{m_{3/2}} \right)^2 \right\} \left\{ 1 + \frac{1}{3} \left(\frac{m_\lambda}{m_{3/2}} \right)^2 \right\}, \end{aligned} \quad (4.60)$$

where m_λ is the gauge fermion mass, and we have assumed that the gauge field A_μ is massless. Notice that in deriving eq.(4.60), we have taken an average of the helicity of initial gravitino. By using eq.(4.60), the decay rate is given by

$$\begin{aligned} \Gamma(\psi_\mu \rightarrow \lambda + A_\nu) &= \frac{|\mathbf{p}_f|}{32\pi^2} \int d\Omega \overline{|\mathcal{M}|^2} \\ &= \frac{1}{32\pi} \frac{m_{3/2}^3}{M^2} \left\{ 1 - \left(\frac{m_\lambda}{m_{3/2}} \right)^2 \right\}^3 \left\{ 1 + \frac{1}{3} \left(\frac{m_\lambda}{m_{3/2}} \right)^2 \right\}, \end{aligned} \quad (4.61)$$

where \mathbf{p}_f is the three momentum of the particle in final state. Notice that if the gauge group G is non-abelian, the above decay rate should be multiplied by the rank of G in order to calculate a total decay rate. Especially in the case $m_{3/2} \gg m_\lambda$, the gravitino lifetime $\tau_{3/2}$ is approximately given by

$$\tau_{3/2}(\psi_\mu \rightarrow \lambda + A_\mu) \simeq 4.0 \times 10^8 \times \left(\frac{m_{3/2}}{100\text{GeV}} \right)^{-3} \text{ sec.} \quad (4.62)$$

For the process $\psi_\mu \rightarrow \phi^i + \bar{\chi}^i$, the invariant amplitude is given by

$$\mathcal{M}(\psi_\mu \rightarrow \phi^i + \bar{\chi}^i) = \frac{1}{2\sqrt{2}M} \bar{\chi} \gamma^\mu \not{A}' (1 + \gamma_5) \tilde{\psi}_\mu, \quad (4.63)$$

and by using a similar method to in the previous case, the decay rate is obtained as

$$\Gamma(\psi_\mu \rightarrow \phi^i + \bar{\chi}^i) = \frac{1}{384\pi} \frac{m_{3/2}^3}{M^2} \left\{ 1 - \left(\frac{m_\phi}{m_{3/2}} \right)^2 \right\}^4, \quad (4.64)$$

where m_ϕ is the mass of ϕ field, and we have assumed that χ is a massless fermion. Notice that the decay rate for the process $\psi_\mu \rightarrow \phi^{i*} + \chi^i$ is equal to the one given in eq.(4.64).

Another application is to calculate the gravitino production cross sections. As one can easily see, the most important processes are those of one gravitino production since the vertices having a gravitino are suppressed by M^{-1} (or its higher power). Amplitudes for the gravitino production processes are obtained by combining the Feynman rules given in Fig. 4.1 with those derived from the ordinary (global) SUSY lagrangian. We have calculated the total cross section for the dominant processes of helicity $\pm \frac{3}{2}$ gravitino production, and the results are shown in Table 4.2.

Process	$\sigma = (g^2/64\pi M^2) \times$
(A) $A^a + A^b \rightarrow \psi + \lambda^{(c)}$	$(8/3) f^{abc} ^2$
(B) $A^a + \lambda^{(b)} \rightarrow \psi + A^c$	$4 f^{abc} ^2 \{-(3/2) + 2 \ln(2/\delta) + \delta - (1/8)\delta^2\}$
(C) $A^a + \phi_i \rightarrow \psi + \chi_j$	$4 T_{ji}^a ^2$
(D) $A^a + \chi_i \rightarrow \psi + \phi_j$	$2 T_{ji}^a ^2$
(E) $\chi_i + \phi_j^* \rightarrow \psi + A^a$	$4 T_{ji}^a ^2$
(F) $\lambda^{(a)} + \lambda^{(b)} \rightarrow \psi + \lambda^{(c)}$	$ f^{abc} ^2 \{-(62/3) + 16 \ln[(2-\delta)/\delta] + 22\delta - 2\delta^2 + (2/3)\delta^3\}$
(G) $\lambda^{(a)} + \chi_i \rightarrow \psi + \chi_j$	$4 T_{ji}^a ^2 \{-2 + 2 \ln(2/\delta) + \delta\}$
(H) $\lambda^{(a)} + \phi_i \rightarrow \psi + \phi_j$	$ T_{ji}^a ^2 \{-6 + 8 \ln(2/\delta) + 4\delta - (1/2)\delta^2\}$
(I) $\chi_i + \bar{\chi}_j \rightarrow \psi + \lambda^{(a)}$	$(8/3) T_{ji}^a ^2$
(J) $\phi_i + \phi_j^* \rightarrow \psi + \lambda^{(a)}$	$(16/3) T_{ji}^a ^2$

Table 4.2: Total cross sections for the helicity $\pm \frac{3}{2}$ gravitino production processes. Spins of the initial states are averaged and those of the final states are summed. f^{abc} and T_{ij}^a represent the structure constants and the generators of the gauge groups, respectively. Notice that for the processes (B), (F), (G) and (H), we cut off the infrared singularities due to the t -, u -channel exchanges of gauge bosons, taking a small but a positive parameter $\delta = (1 \pm \cos \theta)_{min}$ where θ is the scattering angle in the center-of-mass frame.

4.5 Effective lagrangian for light gravitino

In spontaneously broken SUSY models, the massless gravitino field ψ_μ acquires mass by absorbing goldstino modes. Before becoming massive, the gravitino only possesses helicity $\pm \frac{3}{2}$ modes, and the goldstino provides helicity $\pm \frac{1}{2}$ modes of the massive gravitino field. This fact suggests that the helicity $\pm \frac{1}{2}$ mode of the gravitino field behaves like a goldstino. In fact, if the gravitino mass $m_{3/2}$ is much smaller than the mass differences between bosons and fermions in the chiral and gauge multiplets, the above argument is valid and we can obtain an effective lagrangian for the relativistic gravitino field of helicity $\pm \frac{1}{2}$ components. In this section, we will derive the effective lagrangian for the light gravitino field [32] and apply it for calculating some processes.

For the case $\sqrt{s} \gg m_{3/2}$, the wave function of the gravitino of helicity $\pm \frac{1}{2}$ components is approximately proportional to $p_\mu/m_{3/2}$ where p_μ is a momentum of the gravitino. In this case, the helicity $\pm \frac{1}{2}$ component of the gravitino field can be written as

$$\psi_\mu \sim i \sqrt{\frac{2}{3}} \frac{1}{m_{3/2}} \partial_\mu \psi, \quad (4.65)$$

where ψ represents the spin $\frac{1}{2}$ fermionic field which can be interpreted as the goldstino.

Substituting eq.(4.65) into the gravitino interaction lagrangian (4.58), we obtain the effective interaction lagrangian for the goldstino components ψ .

Using the replacement (4.65), the gravitino interaction lagrangian (4.58) becomes

$$\begin{aligned}\mathcal{L}_{\text{eff}} = & \left[\frac{i}{\sqrt{3}Mm_{3/2}} \left\{ (\bar{\psi}\chi_R^i) \partial_\mu \partial^\mu \phi^{i*} - (\bar{\psi} \partial_\mu \partial^\mu \chi_R^i) \phi^{i*} \right\} + h.c. \right] \\ & + \frac{1}{4\sqrt{6}Mm_{3/2}} \bar{\psi} [\gamma^\mu, \gamma^\nu] \gamma^\rho \partial_\rho \lambda^{(a)} F_{\mu\nu}^{(a)} \\ & + (\text{total derivative}),\end{aligned}\tag{4.66}$$

where we have used the relation $\not{\partial}\psi_\mu = 0$ since we are considering processes with a light gravitino in the external line.

The terms in the right-hand side of eq.(4.66) are dimension six operators and one would expect that the processes involving helicity $\pm\frac{1}{2}$ gravitinos have bad high energy behaviors. In supergravity, however, this is not the case since the leading high energy behavior cancels out in the total amplitude. For example, for the helicity $\pm\frac{1}{2}$ gravitino production process $\phi^i + \phi^{*j} \rightarrow \psi_\mu^{(1/2)} + \lambda^{(a)}$, there are s -, t - and u -channel diagrams (see Fig. 4.3), whose leading terms are given by

$$\mathcal{M}_s \simeq i\sqrt{\frac{2}{3}} \frac{g}{m_{3/2}M} (T^a)_{ji} \bar{\psi} \not{p}' \lambda^C, \tag{4.67}$$

$$\mathcal{M}_t \simeq -i\frac{1}{2}\sqrt{\frac{2}{3}} \frac{g}{m_{3/2}M} (T^a)_{ji} \bar{\psi} \not{p}' (1 - \gamma_5) \lambda^C, \tag{4.68}$$

$$\mathcal{M}_u \simeq -i\frac{1}{2}\sqrt{\frac{2}{3}} \frac{g}{m_{3/2}M} (T^a)_{ji} \bar{\psi} \not{p}' (1 + \gamma_5) \lambda^C, \tag{4.69}$$

where p' is the momentum of ϕ^* . As one can see, they cancel out in the total amplitude. This can be understood in the following way. The helicity $\pm\frac{1}{2}$ components of the gravitino field is the unphysical in the symmetric phase, and hence total amplitudes with helicity $\pm\frac{1}{2}$ gravitino at external line should vanish unless SUSY is broken. That is, the total amplitude for the helicity $\pm\frac{1}{2}$ gravitino production should be proportional to some SUSY breaking parameters. Thus, the leading high energy behavior, which is independent of SUSY breaking parameters, cancels out in the total amplitude.

From this fact, we can obtain an effective lagrangian for the helicity $\pm\frac{1}{2}$ light gravitino field by replacing all the derivatives operated on ϕ , χ , and λ in eq.(4.66) by the masses m_ϕ , m_χ , and m_λ of the corresponding fields. When these derivatives are operated on external lines, this replacement is easily justified. On the other hand, if they are operated on propagators, they become internal momenta and seem to make the high energy behavior worse. As mentioned above, however, this bad high energy behavior cancels out, and hence the leading high energy behaviors can be subtracted from the propagators with derivatives in

Process	$\sigma = (g^2 m_G^2 / 24\pi M^2 m_{3/2}^2) \times$
(A) $A^a + A^b \rightarrow \psi + \lambda^{(c)}$	$(1/3) f^{abc} ^2$
(B) $A^a + \lambda^{(b)} \rightarrow \psi + A^c$	$(1/16) f^{abc} ^2 \{-12 + 16 \ln(2/\delta) + 8\delta - \delta^2\}$
(C) $A^a + \phi_i \rightarrow \psi + \chi_j$	$(1/2) T_{ji}^a ^2$
(D) $A^a + \chi_i \rightarrow \psi + \phi_j$	$(1/4) T_{ji}^a ^2$
(E) $\chi_i + \phi_j^* \rightarrow \psi + A^a$	$(1/2) T_{ji}^a ^2$
(F) $\lambda^{(a)} + \lambda^{(b)} \rightarrow \psi + \lambda^{(c)}$	$(1/12) f^{abc} ^2 \{-22 + 24 \ln\{(2-\delta)/\delta\} + 24\delta - 3\delta^2 + \delta^3\}$
(G) $\lambda^{(a)} + \chi_i \rightarrow \psi + \chi_j$	$(1/2) T_{ji}^a ^2 \{-2 + 2 \ln(2/\delta) + \delta\}$
(H) $\lambda^{(a)} + \phi_i \rightarrow \psi + \phi_j$	$(1/32) T_{ji}^a ^2 \{-28 + 32 \ln(2/\delta) + 16\delta - \delta^2\}$
(I) $\chi_i + \bar{\chi}_j \rightarrow \psi + \lambda^{(a)}$	$(1/3) T_{ji}^a ^2$
(J) $\phi_i + \phi_j^* \rightarrow \psi + \lambda^{(a)}$	$(1/6) T_{ji}^a ^2$

Table 4.3: Total cross sections for the helicity $\pm \frac{1}{2}$ gravitino production. Spins of the initial states are averaged and those of the final states are summed. f^{abc} and T_{ij}^a represent the structure constants and the generators of the gauge groups, respectively. Notice that for the processes (B), (F), (G) and (H), we cut off the infrared singularities due to the t -, u -channel exchange of gauge bosons, taking small but positive $\delta = (1 \pm \cos \theta)_{min}$ where θ is the scattering angle in the center-of-mass frame.

the total amplitude;

$$\frac{p^2}{p^2 - m_\phi^2} \rightarrow \frac{p^2}{p^2 - m_\phi^2} - 1 = \frac{m_\phi^2}{p^2 - m_\phi^2}, \quad (4.70)$$

$$P_L \frac{p^2 (\not{p} + m_\chi)}{p^2 - m_\chi^2} P_R \rightarrow P_L \frac{p^2 (\not{p} + m_\chi)}{p^2 - m_\chi^2} P_R - P_L \not{p} P_R = P_L \frac{m_\chi^2 (\not{p} + m_\chi)}{p^2 - m_\chi^2} P_R, \quad (4.71)$$

$$\frac{\not{p} (\not{p} + m_\lambda)}{p^2 - m_\lambda^2} \rightarrow \frac{\not{p} (\not{p} + m_\lambda)}{p^2 - m_\lambda^2} - 1 = \frac{m_\lambda (\not{p} + m_\lambda)}{p^2 - m_\lambda^2}. \quad (4.72)$$

Thus, the derivatives in the interaction lagrangian (4.66) can be replaced by the appropriate masses related to the SUSY breaking, and the lagrangian (4.66) becomes

$$\mathcal{L}_{\text{eff}} = \frac{i(m_\phi^2 - m_\chi^2)}{\sqrt{3}m_{3/2}M} (\bar{\psi}\chi_R) \phi^* + \frac{-im_\lambda}{8\sqrt{6}m_{3/2}M} \bar{\psi} [\gamma^\mu, \gamma^\nu] \lambda^{(a)} F_{\mu\nu}^{(a)} + h.c. \quad (4.73)$$

As one can see, in the SUSY limit (*i.e.* $m_\chi^2 - m_\phi^2 \rightarrow 0$ and $m_\lambda \rightarrow 0$), the above lagrangian vanishes and the helicity $\pm \frac{1}{2}$ modes of the gravitino field decouple from the theory.

In the case of a light gravitino, it is more convenient to use the effective lagrangian (4.73) rather than the full lagrangian (4.58). Feynman rules derived from the lagrangian (4.73) are shown in Fig. 4.4.

By using the effective lagrangian (4.73), we have calculated decay rates and cross sections for some processes including a light gravitino. The decay rate of the process $\lambda \rightarrow \psi + A_\mu$ is given by

$$\Gamma(\lambda \rightarrow \psi + A_\mu) = \frac{1}{48\pi} \frac{m_\lambda^5}{m_{3/2}^2 M^2} \left\{ 1 - \left(\frac{m_{3/2}}{m_\lambda} \right)^2 \right\}^3, \quad (4.74)$$

and that of the process $\phi \rightarrow \psi + \chi$,

$$\Gamma(\phi \rightarrow \psi + \chi) = \frac{1}{48\pi} \frac{m_\phi^5}{m_{3/2}^2 M^2} \left\{ 1 - \left(\frac{m_{3/2}}{m_\phi} \right)^2 \right\}^2. \quad (4.75)$$

Furthermore, total cross sections of some light gravitino production processes are calculated and the results are shown in Table 4.3. Notice that the interaction of the helicity $\pm \frac{1}{2}$ gravitino becomes stronger as the gravitino mass $m_{3/2}$ becomes lighter, as one can see in eq.(4.74), eq.(4.75) and the total cross sections given in Table 4.3.

The results obtained above can be used when the gravitino mass $m_{3/2}$ is much smaller than the SUSY mass splitting in observable sector. Such a situation seems to conflict with the super-trace formula obtained in the previous section. But the super-trace formula is a tree level relation, and the mass splitting in the observable sector may become larger than the gravitino mass due to various radiative corrections. In fact, in some models based on no-scale type Kähler potential [10], the gravitino mass may become much smaller than the electroweak scale. In any case, if the gravitino mass is smaller than the mass splitting in other multiplets, we can use the results obtained in this section.

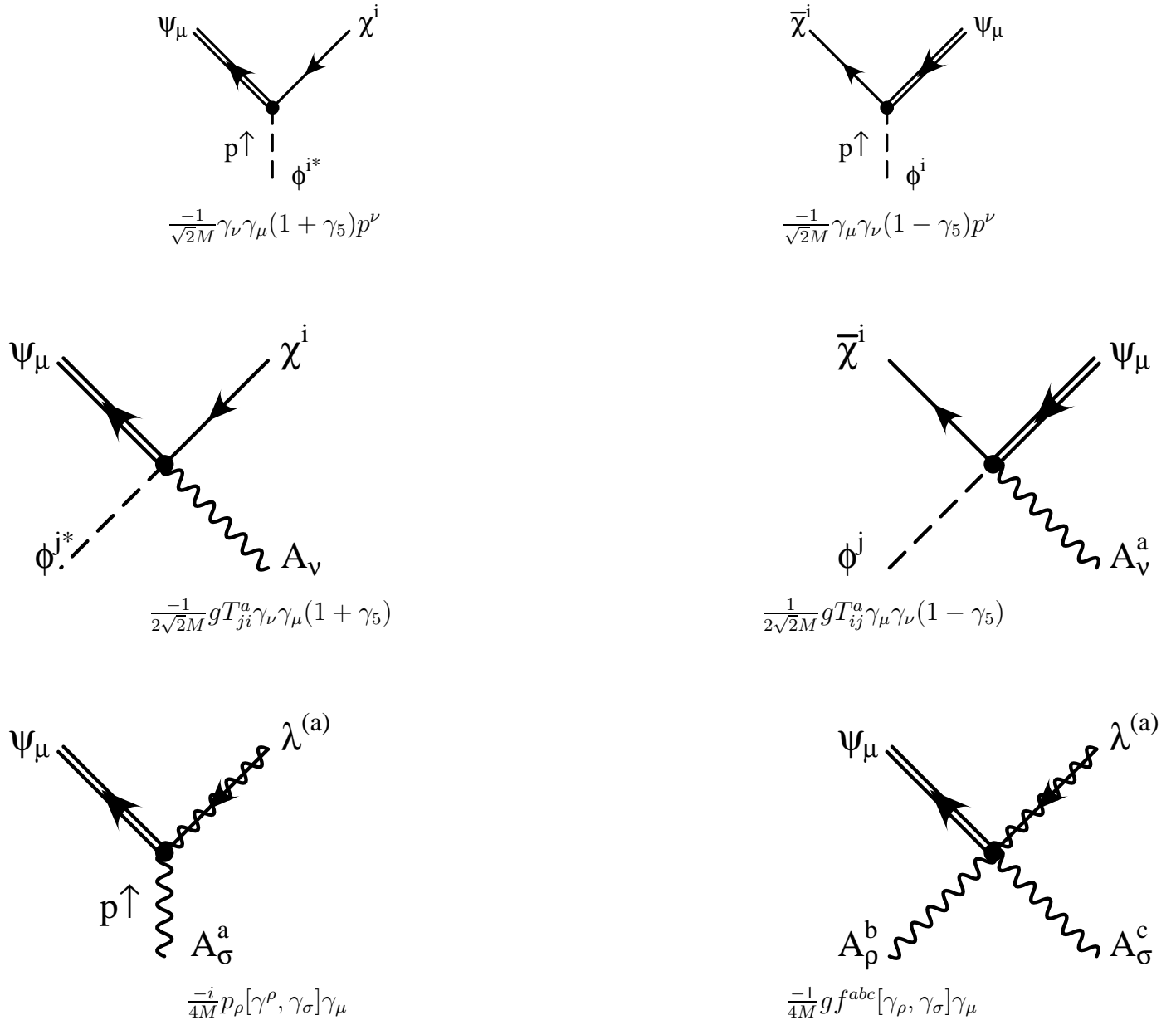


Figure 4.1: Feynman rules for the interactions of gravitino.



Figure 4.2: Feynman diagrams for the processes (a) $\psi_\mu \rightarrow \lambda + A_\mu$, and (b) $\psi_\mu \rightarrow \phi^i + \bar{\chi}^i$.

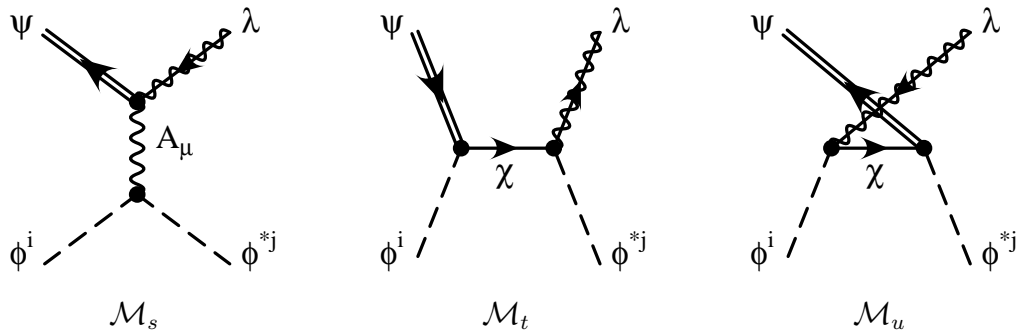


Figure 4.3: Feynman diagrams for the process $\phi^i + \phi^{*j} \rightarrow \psi_\mu + \lambda^{(a)}$.

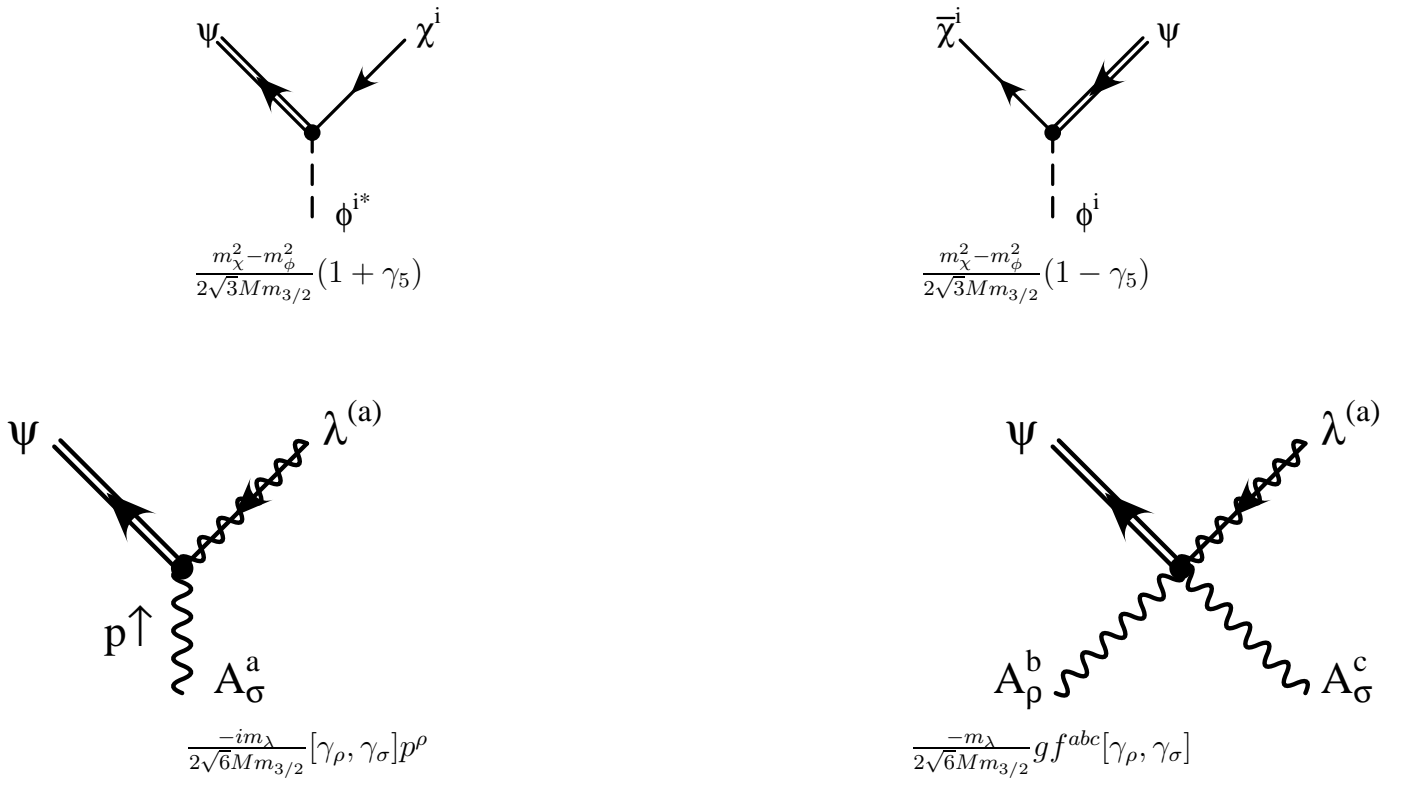


Figure 4.4: Feynman rules for the interactions of a light gravitino.

Chapter 5

Phenomenology of the gravitino : overview

Having Feynman rules with the gravitino field in the previous chapter, we are now at the point to discuss phenomenology of the gravitino. As we will see below, the gravitino is almost nothing to do with collider experiments because its interactions are extremely weak. But if we think of cosmology, effects of the gravitino may become very significant. Our main purpose is to investigate the effects of the gravitino on the inflationary universe quantitatively. Before doing this, we will survey the phenomenological implications of the massive gravitino.

5.1 Collider experiments with the gravitino

In this section, we will give brief comments on collider experiments with the massive gravitino. If the gravitino mass is comparable to the masses of SUSY particles (*i.e.* squarks, sleptons and gauginos), gravitino production cross sections are extremely small since the interaction terms for the gravitino are suppressed by powers of M^{-1} . For example, the helicity $\pm\frac{3}{2}$ gravitino production cross section in e^+e^- collider experiments is estimated to be

$$\sigma(e^+ + e^- \rightarrow \psi_\mu + \lambda) = \frac{1}{96\pi M^2} \left(\frac{1}{2}g_2^2 + \frac{5}{4}g_1^2 \right) \sim 1 \times 10^{-67} \text{cm}^2, \quad (5.1)$$

where we have assumed that \sqrt{s} is much larger than the gravitino and gaugino masses. Compared with the luminosity of LEP $\sim 10^{31} \text{cm}^{-2} \text{sec}^{-1}$, or even with a design luminosity of JLC $\sim 10^{34} \text{cm}^{-2} \text{sec}^{-1}$, we have no hope to have a signal of gravitino production events.

In the case of light gravitino, however, helicity $\pm\frac{1}{2}$ modes of the gravitino interact strongly, and hence one may expect that some signals of the gravitino may be detectable if the gravitino mass is sufficiently small. Bound on the light gravitino mass from collider experiments depends on the mass spectrum of superparticles. The most stringent bound on the gravitino mass is derived for the case where there exists a neutralino lighter than Z^0 -boson. In this

case, Z^0 -decay may contain a single photon balanced by missing transverse momentum in the opposite hemisphere [33]. Such a single photon is expected to arise from the process $Z^0 \rightarrow \psi_\mu + \chi$, $\chi \rightarrow \psi_\mu + \gamma$, where χ is the neutralino. Both of the decay rates for these processes are proportional to $m_{3/2}^{-2}$, and hence such a single photon event is sizable if the gravitino mass is extremely small. This process is analyzed in ref.[33], and the gravitino mass smaller than $\sim 10^{-13}\text{GeV}$ is excluded by the LEP experiments. Notice that this bound ($m_{3/2} \gtrsim 10^{-13}\text{GeV}$) is comparable to that obtained from cosmological considerations. If the neutralino mass is larger than the Z^0 -boson mass m_Z , we cannot use the above arguments, and less stringent bound may be derived.

5.2 Cosmology

Contrary to collider experiments, the mass of gravitino is severely constrained if we assume the standard big-bang cosmology.¹ If the gravitino is unstable, it may decay after the big-bang nucleosynthesis (BBN) and produces an unacceptable amount of entropy, which conflicts with the predictions of BBN. In order to keep the success of BBN, the gravitino mass should be larger than $\sim 10\text{TeV}$ as Weinberg first pointed out [11]. In a model with the gravitino mass larger than $\sim 10\text{TeV}$, the gravitino decay processes produce a large amount of entropy and dilutes the baryon number density of the universe. This requires that the baryon-to-photon ratio before the decay of the gravitino should be extremely large so that the present value of the baryon-to-photon ratio is given by $O(10^{-9} - 10^{-10})$. Furthermore, in a model with R -parity invariance, the gravitino decay also produces an unacceptable amount of LSP which conflicts with the observations of the present mass density of the universe [12]. (These problems are sometimes called “gravitino problem”.)

Meanwhile, in the case of stable gravitino, its mass should be smaller than $\sim 1\text{keV}$ not to overclose the universe [13]. Therefore, the gravitino mass between $\sim 1\text{keV}$ and $\sim 10\text{TeV}$ conflicts with the standard big-bang cosmology.

However, if the universe went through inflation [14], we may avoid the above constraints [15] since the initial abundance of the gravitino is diluted by the exponential expansion of the universe. But even if the initial gravitinos are diluted, the above problems still potentially exist since gravitinos are reproduced by scattering processes off the thermal radiation after the universe has been reheated. The number density of the secondary gravitino is proportional to the reheating temperature and hence upperbound on the reheating temperature should be imposed not to overproduce gravitinos. Therefore, even assuming the inflation, a detailed analysis must be made to obtain the upperbound on the reheating temperature.

¹In the “standard cosmology”, we adopt the following two points. The first point is that the light nuclei were synthesized through the (almost) standard big-bang nucleosynthesis, and the second is that the density parameter Ω of the present universe is smaller than $O(1)$. (For the big-bang nucleosynthesis, see Appendix C.)

For the case of the unstable gravitino, the cosmological considerations on regeneration and decay of the gravitino has been done in many articles [34, 35, 36, 37, 38, 39, 40, 41]. These previous works show that the most stringent upperbound on the reheating temperature comes from the photo-dissociation of light nuclei (D, T, ^3He , ^4He). Once gravitinos are produced in the early universe, most of them decay after BBN since the lifetime of the gravitino of mass $O(100\text{GeV} - 10\text{TeV})$ is $O((10^8 - 10^2)\text{sec})$. If the gravitinos decay radiatively, emitted high energy photons induce cascade processes and affect the result of BBN. Not to change the abundance of light nuclei, we must have a restriction on the number density of gravitinos, and this constraint is translated into the upperbound on the reheating temperature.

In order to analyze the photo-dissociation processes, we must calculate the following two quantities precisely; the number density of the gravitinos produced after the reheating, and the high energy photon spectrum induced by radiative decay of the gravitinos. But the previous estimations of these values are incomplete. As for the number density of gravitino, most of the previous works follow the result of ref.[36], where the number density is underestimated by factor ~ 4 . Furthermore, in many articles the spectrum of high energy photon, which determines the photo-dissociation rates of light elements, is calculated by using a simple fitting formula. In this thesis, we calculate these two quantities precisely and find more precise upperbound on the reheating temperature.

If the gravitino is stable, the situation changes. If a very light gravitino of mass $m_{3/2} \sim O(1\text{ keV})$ was once thermalized, the critical density of the universe is easily obtained, and hence it constitutes a dark matter. For a heavier gravitino, one has to consider inflation. We will find that the requirement that the gravitinos produced after the inflation should not overclose the universe (the closure limit) places a severe upperbound on the reheating temperature [42]. Another stringent constraint comes from the photo-dissociations of light nuclei by high energy photons produced through radiative decays of the next-to-the-lightest superparticle into the gravitinos, which excludes the certain range of the gravitino mass.

In the following chapters, we will investigate these effects quantitatively.

5.3 The Polonyi problem

As we have seen in Chapter 3, there exists a scalar boson with mass of the order of the gravitino mass $m_{3/2}$ in a wide class of models based on supergravity. (Below, we call this scalar field “Polonyi field” ϕ_P and denote its mass m_{ϕ_P} .) If one assumes that the gravitino mass is of the order of the electroweak scale from the naturalness point of view, it has been pointed out that the Polonyi field ϕ_P causes serious cosmological difficulties [30] (so-called “Polonyi problem”) as gravitino does. Though this is not directly related to our present purpose, we briefly discuss this problem because of its significance.

The Polonyi problem stems from the fact that the Polonyi field takes its amplitude of order M at the end of inflation, *i.e.* there is a Bose condensation. Such a condensation cannot be eliminated by inflation since the equation of motion for the Polonyi field is coupled to

that of the inflaton field. Thus, in general the potential minimum of the Polonyi field at zero temperature is not a stationary point during inflation, and hence the Polonyi field does not sit at the origin. Furthermore, it should be noted that scalar fields deviate from the origin due to the quantum fluctuation during the inflation.

As the temperature drops and the expansion rate H of the universe becomes comparable to m_{ϕ_P} , the Polonyi field starts its oscillation, and subsequently dominates the energy density of the universe until it decays. The decay rate of the Polonyi field is estimated as $O(m_{\phi_P}^3/M_{pl}^2) \sim O(m_{3/2}^3/M_{pl}^2)$, and hence it may cause cosmological difficulties as in the gravitino case. That is, the Polonyi field decay releases tremendous amount of entropy and dilutes primordial baryon asymmetry much below what is observed today (which is sometimes called the entropy crisis). Furthermore, the decay of the Polonyi field destroys the successful scenario of the BBN if it occurs after the BBN starts. In fact, the Polonyi problem is more serious than the gravitino problem, since it cannot be solved by inflation. As a result, a wide class of models with the SUSY breaking in hidden sector are excluded by cosmological arguments.

It has been pointed out [43] that the first problem (*i.e.* the entropy crisis) can be cured if the Affleck-Dine mechanism [44] for baryogenesis works in the early universe. Furthermore, the second one can be solved by raising the mass of the Polonyi field up to $O(10\text{TeV})$ so that the reheating temperature by the ϕ_P decay is larger than $O(1\text{MeV})$. Then, the BBN starts after the decay of ϕ_P has completed.

In order to raise Polonyi mass m_{ϕ_P} without raising the SUSY breaking scalar masses in the observable sector, several ideas have been proposed. One of the attractive proposal is to assume a dynamical SUSY breaking scenario. If the SUSY is broken by some dynamics at the energy scale M_I much below the gravitational one, the cut-off scale of the model may become $O(M_I)$. In this case, Kähler potential may contain (non-renormalizable) interaction terms which are suppressed by powers of M_I^{-1} instead of M^{-1} . Then, the Polonyi field may have a mass much larger than that of the gravitino, and hence decays before the BBN starts.

Alternative approach is to consider no-scale type supergravity models [9, 45]. In some class of models with no-scale type Kähler potential, the gravitino mass is not directly related to the SUSY breaking masses of the squarks, sleptons and Higgs bosons. In this case, the gravitino mass (and the mass of the Polonyi field) can become much larger than the electroweak scale without raising the SUSY breaking scalar masses in the observable sector.

Furthermore, in some class of models with fine tuning, mixing between the Polonyi field and the scalar field concerning the fine tuning becomes substantially large [46]. In this case, the Polonyi field decays through the mixing, and the decay rate can be enhanced without increasing the Polonyi mass m_{ϕ_P} . If the mixing is sufficiently large, the Polonyi field decays before the BBN starts. An example of this type of models is the minimal SUSY SU(5) model [6, 7] with a small self-coupling of the **24**-Higgs. In this model, the Polonyi field decays into the flavor Higgs doublets through the mixing to **24**-Higgs.

As we have discussed, there exist some approach to the Polonyi problem. However, they

still have uncertainties, and it is unclear whether these scenarios really work well. Therefore, more efforts are needed in order to check the validity of each scenario. Finally, it should be noted that the cosmological evolution of the Polonyi field may affect the arguments on the gravitino problem. In this thesis, however, we assume that the Polonyi field plays no significant role in cosmology due to some (unknown) mechanism, and hence we ignore its effects in the following chapters.

Chapter 6

Cosmology with unstable gravitino

As mentioned in the previous chapter, the gravitino may affect cosmology. Especially the constraints from the BBN and the present mass density of the universe strongly suggest the inflation if there exists the gravitino. In this chapter, we will consider the effects of the gravitino on the inflationary universe mainly assuming that the gravitino decays only into photon and photino. We will also give the analysis for the case where the gravitino only decays into neutrino and sneutrino.¹

6.1 Gravitino production in the early universe

We will first calculate the number density of the gravitino after the inflation. Once the universe has reheated, gravitinos are reproduced by scattering processes of the thermal radiations and they decay with the decay rate of the order of $m_{3/2}^3/M_{pl}^2$. Since the interactions of gravitino are very weak, the gravitinos cannot be thermalized if the reheating temperature T_R is less than $O(M_{pl})$. In this case, the Boltzmann equation for the gravitino number density $n_{3/2}$ can be written as

$$\frac{dn_{3/2}}{dt} + 3Hn_{3/2} = \langle \Sigma_{tot} v_{rel} \rangle n_{rad}^2 - \frac{m_{3/2}}{\langle E_{3/2} \rangle} \frac{n_{3/2}}{\tau_{3/2}}, \quad (6.1)$$

where H is the expansion rate of the universe, $\langle \cdot \cdot \cdot \rangle$ represents thermal average, n_{rad} the number density of the scalar boson in the thermal bath,

$$n_{rad} = \frac{\zeta(3)}{\pi^2} T^3, \quad (6.2)$$

v_{rel} the relative velocity of the scattering radiations ($\langle v_{rel} \rangle = 1$ in our case), and the factor $m_{3/2}/\langle E_{3/2} \rangle$ the averaged Lorentz factor. For the radiation dominated universe, the expansion

¹This chapter is based on the work in a collaboration with M. Kawasaki [41, 47].

rate H of the universe is given by

$$H \equiv \frac{\dot{R}}{R} = \sqrt{\frac{N_* \pi^2}{90 M^2}} T^2, \quad (6.3)$$

where R is the scale factor and N_* the effective total number of degrees of freedom for effectively massless particles. For the particle content of the MSSM, $N_*(T_R) \sim 228.75$ if T_R is much larger than the masses of the superpartners, and $N_*(T \ll 1\text{MeV}) \sim 3.36$. The total cross section Σ_{tot} in the thermal bath is defined as

$$\Sigma_{tot} = \frac{1}{2} \sum_{x,y,z} \eta_x \eta_y \sigma_{(x+y \rightarrow \psi_\mu + z)}, \quad (6.4)$$

where $\sigma_{(x+y \rightarrow \psi_\mu + z)}$ is the cross section for the process $x + y \rightarrow \psi_\mu + z$ (see Table 4.2), and $\eta_x = 1$ for incoming bosons, $\eta_x = \frac{3}{4}$ for incoming fermions. For the MSSM particle content, Σ_{tot} is given by

$$\Sigma_{tot} = \frac{1}{M^2} \left\{ 2.50 g_1^2(T) + 4.99 g_2^2(T) + 11.78 g_3^2(T) \right\}, \quad (6.5)$$

where g_1 , g_2 and g_3 are the gauge coupling constants of the gauge group $U(1)_Y$, $SU(2)_L$ and $SU(3)_C$, respectively. Notice that in high energy scattering processes, the effect of the renormalization of the gauge coupling constants should be taken into account. Using the one loop β -function of the MSSM, the solution to the renormalization group equation of gauge coupling constants is given by

$$g_i(T) \simeq \left\{ g_i^{-2}(m_Z) - \frac{b_i}{8\pi^2} \ln \left(\frac{T}{m_Z} \right) \right\}^{-1/2}, \quad (6.6)$$

with $b_1 = 11$, $b_2 = 1$, $b_3 = -3$. In this thesis, we use this formula.

At the time right after the end of the reheating, the first term dominates the right-hand side of eq.(6.1) since gravitinos have been diluted by the de Sitter expansion of the universe during the inflation. As a first step to solve eq.(6.1), we assume a “naive” adiabatic expansion of the universe;

$$RT = \text{const.} \quad (6.7)$$

Then using the yield variable $Y_{3/2} \equiv n_{3/2}/n_{rad}$ and ignoring the decay contributions, eq.(6.1) becomes

$$\frac{dY_{3/2}}{dT} = - \frac{\langle \Sigma_{tot} v_{rel} \rangle n_{rad}}{HT}. \quad (6.8)$$

Notice that the right-hand side of this equation is (almost) independent of T , and hence we can easily integrate eq.(6.8).

However, eq.(6.8) does not give a correct value of $Y_{3/2}$ since the conserved quantity is not RT but the entropy per comoving volume;

$$R^3 S = \text{const}, \quad (6.9)$$

with S being the entropy density. Therefore, if the number of the gravitino per comoving volume is conserved, the yield variables $Y_{3/2}$ for different temperature T_1 and T_2 are related as

$$\begin{aligned} Y_{3/2}(T_1) &= \frac{S(T_1)/n_{rad}(T_1)}{S(T_2)/n_{rad}(T_2)} Y_{3/2}(T_2) \\ &= \frac{N_S(T_1)}{N_S(T_2)} Y_{3/2}(T_2), \end{aligned} \quad (6.10)$$

where $N_S \equiv S/S_0$ with $S_0 \equiv (2\pi/45)T^3$. (The prefactor $N_S(T_1)/N_S(T_2)$ is sometimes called a dilution factor.)

Taking this effect into account, the yield of the gravitino at T is given by²

$$Y_{3/2}(T) = \frac{N_S(T)}{N_S(T_R)} \times \frac{n_{rad}(T_R) \langle \Sigma_{tot} v_{rel} \rangle}{H(T_R)}. \quad (6.11)$$

For the MSSM particle content, $N_S(T_R) \sim 228.75$ and $N_S(T \ll 1\text{MeV}) \sim 3.91$. Eq.(6.11) shows that $Y_{3/2}$ is proportional to T_R , *i.e.* as the reheating temperature increases the yield of the gravitino becomes larger. From eq.(6.11), we can derive a simple fitting formula for $Y_{3/2}$;

$$Y_{3/2}(T \ll 1\text{MeV}) \simeq 2.14 \times 10^{-11} \left(\frac{T_R}{10^{10}\text{GeV}} \right) \left\{ 1 - 0.0232 \ln \left(\frac{T_R}{10^{10}\text{GeV}} \right) \right\}, \quad (6.12)$$

where the logarithmic correction term comes from the renormalization of the gauge coupling constants. The difference between the exact formula (6.11) and the above approximated one is within $\sim 5\%$ for $10^6 \text{ GeV} \lesssim T_R \lesssim 10^{14} \text{ GeV}$ (and within $\sim 25\%$ for $10^2 \text{ GeV} \lesssim T_R \lesssim 10^{19} \text{ GeV}$). Notice that the gravitino abundance derived here is about four times larger than the one obtained in ref.[36].

As the temperature of the universe drops and the Hubble time H^{-1} approaches $\tau_{3/2}$, the decay term becomes the dominant part of the right-hand side of eq.(6.1). Ignoring the scattering term, eq.(6.1) can be rewritten as

$$\frac{dY_{3/2}}{dt} = -\frac{Y_{3/2}}{\tau_{3/2}}, \quad (6.13)$$

²In the recent article, Fischler [48] have proposed a new mechanism to produce gravitinos in the thermal bath. If one adopts his mechanism, the number density of the gravitino becomes much larger than the results obtained in this thesis, and hence the constraints obtained below must become more stringent. However, it is not clear to us if his new mechanism is relevant.

where we have taken $m_{3/2}/\langle E_{3/2} \rangle = 1$ since gravitinos are almost at rest. Using eq.(6.11) as a boundary condition, we can solve eq.(6.13) and the solution is given by

$$Y_{3/2}(t) = \frac{n_{3/2}(t)}{n_{rad}(t)} = \frac{N_S(T)}{N_S(T_R)} \times \frac{n_{rad}(T_R) \langle \Sigma_{tot} v_{rel} \rangle}{H(T_R)} e^{-t/\tau_{3/2}}, \quad (6.14)$$

where the relation between t and T can be obtained by solving eq.(6.3) with eq.(6.7);

$$t = \frac{1}{2} \sqrt{\frac{90M^2}{N_* \pi^2}} T^{-2}. \quad (6.15)$$

6.2 Radiative decay of the gravitino

Radiative decays of the gravitino may affect BBN. First, we analyze this effect assuming that the gravitino ψ_μ mainly decays into a photon γ and a photino $\tilde{\gamma}$.

In order to investigate the photo-dissociation processes, we must know the spectra of the high energy photon and electron induced by the gravitino decay. In this section, we will derive these spectra by solving the Boltzmann equations numerically.

Once high energy photons are emitted in the gravitino decay, they induce cascade processes. In order to analyze these processes, we take the following radiative processes into account.

- The high energy photon with energy ϵ_γ produces an $e^+ e^-$ pair by scattering off the background photon if the energy of the background photon is larger than m_e^2/ϵ_γ . We call this process the double photon pair creation. For sufficiently high energy photons, this is the dominant process since the cross section or the number density of the target is much larger than that of other processes. A numerical calculation shows that this process determines the shape of the spectrum of the high energy photon for $\epsilon_\gamma \gtrsim m_e^2/22T$.
- Below the effective threshold of the double photon pair creation, high energy photons lose their energy by the photon-photon scattering. But in the limit of $\epsilon_\gamma \rightarrow 0$, the total cross section for the photon-photon scattering is proportional to ϵ_γ^3 and this process loses its significance.
- Finally, photons lose their energy by scattering off charged particles in the thermal bath. The dominant processes are pair creation in the nuclei and the Compton scattering off the thermal electron.
- Emitted high energy electrons and positrons lose their energy by the inverse Compton scattering off the background photon.
- The source of these cascade processes are the high energy photons emitted in the decay of gravitinos. Notice that we only consider the decay channel $\psi_\mu \rightarrow \gamma + \tilde{\gamma}$ and hence

the energy of the incoming photon $\epsilon_{\gamma 0}$ is monochromatic.

The Boltzmann equations for the photon and the electron distribution function f_γ and f_e are given by

$$\begin{aligned} \frac{\partial f_\gamma(\epsilon_\gamma)}{\partial t} = & \left. \frac{\partial f_\gamma(\epsilon_\gamma)}{\partial t} \right|_{\text{DP}} + \left. \frac{\partial f_\gamma(\epsilon_\gamma)}{\partial t} \right|_{\text{PP}} + \left. \frac{\partial f_\gamma(\epsilon_\gamma)}{\partial t} \right|_{\text{PC}} + \left. \frac{\partial f_\gamma(\epsilon_\gamma)}{\partial t} \right|_{\text{CS}} \\ & + \left. \frac{\partial f_\gamma(\epsilon_\gamma)}{\partial t} \right|_{\text{IC}} + \left. \frac{\partial f_\gamma(\epsilon_\gamma)}{\partial t} \right|_{\text{DE}}, \end{aligned} \quad (6.16)$$

$$\frac{\partial f_e(E_e)}{\partial t} = \left. \frac{\partial f_e(E_e)}{\partial t} \right|_{\text{DP}} + \left. \frac{\partial f_e(E_e)}{\partial t} \right|_{\text{PC}} + \left. \frac{\partial f_e(E_e)}{\partial t} \right|_{\text{CS}} + \left. \frac{\partial f_e(E_e)}{\partial t} \right|_{\text{IC}}, \quad (6.17)$$

where DP (PP, PC, CS, IC, and DE) represents double photon pair creation (photon-photon scattering, pair creation in nuclei, Compton scattering, inverse Compton scattering, and the contribution from the gravitino decay). Full details are shown in Appendix B.

By solving the Boltzmann equations (6.16) and (6.17) numerically, we obtain the time evolution of the photon and the electron spectra. The typical time evolutions of the photon spectrum are shown in Figs.6.1.

6.3 BBN with high energy photon injection

BBN is one of great successes of the standard big bang cosmology. It is believed that light elements with atomic number less than 7 are produced when the cosmic temperature is between 1MeV and 10keV. Theoretical predictions for abundances of light elements are excellently in good agreement with the observations if the baryon-to-photon ratio η_B is about 3×10^{-10} [49]. (For a review, see Appendix C.)

However, the presence of the gravitino might destroy this success of the BBN. Gravitino may have three effects on BBN. First the energy density of the gravitino at $T \sim 1\text{MeV}$ speeds up the cosmic expansion and leads to increase the n/p ratio and hence ${}^4\text{He}$ abundance also increases. Second, the radiative decay of gravitino reduces the baryon-to-photon ratio and results in too baryon-poor universe. Third, the high energy photons emitted in the decay of gravitino destroy the light elements. Among three effects, photo-dissociation by the high energy photons is the most dangerous for the gravitino with mass less than $\sim 1\text{TeV}$. In the following we investigate the photo-dissociation of light elements.

The high energy photons emitted in the decay of gravitinos lose their energy during multiple electro-magnetic processes described in the previous section. Surviving soft photons can destroy the light elements (D, T, ${}^3\text{He}$, ${}^4\text{He}$) if their energy are greater than the threshold of the photo-dissociation reactions. In this thesis, we consider the photo-dissociation reactions listed in Table 6.1. For the process $\text{D}(\gamma, n)p$, we use the cross section in analytic form which is given in ref.[50], and the cross sections for other reactions are taken from the experimental data. (For references, see Table 6.1). We neglect the reactions ${}^4\text{He}(\gamma, \text{D})\text{D}$ and ${}^4\text{He}(\gamma, 2p)$

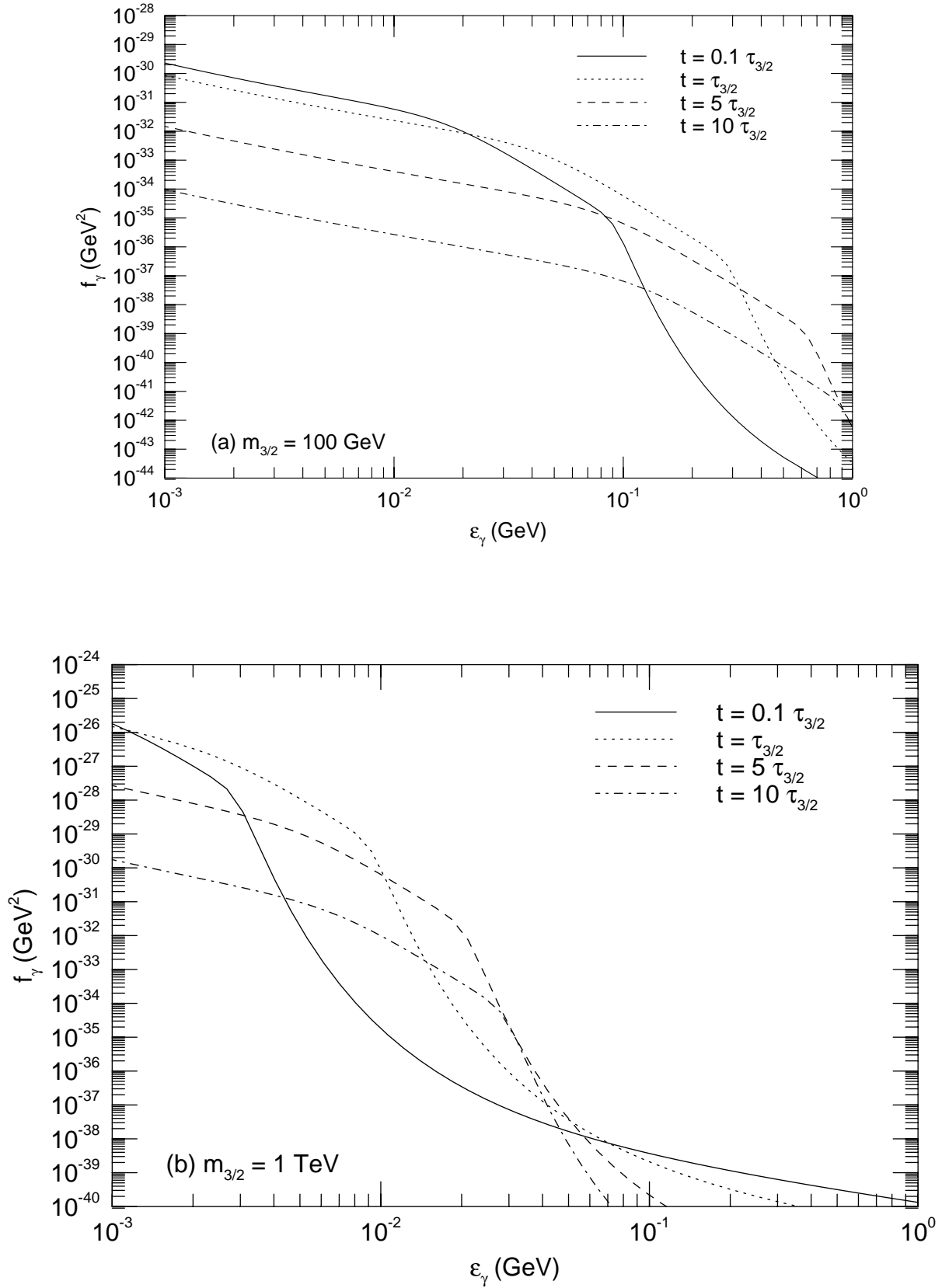


Figure 6.1: Time evolution of the photon spectrum with the case of $T_R = 10^{10} \text{ GeV}$, and (a) $m_{3/2} = 100 \text{ GeV}$, and (b) $m_{3/2} = 1 \text{ TeV}$. The solid lines (the dotted lines, the dashed lines, and the dotted-dashed lines) correspond to the photon spectra at the time $t = 0.1 \tau_{3/2}$ ($t = \tau_{3/2}$, $t = 5 \tau_{3/2}$, and $t = 10 \tau_{3/2}$).

Reaction	Threshold (MeV)	Reference
$D + \gamma \rightarrow n + p$	2.225	[50]
$T + \gamma \rightarrow n + D$	6.257	[51, 52]
$T + \gamma \rightarrow p + n + n$	8.482	[52]
${}^3\text{He} + \gamma \rightarrow p + D$	5.494	[53]
${}^3\text{He} + \gamma \rightarrow p + D$	7.718	[53]
${}^4\text{He} + \gamma \rightarrow p + T$	19.815	[54]
${}^4\text{He} + \gamma \rightarrow n + {}^3\text{He}$	20.578	[55, 56]
${}^4\text{He} + \gamma \rightarrow p + n + D$	26.072	[54]

Table 6.1: Photo-dissociation reactions.

2n) since their cross sections are small compared with the other reactions. Furthermore, we do not include the photo-dissociation processes for ${}^7\text{Li}$ and ${}^7\text{Be}$ because the data of the cross section for ${}^7\text{Be}$ is not available, and hence we cannot predict the abundance of ${}^7\text{Li}$ a part of which comes from ${}^7\text{Be}$.

The time evolution of the light elements are described by

$$\begin{aligned} \frac{dn_D}{dt} + 3Hn_D &= -n_D \sum_i \int_{E_i} d\epsilon_\gamma \sigma_{D \rightarrow a}^i(\epsilon_\gamma) f_\gamma(\epsilon_\gamma) \\ &\quad + \sum_i \int_{E_i} d\epsilon_\gamma \sigma_{a \rightarrow D}^i(\epsilon_\gamma) n_a f_\gamma(\epsilon_\gamma), \end{aligned} \quad (6.18)$$

$$\begin{aligned} \frac{dn_T}{dt} + 3Hn_T &= -n_T \sum_i \int_{E_i} d\epsilon_\gamma \sigma_{T \rightarrow a}^i(\epsilon_\gamma) f_\gamma(\epsilon_\gamma) \\ &\quad + \sum_i \int_{E_i} d\epsilon_\gamma \sigma_{a \rightarrow T}^i(\epsilon_\gamma) n_a f_\gamma(\epsilon_\gamma), \end{aligned} \quad (6.19)$$

$$\begin{aligned} \frac{dn_{{}^3\text{He}}}{dt} + 3Hn_{{}^3\text{He}} &= -n_{{}^3\text{He}} \sum_i \int_{E_i} d\epsilon_\gamma \sigma_{{}^3\text{He} \rightarrow a}^i(\epsilon_\gamma) f_\gamma(\epsilon_\gamma) \\ &\quad + \sum_i \int_{E_i} d\epsilon_\gamma \sigma_{a \rightarrow {}^3\text{He}}^i(\epsilon_\gamma) n_a f_\gamma(\epsilon_\gamma), \end{aligned} \quad (6.20)$$

$$\begin{aligned} \frac{dn_{{}^4\text{He}}}{dt} + 3Hn_{{}^4\text{He}} &= -n_{{}^4\text{He}} \sum_i \int_{E_i} d\epsilon_\gamma \sigma_{{}^4\text{He} \rightarrow a}^i(\epsilon_\gamma) f_\gamma(\epsilon_\gamma) \\ &\quad + \sum_i \int_{E_i} d\epsilon_\gamma \sigma_{a \rightarrow {}^4\text{He}}^i(\epsilon_\gamma) n_a f_\gamma(\epsilon_\gamma), \end{aligned} \quad (6.21)$$

where $\sigma_{a \rightarrow b}^i$ is the cross section of the photo-dissociation process i ; $a + \gamma \rightarrow b + \dots$, and E_i is the threshold energy of reaction i . When the energy of the high energy photon is relatively low, *i.e.* $2\text{MeV} \lesssim \epsilon_\gamma \lesssim 20\text{MeV}$, D , T and ${}^3\text{He}$ are destroyed and their abundances decrease. On the other hand, if the photons have energy high enough to destroy ${}^4\text{He}$, it seems that such high energy photons decrease the abundance of all light elements. However, since D , T and ${}^3\text{He}$ are produced by the photo-dissociation of ${}^4\text{He}$ whose abundance is much higher than the other elements, their abundances increase or decrease depending on the number

density of high energy photon. When the number density of high energy photons with their energy greater than $\sim 20\text{MeV}$ (*i.e.* the threshold energy for ^4He destruction) is extremely high, all light elements are destroyed. But as the photon density becomes lower, there is some range of the high energy photon density in which the overproduction of D, T and ^3He becomes significant. And if the density is sufficiently low, the high energy photon does not affect the BBN at all.

From various observations, the primordial abundances of light elements (D, ^3He , ^4He) are estimated [49] as

$$0.22 < Y_p \equiv \left[\frac{\rho_{^4\text{He}}}{\rho_B} \right]_p < 0.24, \quad (6.22)$$

$$\left[\frac{n_D}{n_H} \right]_p > 1.8 \times 10^{-5}, \quad (6.23)$$

$$\left[\frac{n_D + n_{^3\text{He}}}{n_H} \right]_p < 1.0 \times 10^{-4}, \quad (6.24)$$

where $\rho_{^4\text{He}}$ and ρ_B are the mass densities of ^4He and baryon. (For details, see Appendix C.) The abundances of light elements modified by the gravitino decay must satisfy the observational constraints above. In order to make precise predictions for the abundances of light elements, the evolution equations (6.18) – (6.21) should be incorporated in the nuclear network calculation of BBN. Therefore, we modify the Kawano computer code [57] to include the photo-dissociation processes.

From the above arguments it is clear that there are at least three free parameters, *i.e.* the mass of gravitino $m_{3/2}$, the reheating temperature T_R and the baryon-to-photon ratio η_B . Furthermore, we also study the case in which the gravitino has other decay channels. Here, we do not specify other decay channel. Instead, we introduce another free parameter B_γ which is the branching ratio for the channel $\psi_\mu \rightarrow \gamma + \tilde{\gamma}$. Therefore, we must study the effect of gravitino decay on BBN in four dimensional parameter space. However, in the following arguments it will be shown that the baryon-to-photon ratio η_B is not an important parameter in the present calculation because the allowed value for η_B is almost the same as that in the standard case (*i.e.* without gravitino).

First we investigate the photo-dissociation effect when all gravitinos decay into photons and photinos ($B_\gamma = 1$). We take the range of three free parameters as $10\text{GeV} \leq m_{3/2} \leq 10\text{TeV}$, $10^5\text{GeV} \leq T_R \leq 10^{13}\text{GeV}$ and $10^{-10} \leq \eta_B \leq 10^{-9}$. In this calculation, we assume that the photino is massless.³ The contours for the critical abundances of the light elements D, (D+ ^3He) and ^4He in the $\eta_B - T_R$ plane are shown in Fig. 6.2 – Fig. 6.5 for $m_{3/2} = 10\text{GeV}$, 100GeV , 1TeV and 10TeV . For lower reheating temperatures ($T_R \lesssim 10^6\text{GeV}$), the number density of the gravitino is very low and hence the number density of the induced high energy photons is too low to affect the BBN. Therefore, the resultant abundances of light elements

³Constraints from the photo-dissociation of the light elements are almost independent of the photino mass if the photino is sufficiently lighter than the gravitino.

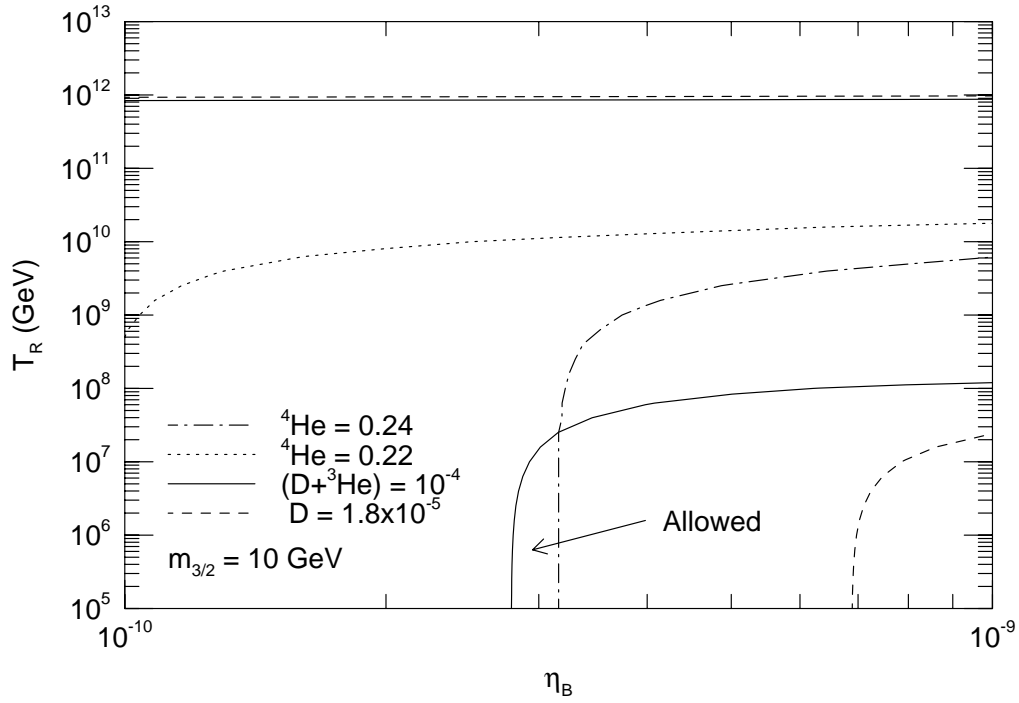


Figure 6.2: Contours for critical abundance of light elements in the $\eta_B - T_R$ plane for $m_{3/2} = 10 \text{ GeV}$. The solid line (dashed line, dotted line, dotted-dashed line) represents the constraints from overproduction of $(D+{}^3\text{He})$ (overdestruction of D, overdestruction of ${}^4\text{He}$, overproduction of ${}^4\text{He}$).

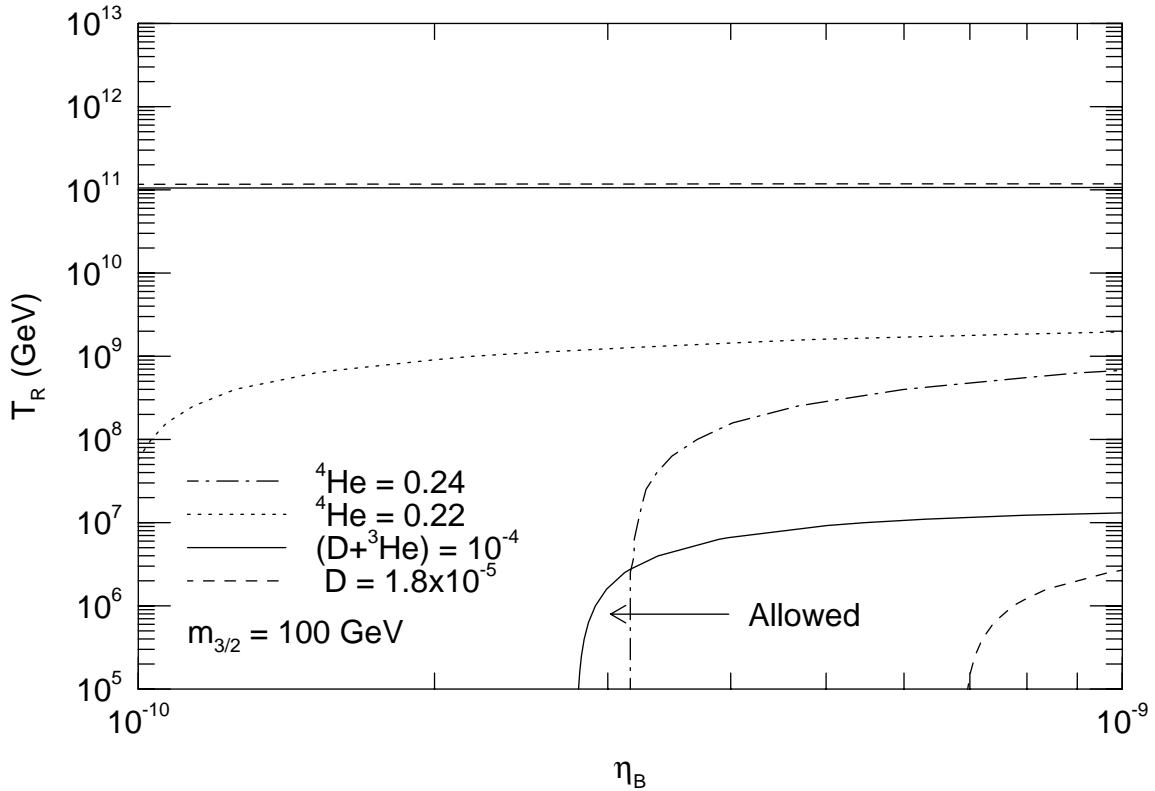


Figure 6.3: Same as Fig. 6.2 except for $m_{3/2} = 100 \text{ GeV}$.

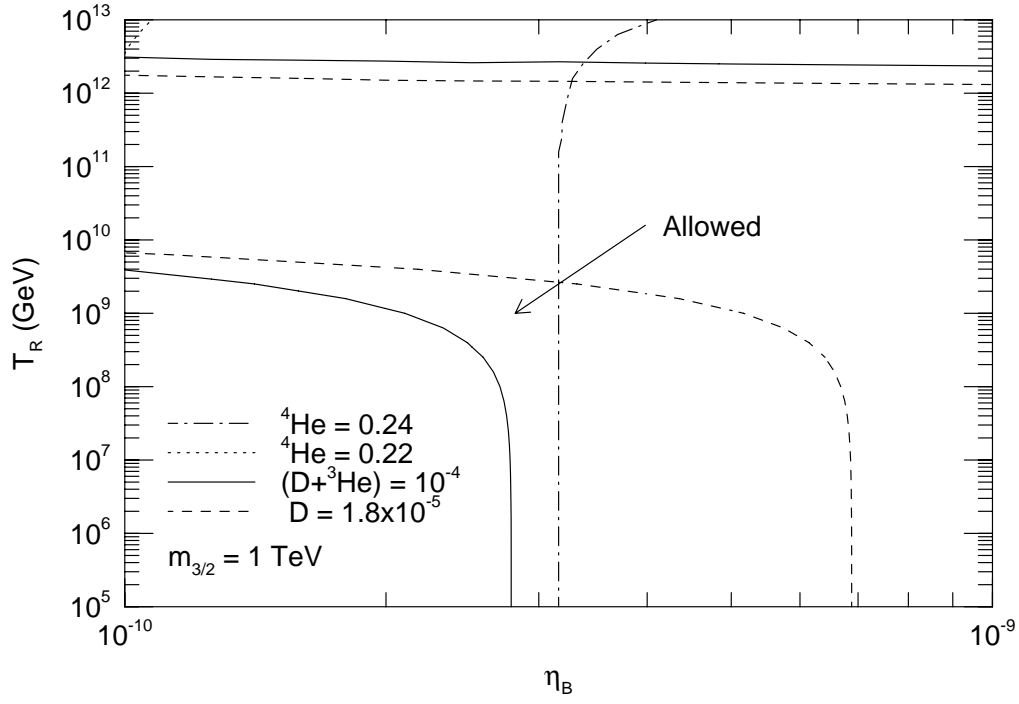


Figure 6.4: Same as Fig. 6.2 except for $m_{3/2} = 1$ TeV.

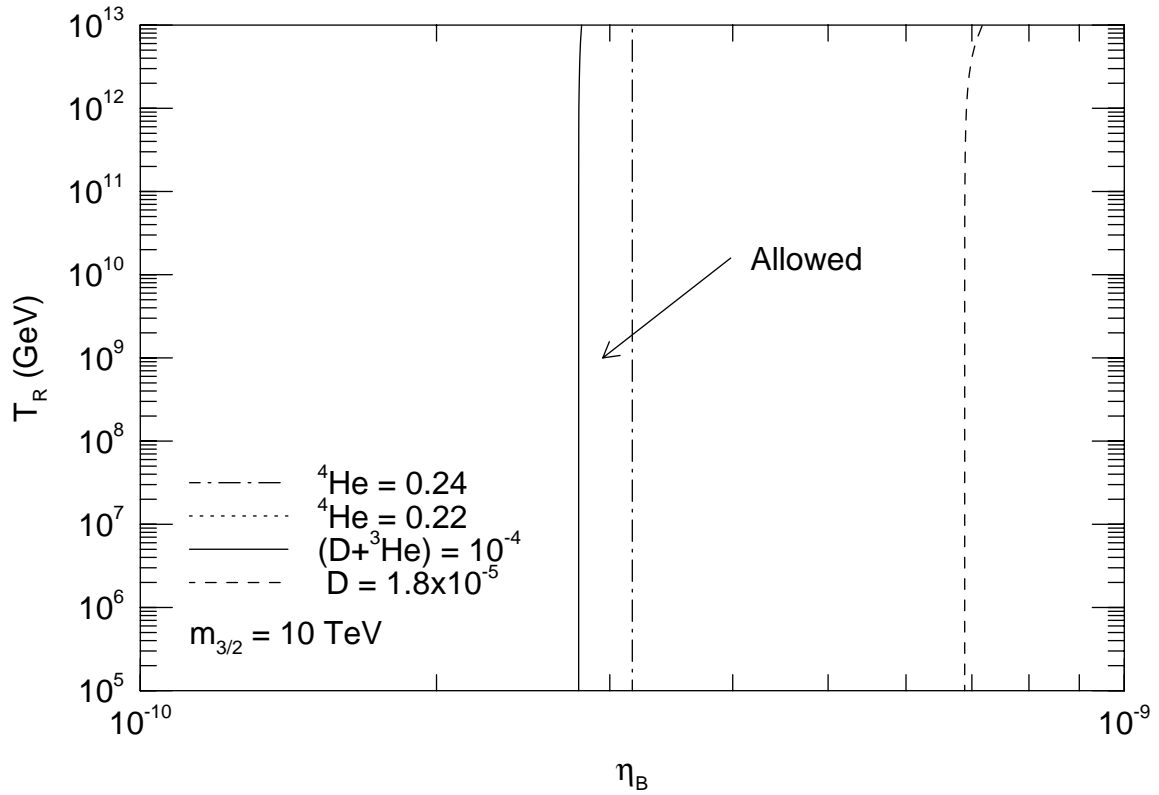


Figure 6.5: Same as Fig. 6.2 except for $m_{3/2} = 10$ TeV.

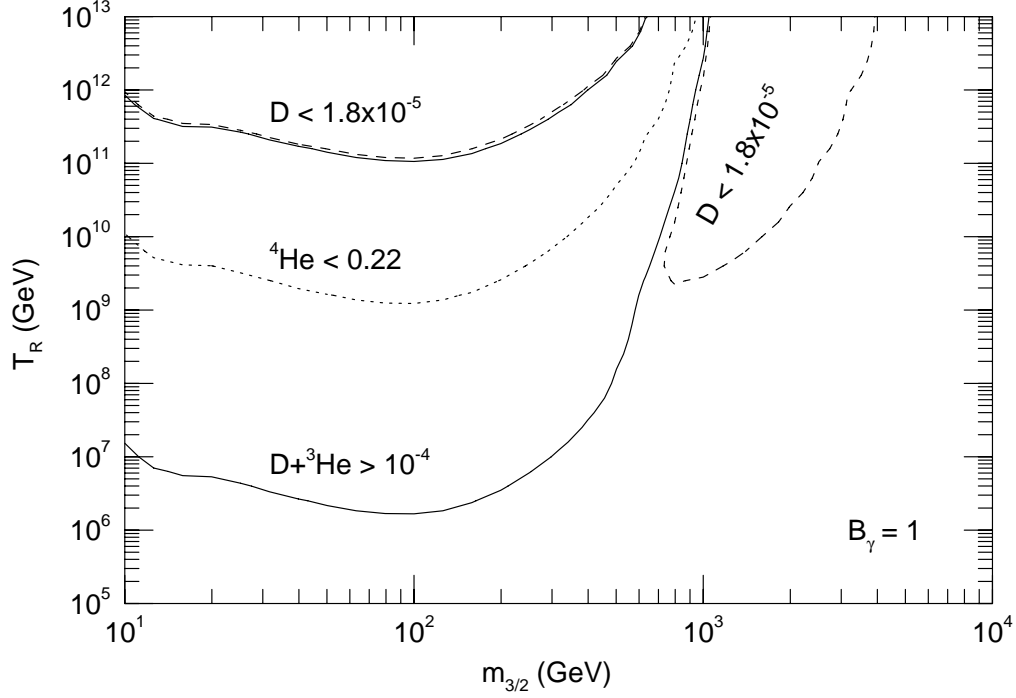


Figure 6.6: Upperbound on T_R as a function of $m_{3/2}$. Here, we take $B_\gamma = 1$. In the region above the solid curve ${}^3\text{He}$ and D are overproduced, the abundance of ${}^4\text{He}$ is less than 0.22 above the dotted curve and the abundance of D is less than 1.8×10^{-5} above the dashed curve.

are the same as those in the standard BBN. The effect of the photo-dissociation due to gravitino decay becomes significant as the reheating temperature increases.

As seen in Fig. 6.2 – Fig. 6.5, the allowed range of the baryon-to-photon ratio is almost same as that without gravitino for $m_{3/2} \lesssim 1\text{TeV}$, *i.e.* a very narrow range around $\eta_B \sim 3 \times 10^{-10}$ is allowed. However, for the cases of $m_{3/2} \sim 1\text{TeV}$ and $T_R \sim 10^9\text{GeV}$ or $m_{3/2} \sim 1\text{TeV}$ and $T_R \sim 10^{12}\text{GeV}$, lower values of η_B are allowed (Fig. 6.4). In this case, the critical photon energy ($\sim m_e^2/22T$) for the double photon pair creation process is lower than the threshold of photo-dissociation reaction of ${}^4\text{He}$. Therefore, for $T_R \lesssim 10^{12}\text{GeV}$, the abundance of ${}^4\text{He}$ is not affected by the gravitino decay. Then, the emitted photons only destroy ${}^3\text{He}$ and D whose abundances would be larger than the observational constraints for low baryon density if gravitino did not exist. Therefore one sees the narrow allowed band at $T_R \simeq 10^9\text{GeV}$ where only a small number of ${}^3\text{He}$ and D are destroyed to satisfy the constraints (6.23) and (6.24). For $T_R \gtrsim 10^{12}\text{GeV}$, since a large number of high energy photons are produced even above the threshold of double photon pair creation, a part of ${}^4\text{He}$ are destroyed to produce ${}^3\text{He}$ and D , which leads to the very narrow allowed region at $T_R \sim 10^{12}\text{GeV}$. However, even in this special case the upper limit of allowed reheating temperature changes very little between $\eta_B = 10^{-10}$ and $\eta_B \sim 3 \times 10^{-10}$. This allows us to fix $\eta_B = 3.0 \times 10^{-10}$ in deriving the upperbound on the reheating temperature.

The allowed regions that satisfy the observational constraints (6.22) – (6.24) are also

shown in Fig. 6.6 in the $m_{3/2} - T_R$ plane for the case of $\eta_B = 3 \times 10^{-10}$ and $B_\gamma = 1$. In Fig. 6.2 – Fig. 6.5 and Fig. 6.6 one can see four typical cases depending on T_R and $m_{3/2}$.

- $m_{3/2} \lesssim 1\text{TeV}$, $T_R \lesssim 10^{11}\text{GeV}$;

In this case the lifetime of the gravitino is so long that the critical energy for the double photon process ($\sim m_e^2/22T$) is higher than the threshold of the photo-dissociation reactions for ^4He at the decay time of gravitino. Thus ^4He is destroyed to produce T, ^3He and D. (Since T becomes ^3He by β -decay, hereafter we denote T and ^3He by the word “ ^3He ”.) Since the reheating temperature is not so high, the number density of gravitino is not high enough to destroy all the light elements completely. As a result, ^3He and D are produced too much and the abundance of ^4He decreases. To avoid the overproduction of ($^3\text{He} + \text{D}$), the reheating temperature should be less than $\sim (10^6 - 10^9)\text{GeV}$.

- $m_{3/2} \lesssim 1\text{TeV}$, $T_R \gtrsim 10^{11}\text{GeV}$;

The lifetime is long enough to destroy ^4He and the gravitino abundance is so large that all the light elements are destroyed since the reheating temperature is high enough. This parameter region is strongly excluded by the observation.

- $1\text{TeV} \lesssim m_{3/2} \lesssim 3\text{TeV}$;

The lifetime becomes shorter as the mass of gravitino increases, and the decay occurs when the double photon pair creation process works well. If the cosmic temperature at $t \sim \tau_{3/2}$ is greater than $\sim m_e^2/22E_{^4\text{He}}$ (where $E_{^4\text{He}} \sim 20\text{MeV}$ represents the typical threshold energy of ^4He destruction processes), ^4He abundance is almost unaffected by the high energy photons as can be seen in Fig. 6.4. In this parameter region, the overproduction of ($\text{D} + ^3\text{He}$) cannot occur since ^4He is not destroyed. In this case, the destruction of D is the most important to set the limit of the reheating temperature. This gives the constraint of $T_R \lesssim (10^9 - 10^{12})\text{GeV}$.

- $m_{3/2} \gtrsim 3\text{TeV}$;

In this case the gravitinos decay when the temperature of the universe is so high that all high energy photons are quickly thermalized by the double photon process before they destroy the light elements. Therefore, the effect on the BBN is negligible. Fig. 6.5 is an example of this case. The resultant contours for abundances of light elements are almost identical as those without the decaying gravitino.

So far we have assumed that all gravitinos decay into photons and photinos. But if other superpartners are also lighter than the gravitino, the decay channels of gravitino increases and the branching ratio for the channel $\psi_\mu \rightarrow \gamma + \tilde{\gamma}$ becomes less than 1. In this case, various decay products affect the evolution of the universe and BBN. In this thesis, instead of studying all decay channels, we consider only the $\gamma + \tilde{\gamma}$ channel with taking the branching ratio B_γ as another free parameter. With this simplification, the effect of all possible decay

products other than photon is not taken into account. Therefore, the resultant constraints on the reheating temperature and the mass of gravitino should be taken as the conservative constraints since other decay products may destroy more light elements and make the constraints more stringent.

Although we have four free parameters in the present case, the result for $B_\gamma = 1$ implies that the allowed range of T_R and $m_{3/2}$ is obtained taking the baryon-to-photon ratio to be 3×10^{-10} . Since our main concern is to set the constraints on T_R and $m_{3/2}$, we can safely fix η_B as 3×10^{-10} .

The constraints for $B_\gamma = 0.1$ and $B_\gamma = 0.01$ are shown in Fig. 6.7 and Fig. 6.8 which should be compared with Fig. 6.6 (*i.e.* the case of $B_\gamma = 1$). Since the number density of the high energy photons is proportional to B_γ , the constraint on the reheating temperature becomes less stringent as B_γ decreases. In addition, the total lifetime of gravitino is given by

$$\tau_{3/2} = \tau(\psi_\mu \rightarrow \gamma + \tilde{\gamma}) \times B_\gamma. \quad (6.25)$$

Thus the gravitinos decay earlier than for the $B_\gamma = 1$ case, and hence the constraints from ($^3\text{He} + \text{D}$) overproduction becomes less stringent. This effect can be seen in Fig. 6.7, where the constraint due to the overproduction of ($^3\text{He} + \text{D}$) has a cut at $m_{3/2} \simeq 400\text{GeV}$ compared with $\sim 1\text{TeV}$ for $B_\gamma = 1$.

In Fig. 6.9, the contours for the upperbound on reheating temperature are shown in the $m_{3/2} - B_\gamma$ plane. One can see that the stringent constraint on T_R is obtained for $m_{3/2} \lesssim 100\text{GeV}$ even if the branching ratio is small. Notice that the actual constraint may become more stringent if we take the effects of other decay products into account.

6.4 BBN with high energy neutrino injection

As seen in the previous section, the existence of the unstable gravitino which decays into a photon and a photino set a stringent upperbound on the reheating temperature T_R . However, the constraints might become much weaker when the gravitino decays only into weakly interacting particles. In the particle content of the MSSM, the only candidate is the decay into a neutrino and a sneutrino.

Even if the gravitino decays only into a neutrino and a sneutrino, the emitted high energy neutrino may scatter off the background neutrino and produce an electron-positron (or muon-anti-muon) pair, which then produces many soft photons through electro-magnetic cascade processes and destruct light elements. Since the interaction between the high energy neutrinos and the background neutrinos is weak, it seems that the destruction of the light elements is not efficient. In fact, Gratsias, Scherrer and Spergel [58] showed that the constraint is not so stringent for the case where the gravitino decays into a neutrino and a sneutrino. However the previous analysis seems to be incomplete in a couple of points. First, Gratsias et al. [58] totally neglected the secondary high energy neutrinos which are produced by the neutrino-neutrino scattering. The effect of the secondary neutrino may

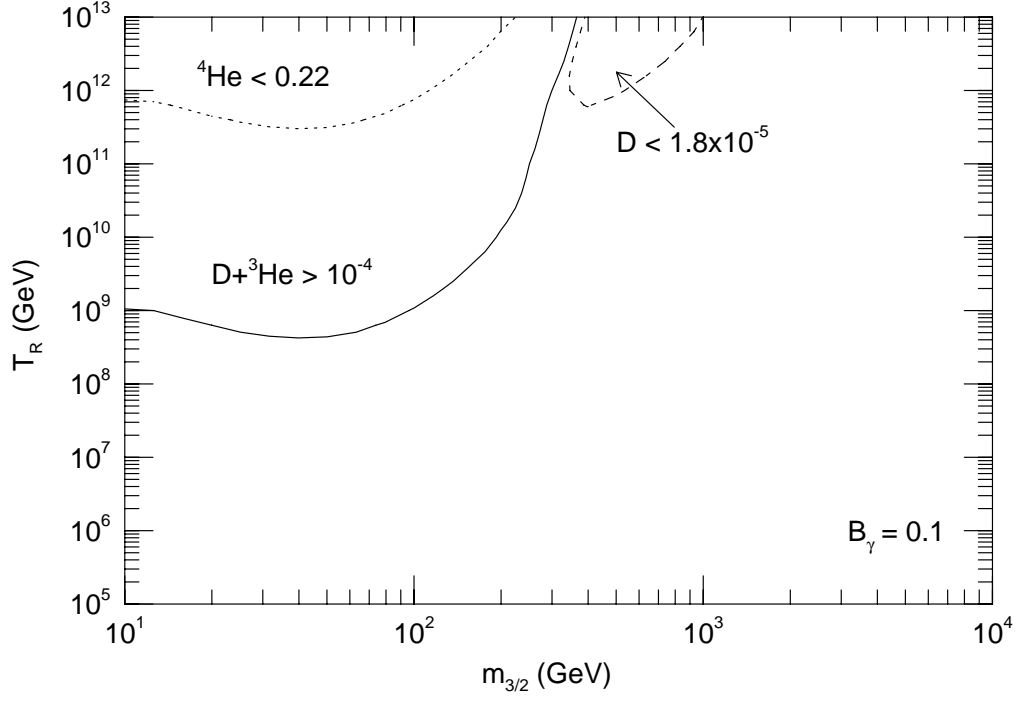


Figure 6.7: Same as Fig. 6.6 except for $B_\gamma = 0.1$.

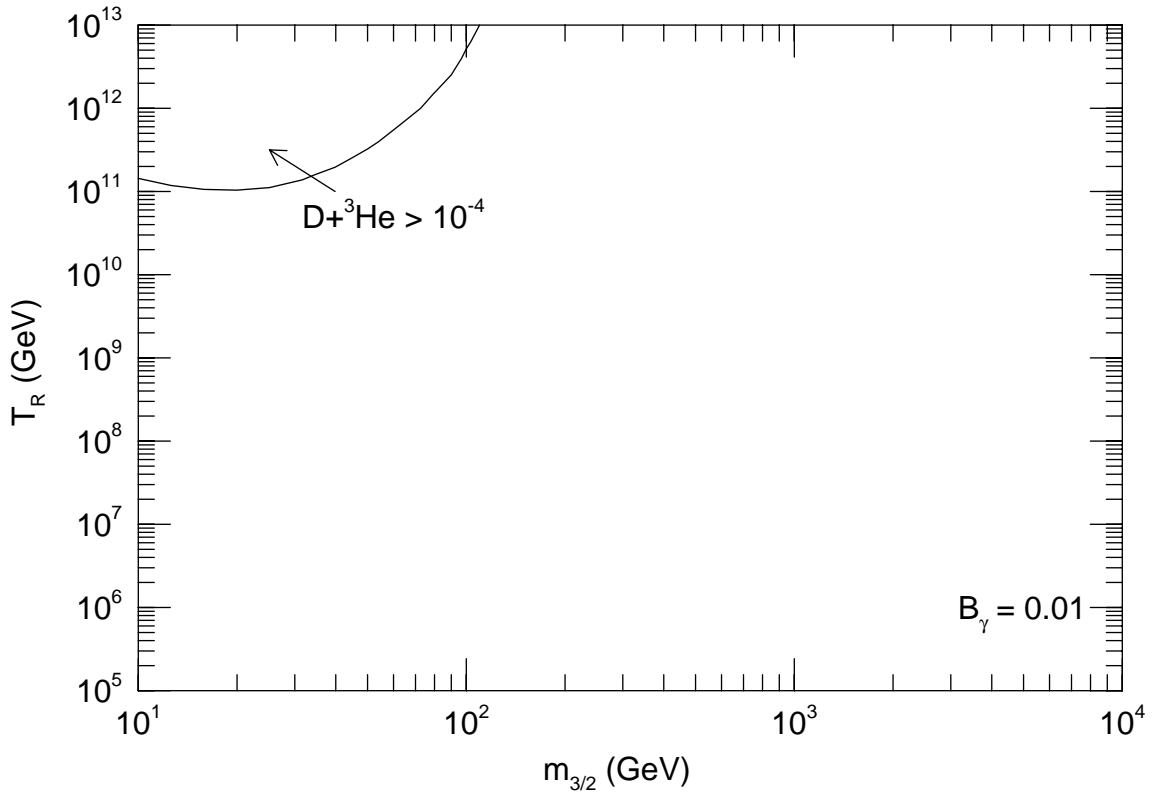


Figure 6.8: Same as Fig. 6.6 except for $B_\gamma = 0.01$.

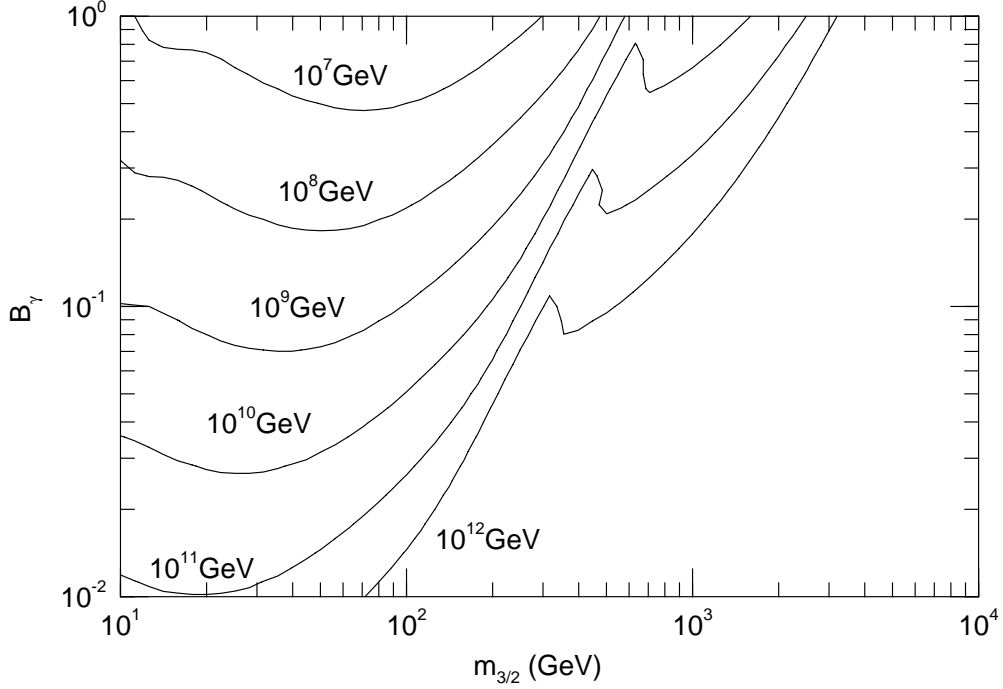


Figure 6.9: Contours for the upper limits of the reheating temperature in the $m_{3/2} - B_{\gamma}$ plane. The numbers in the figure denote the limit of the reheating temperature.

be important for the heavy gravitino case ($m_{3/2} \gtrsim 1\text{TeV}$). Second, they only studied the case where the destruction of ^4He results in the overproduction of ($^3\text{He} + \text{D}$). However, for the heavy gravitino which decays in early stage of the BBN, the destruction of D is more important since the electro-magnetic cascade process is so efficient that the energy of soft photons becomes less than the threshold of ^4He destruction. Furthermore, as pointed out in the previous section, the previous estimation of the gravitino production in the reheating epoch after the inflation is underestimated. Those effects which are not taken into account in ref.[58] may lead to a more stringent constraint on the reheating temperature. Therefore, in this section we reexamine the effects of the decay of the gravitino into a neutrino and a sneutrino ($\psi_{\mu} \rightarrow \nu + \tilde{\nu}$) with taking all relevant processes into account [47].

The high energy neutrinos ν produced in the gravitino decay scatter off the thermal neutrino ν_b in the background through the following processes;

$$\nu_i + \nu_{i,b} \rightarrow \nu_i + \nu_i, \quad (6.26)$$

$$\nu_i + \bar{\nu}_{i,b} \rightarrow \nu_i + \bar{\nu}_i, \quad (6.27)$$

$$\nu_i + \bar{\nu}_{i,b} \rightarrow \nu_j + \bar{\nu}_j, \quad (6.28)$$

$$\nu_i + \nu_{j,b} \rightarrow \nu_i + \nu_j, \quad (6.29)$$

$$\nu_i + \bar{\nu}_{j,b} \rightarrow \nu_i + \bar{\nu}_j, \quad (6.30)$$

$$\nu_i + \bar{\nu}_{i,b} \rightarrow e^- + e^+, \quad (6.31)$$

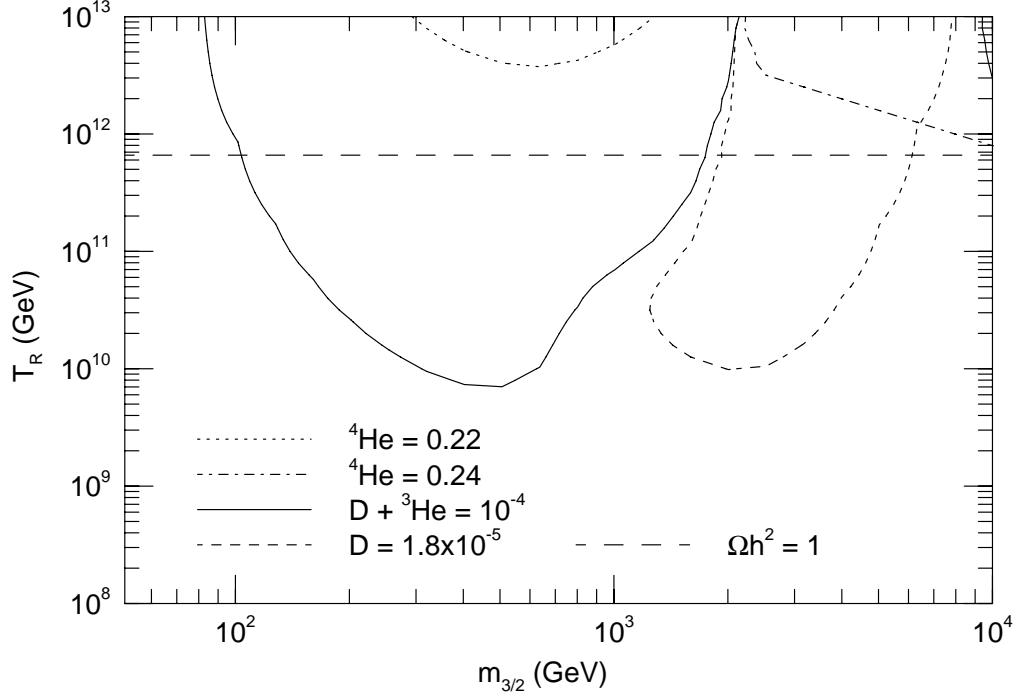


Figure 6.10: Upperbound on the reheating temperature from BBN and the present mass density of the sneutrino. The region above the curves is excluded.

$$\nu_i + \bar{\nu}_{i,b} \rightarrow \mu^- + \mu^+, \quad (6.32)$$

where index i and j represent e , μ and τ with $i \neq j$. The primary and secondary high energy neutrinos scatter off the background neutrinos and produce charged lepton pairs. Then, the charged leptons produced in the processes (6.31) and (6.32) induce the electro-magnetic cascade processes. By the same procedure as in the previous section, we obtain the high energy photon and the electron spectra. The detailed analysis of the neutrino spectrum is given in Appendix B.

The photo-dissociation of the light elements are analyzed in the same way as in the previous section. In the present calculation, there are at least three free parameters, *i.e.* the mass of the gravitino $m_{3/2}$, the reheating temperature T_R and the baryon-to-photon ratio η_B . However as shown in the previous section, the baryon-to-photon ratio η_B is not important parameter because the allowed value for η_B is almost the same as that in the standard case (*i.e.* without gravitino). Therefore, we fix $\eta_B = 3 \times 10^{-10}$ in the following analysis.

The allowed regions that satisfy the observational constraints (6.22) – (6.24) are shown in the $m_{3/2} - T_R$ plane in Fig. 6.10. In Fig. 6.10 one can see that for the gravitino of mass between 100GeV and 1TeV, the overproduction of D and ^3He gives the most stringent constraint, while the upperbound on the reheating temperature is determined from the destruction of D for $m_{3/2} \simeq (1 - 3)\text{TeV}$. Notice that D destruction was not considered in the previous work [58]. Furthermore, the constraint from $(\text{D} + ^3\text{He})$ overproduction is more

stringent. The reasons why we obtain the more stringent constrain are (i) the gravitino abundance is $(4 - 5)$ times larger than the one that the previous authors used, (ii) the secondary neutrinos are taken into account in our calculation, and (iii) the gravitino lifetime for $\psi_\mu \rightarrow \nu + \tilde{\nu}$ is longer by a factor 2 than the lifetime for $\psi_\mu \rightarrow \gamma + \tilde{\gamma}$. (In ref.[58] it is presumed that $\Gamma_{3/2}(\psi_\mu \rightarrow \nu + \tilde{\nu}) = \Gamma_{3/2}(\psi_\mu \rightarrow \gamma + \tilde{\gamma})$.)

6.5 Discussion about hadron injection

In the previous sections, we have assumed that the gravitino only decays into non-hadronic particles, and derived constraints on the reheating temperature. If the gravitino produces hadronic decay products, however, the previous constraints may change. In this section, we will briefly discuss the effect of such strongly interacting decay products.

The effects of the hadronic decay products on the BBN are investigated by several authors [59, 60, 61], and the standard BBN scenario may be affected by the following processes.

- Injecting high energy particles at the time $(1 - 10^2)\text{sec}$ cause non-standard $p \leftrightarrow n$ conversion processes. The major effect is to induce $p \rightarrow n$ reactions because there are more target protons than target neutrons. The extra neutrons produced in this period results in overproduced ^4He abundance.
- Hadronic decay of the gravitino with lifetime $\tau_{3/2} \gtrsim 10^2 \text{ sec}$ causes dissociation processes of light elements. Especially even in the case $\tau_{3/2} \lesssim 10^4 \text{ sec}$ in which the light element photo-dissociation processes are not effective, ^4He may be significantly destroyed to produce D and ^3He .

In the following, we discuss the above effects.

The $p \leftrightarrow n$ conversion induced by hadronic injection was studied by Reno and Seckel [59] in details. In the standard BBN scenario, the neutron fraction in the thermal bath changes from ~ 0.16 (at $T \sim 0.7\text{MeV}$) to ~ 0.12 (at $T \sim 0.08\text{MeV}$). Hadronic injection at this period ($0.7\text{MeV} \lesssim T \lesssim 0.08\text{MeV}$) affects this evolution. Reno and Seckel claimed that the yield of the gravitino $Y_{3/2}$ should be smaller than $O(10^{-11} - 10^{-12})$ in order not to overproduce ^4He . From this bound, we can estimate that the reheating temperature T_R should be lower than $O((10^{10} - 10^{11})\text{GeV})$ for the case $10\text{TeV} \lesssim m_{3/2} \lesssim 100\text{TeV}$.

If the gravitino lifetime is longer than $\sim 100\text{sec}$, gravitinos decay after the “deuterium bottleneck” breaks. In this case, emitted hadrons induce light element destruction processes, which give more stringent constraint than that from ^4He overproduction. These processes are analyzed in ref.[59] (for the case $\tau_{3/2} \lesssim 10^4\text{sec}$), and in refs.[60, 61] (for the case $\tau_{3/2} \gtrsim 10^4\text{sec}$).

For the case $10^2\text{sec} \lesssim \tau_{3/2} \lesssim 10^4\text{sec}$, $(\text{D} + ^3\text{He})$ overproduction induced by ^4He destruction gives a constraint. According to ref.[59], the reheating temperature T_R should be lower than $O((10^8 - 10^{11})\text{GeV})$ if the gravitino mass is given by $(1-10)\text{TeV}$.

If the gravitino lifetime is longer than $\sim 10^4\text{sec}$, photo-dissociation of light elements becomes effective. In this case, we should take the effects of high energy photons as well as

injected hadrons into account. As discussed in refs. [60, 61], the main effects of the hadronic injection in this case is the destruction of ${}^4\text{He}$, and the creation of D, ${}^3\text{He}$, ${}^6\text{Li}$ and ${}^7\text{Li}$. According to refs. [60, 61], the hadronic branching ratio must be very small in order not to overproduce (D+ ${}^3\text{He}$), and hence the constraint is almost the same as in the case $B_\gamma = 1$, except for the case $\tau_{3/2} \sim 10^{5-6}\text{sec}$. In a small parameter region $\tau_{3/2} \sim 10^{5-6}\text{sec}$, one may avoid the severe constraint even in the case $B_\gamma = 1$ by assuming the non-vanishing hadronic branching ratio, since the effect of photo-dissociation of D is compensated by the supply of D through the ${}^4\text{He}$ destruction processes. However in this case, ${}^6\text{Li}$ and ${}^7\text{Li}$ seem to be overproduced. Furthermore, as discussed in ref.[60] some uncertainties exist in the analysis of refs.[60, 61]. The most important source of uncertainty is in the experimental data of hadron scattering processes, especially those concerning Li. Therefore, it is unclear to us if the scenario proposed in refs.[60, 61] works well.

6.6 Other constraints

In the previous sections, we have considered the constraints from the photo-dissociation of light elements. But as we have seen, if the mass of the gravitino is larger than a few TeV, the gravitino decay does not induce light element photo-dissociation and no constraints have been obtained. In this case, we must consider other effects of the gravitino.

If we consider the present mass density of the LSP produced by the gravitino decay, we can get the upperbound on the reheating temperature. In SUSY models with R -invariance (which is an usual assumption), the LSP (in the previous cases, photino or sneutrino) is stable. Thus the LSPs produced by the decay of gravitinos survive until today, and they contribute to the energy density of the present universe. Since one gravitino produces one LSP, we can get the present number density of the LSP n_{LSP} as

$$n_{LSP} = Y_{3/2}(T \ll 1\text{MeV}) \times \frac{\zeta(3)}{\pi^2} T_{NOW}^3, \quad (6.33)$$

where $T_{NOW} \simeq 2.7\text{K}$ is the present temperature of the universe.⁴ The density parameter of the LSP

$$\Omega_{LSP} \equiv \frac{m_{LSP} n_{LSP}}{\rho_c}, \quad (6.34)$$

can be easily calculated, where m_{LSP} is the mass of the LSP, $\rho_c \simeq 8.1 \times 10^{-47} h^2 \text{GeV}^4$ is the

⁴In calculating eq.(6.33), we have ignored the effect of the pair annihilation of the LSP ($\tilde{\gamma} + \tilde{\gamma} \rightarrow f + \bar{f}$, or $\tilde{\nu} + \tilde{\nu}^* \rightarrow f + \bar{f}$). For the pair annihilation processes, the cross section is roughly estimated as $\sigma v \lesssim \alpha_W / m_{LSP}^2$ (where α_W is the coupling factor and v is the relative velocity), and the condition for sufficiently large pair annihilation rate ($n_{LSP} \sigma v \gtrsim H$, with n_{LSP} being the number density of the LSP) reduces to $n_{LSP} / n_\gamma \gtrsim 10^{-7}$ (with Y_{LSP} being the yield variable for the LSP), which is less stringent than the constraint (6.35). However, if the LSP mass is small enough to hit the pole of the Z^0 -boson propagator, the constraint (6.35) may become weaker, and the constraint from the ${}^4\text{He}$ overproduction may become significant for the large gravitino mass case ($m_{3/2} \gtrsim 3\text{TeV}$).

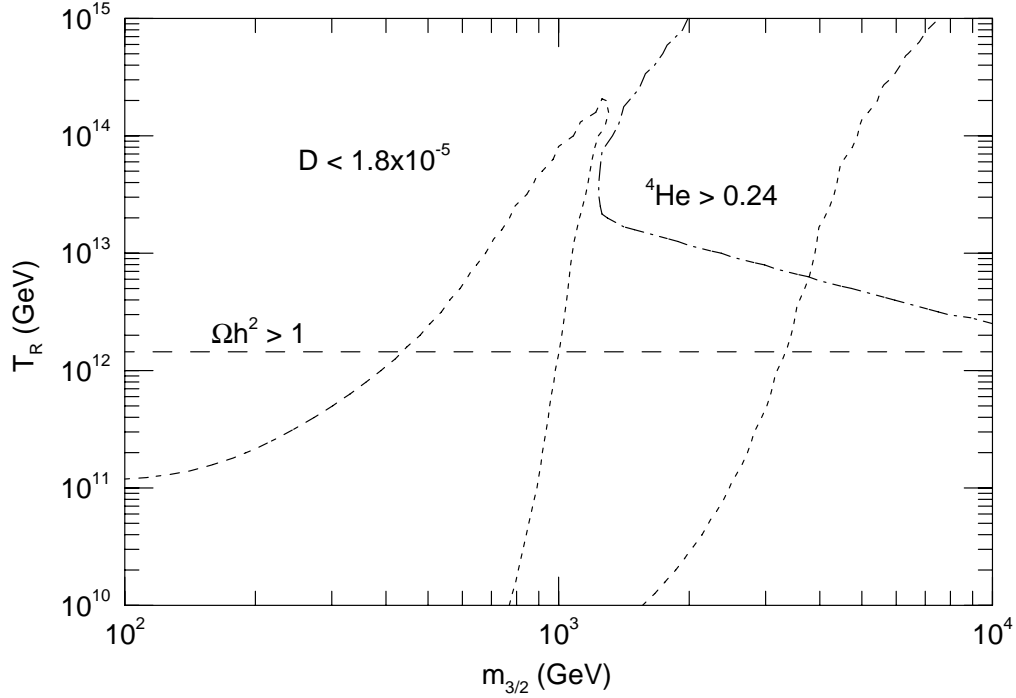


Figure 6.11: Upperbound of the reheating temperature. Dashed line represents the constraint from the present mass density of photino. Dotted-dashed line represents the upperbound requiring ${}^4\text{He} < 0.24$. Constraints from D photo-dissociation is also shown by dotted line.

critical density of the universe and h is the Hubble parameter in units of 100km/sec/Mpc. If we impose $\Omega_{LSP} \leq 1$ in order not to overclose the universe, the upperbound on the reheating temperature is given by

$$T_R \leq 2.7 \times 10^{11} \left(\frac{m_{LSP}}{100\text{GeV}} \right)^{-1} h^2 \text{ GeV}, \quad (6.35)$$

where we have ignored the logarithmic correction term of Σ_{tot} .

To set the upperbound on the reheating temperature, we need to know the mass of the LSP. First let us consider the case where the LSP is photino. In this case, if one assumes the gaugino-mass unification condition, the lower limit of the mass of photino is 18.4GeV [62]. Then we can get the following upperbound on the reheating temperature;

$$T_R \leq 1.5 \times 10^{12} h^2 \text{ GeV} \quad (\text{if the LSP is photino}). \quad (6.36)$$

This constraint is shown in Fig. 6.11. Notice that this bound is independent of the gravitino mass and branching ratio. If the LSP is sneutrino, the present limit on sneutrino mass 41.8GeV [24] sets the upperbound on the reheating temperature;

$$T_R \leq 6.6 \times 10^{11} h^2 \text{ GeV} \quad (\text{if the LSP is sneutrino}), \quad (6.37)$$

which is also shown in Fig. 6.10.

Another important constraint comes from the effect on the cosmic expansion rate at the BBN. As mentioned before, if the density of gravitino in the nucleosynthesis epoch becomes higher, the expansion of the universe increases, which leads to more abundance of ^4He . We study this effect by using the modified Kawano code and show the result in Fig. 6.11. In the calculation, we take $\eta_B = 2.8 \times 10^{-10}$ and $\tau_n = 887 \text{ sec}$ (where $\tau_n = (889 \pm 2.1) \text{ sec}$ is the neutron lifetime [24]) so that the predicted ^4He abundance is minimized without conflicting the observational constraints on other light elements. The resultant upperbound on the reheating temperature is approximately given by

$$T_R \lesssim 2 \times 10^{13} \text{ GeV} \left(\frac{m_{3/2}}{1 \text{ TeV}} \right)^{-1}, \quad (6.38)$$

for $m_{3/2} \geq 1 \text{ TeV}$.⁵ This bound is also shown in Fig. 6.11 by the solid line. Notice that this bound is derived irrespective of the species of the LSP.

⁵For the case $m_{3/2} \leq 1 \text{ TeV}$, primordial ^4He is destroyed by the high energy photons induced by the decay of the gravitino, and hence the constraint (6.38) becomes insignificant. However, if the gravitino decays into a neutrino and a sneutrino, this is not the case.

Chapter 7

Cosmology with stable gravitino

In the previous chapter, we have studied cosmology with unstable gravitino and derived constraints on the reheating temperature after inflation. However, there is another possibility that the gravitino is stable and hence it is the LSP. In this case, the constraints obtained in the previous chapter are not appropriate. In this chapter, we study cosmological constraints when the gravitino is the LSP.¹

7.1 Constraints from the mass density of the universe

In the case of the stable gravitino, the Boltzmann equation for the gravitino number density $n_{3/2}$ is given by

$$\frac{dn_{3/2}}{dt} + 3Hn_{3/2} = \left\langle \Sigma_{tot}^{(1/2)} v_{rel} \right\rangle n_{rad}^2 + \sum_{\tilde{i}} n_{\tilde{i}} \frac{m_{\tilde{i}}}{\langle E_{\tilde{i}} \rangle} \Gamma_{\tilde{i}}, \quad (7.1)$$

where $n_{\tilde{i}}$ is the number density of the superparticle \tilde{i} , $\Gamma_{\tilde{i}}$ the decay rate of \tilde{i} into its superpartner and a gravitino, and $m_{\tilde{i}}/\langle E_{\tilde{i}} \rangle$ the Lorentz factor. Notice that the first term in the right-hand side of eq.(7.1) represents the contribution from the scattering processes off thermal radiations, while the second one is that from the decay of superparticles into a gravitino and some ordinary particles.²

Here we comment on $\Sigma_{tot}^{(1/2)}$. If the gravitino mass is small compared with the typical mass splitting in the matter sector, interactions of the helicity $\pm\frac{1}{2}$ modes of the gravitino become stronger than that of the helicity $\pm\frac{3}{2}$ modes. From this fact, we conclude that the helicity $\pm\frac{1}{2}$ gravitino production processes are the most significant in this case. As we can see in eq.(4.73), the interactions of the gravitino to gauge multiplets are described by dimension-five operators and those to chiral multiplets by dimension-four ones. Therefore, the former

¹This chapter is based on the work in a collaboration with H. Murayama and M. Yamaguchi [42].

²In the case of heavy unstable gravitino analyzed in the previous chapter, we have ignored the contribution from the decay of the superparticles (or its inverse processes). In fact, these contributions are significant only for the case of extremely light gravitino ($m_{3/2} \lesssim 10^{-4}\text{GeV}$, as we will see later), and hence our approximation is justified.

dominates the gravitino production at high temperatures. For the MSSM particle content, $\Sigma_{tot}^{(1/2)}$ is given by

$$\begin{aligned}\Sigma_{tot}^{(1/2)} &= \frac{1}{2} \sum_{x,y,z} \eta_x \eta_y \sigma(x+y \rightarrow \psi+z) \\ &= \frac{1}{24\pi m_{3/2}^2 M^2} \left(2.44 g_1^2 m_{G1}^2 + 9.16 g_2^2 m_{G2}^2 + 26.00 g_3^2 m_{G3}^2 \right),\end{aligned}\quad (7.2)$$

where $\sigma(x+y \rightarrow \psi+z)$ is the helicity $\pm\frac{1}{2}$ gravitino production cross section (see Table 4.3), $m_{G3} - m_{G1}$ are the gauge fermion masses, and $g_3 - g_1$ are the gauge coupling constants.

Using the yield variable $Y_X \equiv n_X/n_{rad}$ and the condition of “naive” adiabatic expansion (6.7), eq.(7.1) is rewritten as

$$\frac{dY_{3/2}}{dT} = -\frac{n_{rad} \langle \Sigma_{tot} v_{rel} \rangle}{HT} - \sum_{\tilde{i}} \frac{m_{\tilde{i}} \langle E_{\tilde{i}} \rangle}{HT} \Gamma_{\tilde{i}} Y_{\tilde{i}}. \quad (7.3)$$

Integrating this equation from T_R to T ($T_R \gg T$) and taking the effects of the dilution factor ($N_S(T)/N_S(T_R)$) into account, we get

$$Y_{3/2}(T) = \frac{N_S(T)}{N_S(T_R)} \times \left\{ \bar{Y}_{scatt}(T) + \bar{Y}_{decay}(T) \right\}. \quad (7.4)$$

with

$$\bar{Y}_{scatt} = \frac{n_{rad}(T_R) \langle \Sigma_{tot}^{(1/2)} v_{rel} \rangle}{H(T_R)}, \quad (7.5)$$

$$\bar{Y}_{decay} = \int_T^{T_R} \frac{dT}{T} \sum_{\tilde{i}} \frac{m_{\tilde{i}} \Gamma_{\tilde{i}}}{\langle E_{\tilde{i}} \rangle H}. \quad (7.6)$$

From eq.(7.5), we can see that \bar{Y}_{scatt} is proportional to the reheating temperature T_R . On the other hand, \bar{Y}_{decay} is almost independent of T_R as far as the reheating temperature is higher than the masses of the superparticles. Notice that effects of the gravitino annihilation processes cannot be ignored in eq.(7.1) if the \bar{Y}_{scatt} in eq.(7.5) or the \bar{Y}_{decay} in eq.(7.6) becomes $O(1)$. We take these effects into account by the following simple method; in the case where the sum of the right hand sides of eq.(7.5) and eq.(7.6), which is the yield of the thermal helicity $\pm\frac{1}{2}$ gravitino, is larger than $\frac{3}{2}$, we consider that the gravitinos are thermalized and take $\bar{Y}_{scatt} + \bar{Y}_{decay} = \frac{3}{2}$.

Using eq.(7.5) and eq.(7.6), we estimate the present gravitino number density and determine the upperbound on the reheating temperature by using the closure limit. In our numerical calculation, we take all the squark and slepton masses to be 1 TeV and the GUT

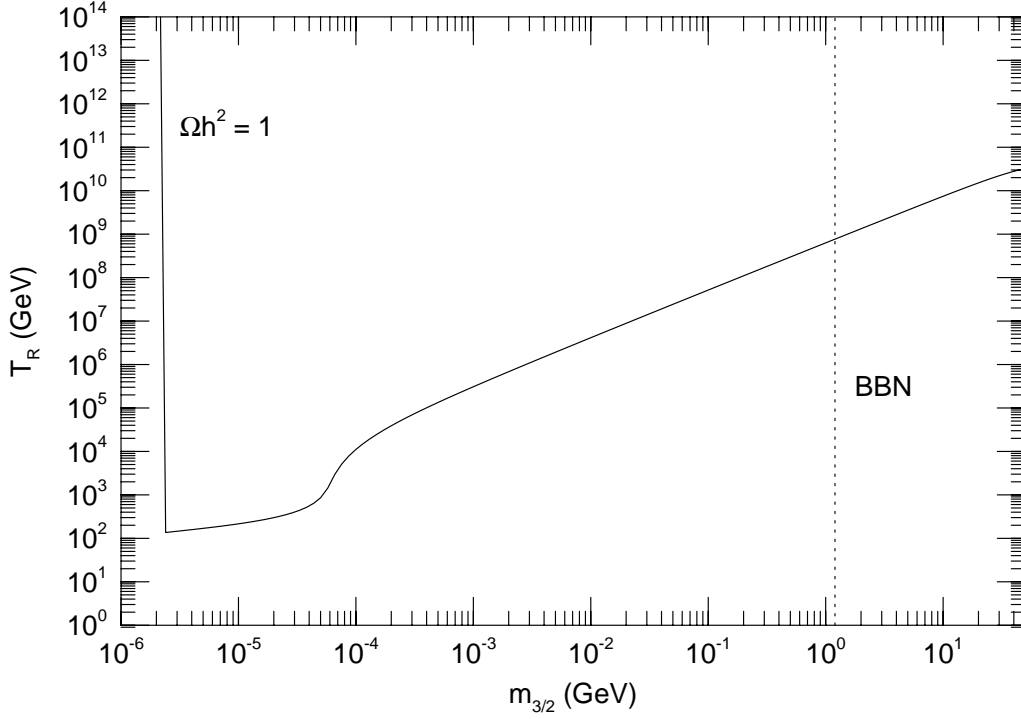


Figure 7.1: Cosmological constraints on the gravitino mass $m_{3/2}$ and the reheating temperature T_R in the framework of the MSSM when the gravitino is the LSP. We take all the squark and slepton masses to be 1 TeV, $m_{G1} = m_{NSP} = 50\text{GeV}$ and the GUT relation on the gauge fermion masses is assumed. The solid line denotes the upperbound on the reheating temperature from the closure limit. The dotted line is the upperbound on the gravitino mass from light element photo-dissociation. We assume the NSP relic density as given in eq.(7.11), and require the NSP lifetime to be shorter than 2.6×10^6 sec.

relation on the gaugino masses;

$$\frac{3}{5} \frac{m_{G1}}{g_1^2} = \frac{m_{G2}}{g_2^2} = \frac{m_{G3}}{g_3^2}. \quad (7.7)$$

Energy density of the gravitino $\rho_{3/2}$ is given by

$$\rho_{3/2}(T) = m_{3/2} Y_{3/2}(T) n_{rad}(T), \quad (7.8)$$

and we determine the upperbound on T_R by the condition

$$\rho_{3/2}(T_{NOW}) \leq \rho_c, \quad (7.9)$$

where $T_{NOW} \simeq 2.7\text{K}$ and $\rho_c \simeq 8.1 \times 10^{-47} h^2 \text{ GeV}^4$ ($0.4 \lesssim h \lesssim 1$) is the critical density of the present universe.

The result is shown in Fig. 7.1. Here we take $m_{G1} = m_{NSP} = 50 \text{ GeV}$ with m_{NSP} being the mass of the next-to-the-lightest superparticle (NSP), and to get a conservative bound we

take $h = 1$. For $m_{3/2} \gtrsim 10^{-4}$ GeV, the upperbound on T_R is approximately proportional to $m_{3/2}$. When 2×10^{-6} GeV $\lesssim m_{3/2} \lesssim 10^{-4}$ GeV, the upperbound on T_R is around $O(100 \text{ GeV})$. And for the very light gravitino case ($m_{3/2} \lesssim 2 \times 10^{-6}$ GeV), there is no constraint on T_R . These features can be understood in the following way. When the gravitino mass is larger than about 10^{-4} GeV, interactions are so weak that decaying processes cannot produce sufficient gravitinos to overclose the universe. Therefore, it is the scattering process that is important to estimate the number density of the gravitino. In this case,

$$Y_{3/2}(T_{NOW}) = \frac{N_S(T_{NOW})}{N_S(T_R)} \frac{\sqrt{90}\zeta(3)M}{\pi^3\sqrt{N_*}} T_R \langle \Sigma_{tot} v_{rel} \rangle, \quad (7.10)$$

from eq.(7.5). Combining eq.(7.10) with eq.(7.9), we get the upperbound on the reheating temperature, which is approximately proportional to the gravitino mass. On the other hand, if 2×10^{-6} GeV $\lesssim m_{3/2} \lesssim 10^{-4}$ GeV, the decay processes become significant. In this case, $\rho_{3/2}$ is larger than ρ_c unless the reheating temperature is smaller than the squark and slepton masses. Therefore, it is necessary to lower the reheating temperature below the squark and slepton mass scale in order not to overclose the universe. And when $m_{3/2} \lesssim 2 \times 10^{-6}$ GeV, the gravitino mass is so small that $\rho_{3/2}$ cannot exceed ρ_c even if the gravitino is thermalized.

7.2 Constraint from BBN

Next, let us consider the constraint from the light element photo-dissociation. If a decay of a heavy particle produces high energy photons after the primordial nucleosynthesis, we must require that these photons do not change the abundance of the light elements. Here we consider the decay of the NSP. Since the gravitino is the LSP, the NSP can decay only into a gravitino and some ordinary particles through the supergravity interaction. Therefore, the NSP have much longer lifetime than other superparticles and may affect the predictions of the BBN.

If the NSP were stable, it would survive until today. Its relic density in this case has been calculated [63, 64, 65]. For the neutralinos, in a wide range of parameters, the relic density is larger than 10^{-3} to the critical one. This relic density can be translated into $m_{NSP}Y_{NSP} \geq 5.0 \times 10^{-11} \text{ GeV}$,³ where m_{NSP} and Y_{NSP} are the mass and yield of the NSP. In the following analysis, we conservatively take

$$m_{NSP}Y_{NSP} = 5.0 \times 10^{-11} \text{ GeV}, \quad (7.11)$$

and assume that the NSP decay produces high energy photons. Photo-dissociation of light elements by the NSP decay can be analyzed in the same way as in the case of unstable gravitino. Detailed analysis shows that the energy density of the NSP as large as the one given in eq.(7.11) will overproduce ($^3\text{He} + \text{D}$) unless the lifetime of the NSP is shorter than

³It is plausible that this bound is also valid when a slepton or a chargino is the lightest.

about $2.6 \times 10^6 \text{sec}$. (See Fig. 8.1 – Fig. 8.3 in the next chapter.) Therefore, we impose

$$\left[\frac{1}{48\pi} \frac{m_{NSP}^5}{m_{3/2}^2 M^2} \left\{ 1 - \left(\frac{m_{3/2}}{m_{NSP}} \right)^2 \right\}^3 \right]^{-1} \leq 2.6 \times 10^6 \text{sec}. \quad (7.12)$$

Here, we assume that the NSP is the $U(1)_Y$ gauge fermion (bino) and used eq.(4.74) for the decay rate of the NSP.⁴ The right hand side of eq.(7.12) strongly depends on the NSP mass and especially when the NSP mass is small, a severe upperbound on the gravitino mass is obtained. The bound we obtained is $m_{3/2} \leq 1.2 \text{ GeV}$ (6.7 GeV, 244.4 GeV, 711.0 GeV) for $m_{NSP} = 50 \text{ GeV}$ (100 GeV, 500 GeV, 1 TeV). This bound for the case of $m_{NSP} = 50 \text{ GeV}$ is also shown in Fig. 7.1. If the reheating temperature is sufficiently low compared to the NSP mass, the NSP is not produced significantly and the above constraint can be avoided. Furthermore, the constraint is not significant when the NSP decay does not produce sufficient photons. This is the case if the NSP is a sneutrino.

7.3 Remarks

Before closing this chapter, we would like to consider phenomenological implications of the gravitino LSP. As we discussed previously, the lightest among the superpartners of the standard model particles is no longer stable. Therefore, this particle (NSP) can be charged or even colored. In a supergravity model with a no-scale like Kähler potential [66], squarks and sleptons are massless at the tree-level. Although they acquire their masses from gaugino masses through radiative corrections, a right-handed charged slepton tends to be the lightest. Indeed with the GUT relation of the gaugino masses, the mass of the right-handed slepton is very close to the $U(1)_Y$ gaugino mass. Detailed analysis showed that a neutral superparticle is the lightest only when its mass is lighter than $\sim 150 \text{ GeV}$ [67, 68]. The gravitino LSP can cure this difficulty of the fascinating class of supergravity model which might be derived from superstring compactification [69]. It can also solve the conflict [70, 71, 72] between the constraints from the mass density of the neutralino LSPs and those from the proton decay in the minimal SUSY $SU(5)$ GUT, because the former gets meaningless when there is a superparticle lighter than the neutralino. In accelerator experiments, the most drastic change occurs when the NSP is charged. Then, we have a chance to find a spectacular track of the charged NSP in a detector.

Finally, we comment on the case where the gravitino is extremely light ($m_{3/2} \ll 1 \text{ keV}$) and interacts strongly. In this case, the gravitino decouples from the thermal bath at temperature well below the electroweak scale. The standard nucleosynthesis scenario constrains the number of the species of the neutrino-like light particles to be smaller than

⁴If the bino is the NSP, it decays into a gravitino and a photon, and into a gravitino and a Z^0 -boson. But when the bino is lighter than the Z^0 -boson, the latter decay channel is forbidden kinematically and the decay rate of the bino is $\sin^2 \theta_W \simeq 0.23$ times smaller than the value of eq.(4.74). For the case $m_{NSP} = 50 \text{ GeV}$, we have considered this effect.

3.3 [49].⁵ Therefore, in order to get a sufficient dilution, the gravitino must decouple before $T \simeq 200$ MeV. After the QCD phase transition, $l + \bar{l} \leftrightarrow \psi + \psi$ scatterings become the most important in the thermalization processes of the gravitino, where l denotes e , μ , ν_e , ν_μ or ν_τ , and \bar{l} its anti-particle. Comparing the gravitino production rate of these processes with the expansion rate of the universe, we get

$$m_{3/2} \gtrsim 10^{-13} \text{ GeV} \times \left(\frac{m_{\tilde{l}}}{100 \text{ GeV}} \right), \quad (7.13)$$

where $m_{\tilde{l}}$ is the slepton mass.⁶ Remember that the interactions of the light gravitino are proportional to $m_{3/2}^{-1}$ as we have seen in Chapter 4, and hence the lowerbound on the gravitino mass is obtained here.

⁵In a recent paper, Kernan and Krauss [73] has claimed that the number of the species of neutrinos N_ν should be smaller than 3.04. In this thesis, however, we use $N_\nu \leq 3.3$ in order to derive a conservative constraint.

⁶One can also consider the constraints from the collider experiments [32, 33] or from the cooling of the red supergiant star [74]. These arguments give similar bound on the gravitino mass.

Chapter 8

Conclusions and discussion

8.1 Summary of conclusions

We summarize the effects of the massive gravitino on the inflationary universe. If the gravitino is unstable and decays only into a photon and a photino, stringent constraints on the reheating temperature are obtained. In the case where the gravitino mass $m_{3/2}$ is less than $\sim 1\text{TeV}$, $(\text{D} + {}^3\text{He})$ overproduction due to the photo-dissociation of ${}^4\text{He}$ set the upperbound on the reheating temperature T_R , $T_R \lesssim 10^{6-9}\text{GeV}$. Constraints in the case $1\text{TeV} \lesssim m_{3/2} \lesssim 3\text{TeV}$, the photo-dissociation of D gives the upperbound on the reheating temperature, $T_R \lesssim 10^{9-12}\text{GeV}$. If the gravitino mass is heavier than $\sim 3\text{TeV}$, the reheating temperature is constrained to be lower than $\sim 10^{12}\text{GeV}$ not to overclose the universe. These constraints are shown in Fig. 6.11;

$$T_R \lesssim 10^{6-7}\text{GeV} \quad (m_{3/2} \lesssim 100\text{GeV}), \quad (8.1)$$

$$T_R \lesssim 10^{7-9}\text{GeV} \quad (100\text{GeV} \lesssim m_{3/2} \lesssim 1\text{TeV}), \quad (8.2)$$

$$T_R \lesssim 10^{9-12}\text{GeV} \quad (1\text{TeV} \lesssim m_{3/2} \lesssim 3\text{TeV}), \quad (8.3)$$

$$T_R \lesssim 10^{12}\text{GeV} \quad (3\text{TeV} \lesssim m_{3/2} \lesssim 10\text{TeV}). \quad (8.4)$$

If most of the decay products of the gravitino are charged particles, above constraints are expected to be valid since the spectrum of the high energy photon is fixed mainly by the total amount of energy injection. An exception is the case where the gravitino only decays into a neutrino and a sneutrino. In this case, the constraints are less stringent than in the case of high energy photon injection, and the constraints are given by

$$T_R \lesssim 10^{12}\text{GeV} \quad (m_{3/2} \lesssim 100\text{GeV}), \quad (8.5)$$

$$T_R \lesssim 10^{10-12}\text{GeV} \quad (100\text{GeV} \lesssim m_{3/2} \lesssim 5\text{TeV}), \quad (8.6)$$

$$T_R \lesssim 10^{12}\text{GeV} \quad (5\text{TeV} \lesssim m_{3/2} \lesssim 10\text{TeV}), \quad (8.7)$$

which are also shown in Fig. 6.10.

If the gravitino is light and stable, interactions of helicity $\pm\frac{1}{2}$ gravitino become strong and a more stringent bound on the reheating temperature is derived from the closure limit;

$$T_R \lesssim 10^{12} \text{GeV} \times \left(\frac{m_{3/2}}{100 \text{GeV}} \right). \quad (8.8)$$

Notice that this constraint is not appropriate for the case $m_{3/2} \lesssim 1 \text{keV}$. Furthermore, the effects of the NSP decay on BBN set the upperbound on the gravitino mass. The detailed value of the upperbound depends on the mass of the NSP. For example, the gravitino mass larger than $\sim 1 \text{GeV}$ is excluded for the case of $m_{NSP} = 50 \text{GeV}$.

8.2 Discussion

We have derived constraints on the reheating temperature after inflation by assuming the existence of the massive gravitino field. As we have seen, cosmological arguments give stringent upperbound on the reheating temperature.

Some comments on our results are in order. When the gravitino is unstable and its mass is smaller than $\sim 1 \text{TeV}$, the upperbound on the reheating temperature is given by $(10^6 - 10^9) \text{GeV}$. This constraint seems to be very stringent since such a low reheating temperature requires very small decay rate of the inflaton field. For example, in a chaotic inflation [77] with a inflaton whose interactions are suppressed by M^{-1} , the decay rate of the inflaton is expected to be $\Gamma_{\text{inf}} \sim m_{\text{inf}}^3/M_{\text{pl}}^2$ with m_{inf} being the inflaton mass, and hence the reheating temperature is estimated as [79]

$$T_R \sim 0.1 \sqrt{\Gamma_{\text{inf}} M_{\text{pl}}} \sim 10^9 \text{GeV}, \quad (8.9)$$

requiring that the inflaton field should produce the density perturbations observed by COBE ($m_{\text{inf}} \sim 10^{13} \text{GeV}$) [78]. Notice that if the interaction of the inflaton becomes stronger, the decay rate becomes larger and hence a higher reheating temperature is obtained. Thus, in the case that the gravitino is lighter than $\sim 1 \text{TeV}$ (which is favored from the naturalness point of view), we have to adopt an inflaton with extremely small decay rate.

Let us compare our results with those in other literatures. The gravitino number density and the photon spectrum are the essential quantity for the analysis. Our number density of gravitino produced in the reheating epochs of the inflationary universe is about four times larger than one given in ref.[36]. Since the authors of ref.[36] neglected the interactions between the gravitino and chiral multiplets (which is the second term in eq.(4.58)), they might underestimate the total cross section for the production of gravitino. All previous works concerning the gravitino problem were based on the gravitino number density given in ref.[36]. Therefore our constraints are more stringent than others.

Furthermore, our photon spectrum is different from that in ref.[40] as shown in Fig.B.2. The spectrum adopted by ref.[40] has more power to destroy light elements above threshold

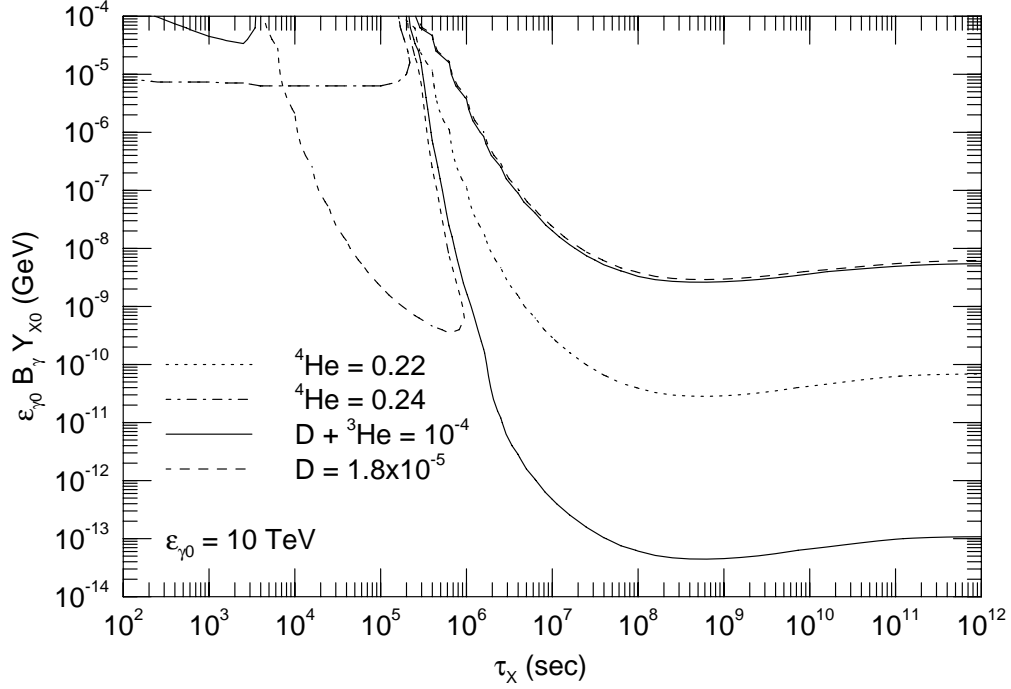


Figure 8.1: Contours for critical abundance of light elements in the $\tau_X - \epsilon_{\gamma 0} B_\gamma Y_{X0}$ plane for $\epsilon_0 = 10\text{TeV}$. The solid line (dashed line, dotted line, dotted-dashed line) is a bound from overproduction of ($D+{}^3\text{He}$) (overdestruction of D , overdestruction of ${}^4\text{He}$, and overproduction of ${}^4\text{He}$). In deriving the mass density of X , we take $B_\gamma = 1$ and $m_X = 2\epsilon_{\gamma 0}$.

for the photon-photon scattering and less power below the threshold. In refs.[75, 76], the Compton scattering process was not taken into account in calculating the photon spectrum which the authors of ref.[40] used to derive a fitting formula for the high energy photon spectrum. Therefore, it is expected that the difference comes mainly from the neglect of Compton scattering off the thermal electron, which is the most dominant process for the relatively low energy photons.

Finally, we discuss applications of the cosmological arguments to other cases. If some exotic particle decays radiatively with a lifetime longer than $\sim 1\text{sec}$, the standard BBN scenario may be affected. The constraints we have used in the case of massive gravitino can be applied to other cases of exotic particle X . Using the similar method as in the gravitino case, we derive constraints from the BBN on radiatively decaying weakly interacting particles. The results are given in Fig.8.1 – Fig.8.3, where τ_X is the lifetime of X , Y_{X0} the yield of X before X decays, $\epsilon_{\gamma 0}$ the energy of the primary photon, and B_γ the branching ratio of radiative decay channel. The evolution of the yield variable $Y_X \equiv n_X/n_{rad}$ of X is given by $Y_X(t) = Y_{X0}e^{-t/\tau_X}$. Notice that we assume that the emitted photon is monochromatic, and that the number of photons emitted from one decay process is one. As we can see, the constraint on the combination $\epsilon_{\gamma 0} B_\gamma Y_{X0}$ is almost the same as in the cases of $\epsilon_{\gamma 0} = 10\text{GeV}$ and $\epsilon_{\gamma 0} = 10\text{TeV}$ since the spectrum of the energetic photon depends almost only on the total amount of energy injection, while for the case of $\epsilon_{\gamma 0} = 10\text{MeV}$ the constraint from

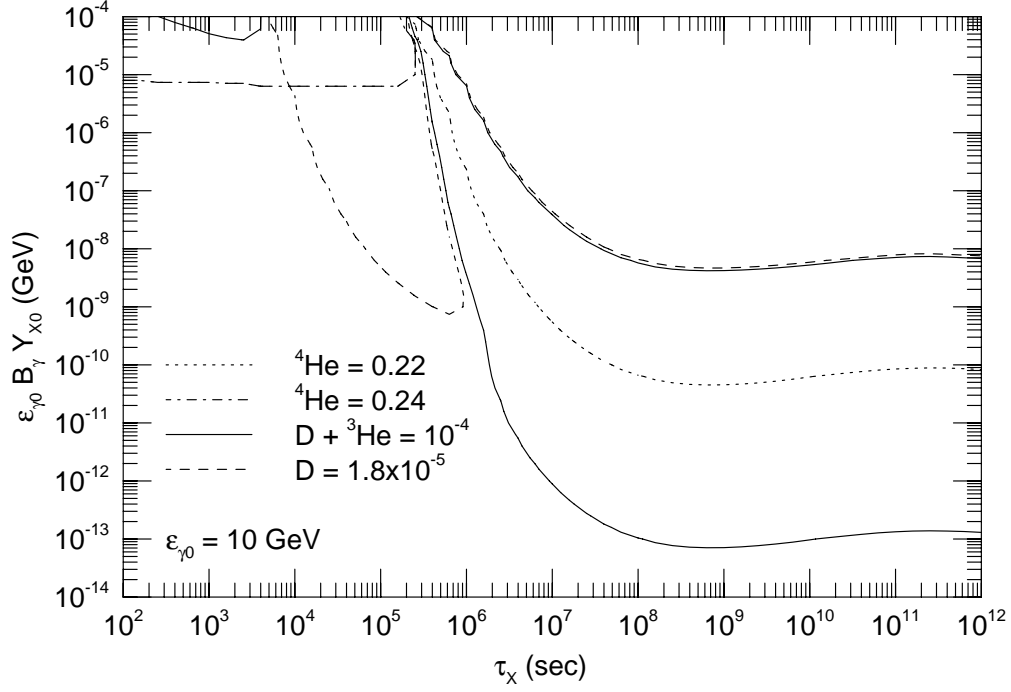


Figure 8.2: Same as Fig. 8.1 except for $\epsilon_{\gamma 0} = 10$ GeV.

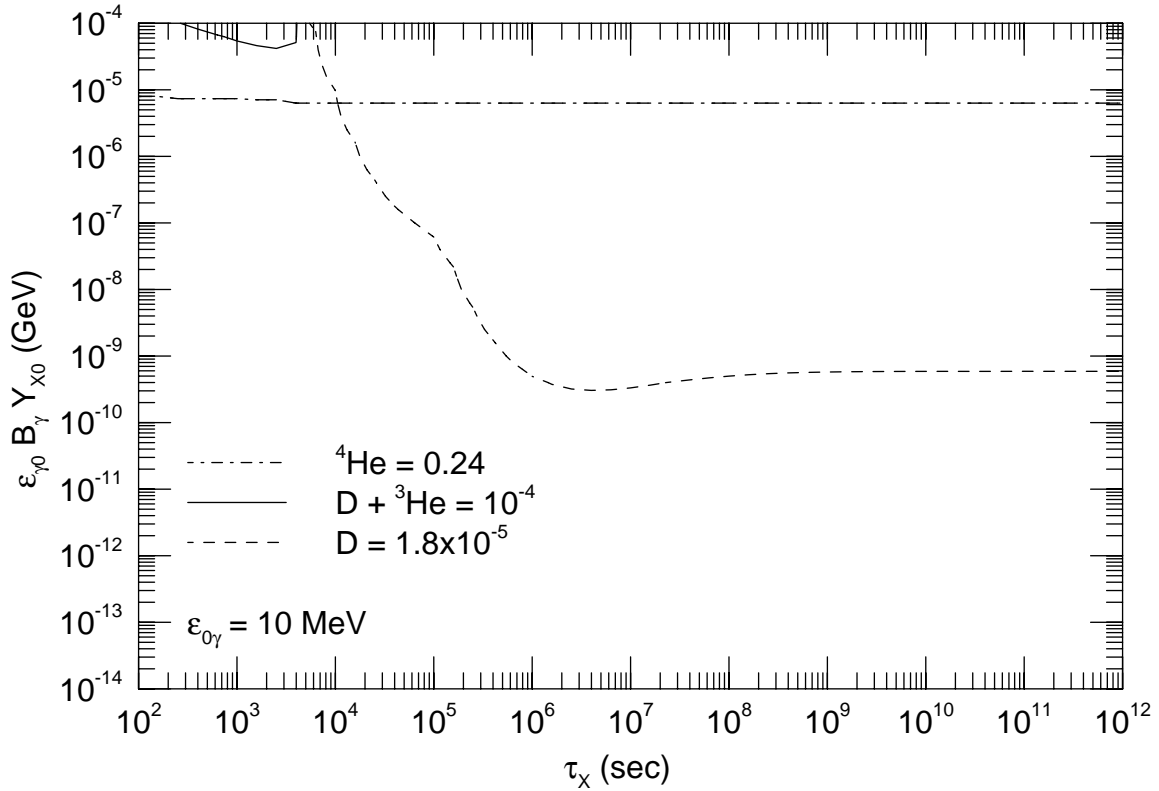


Figure 8.3: Same as Fig. 8.1 except for $\epsilon_{\gamma 0} = 10$ MeV.

($D + {}^3\text{He}$) is negligible since the energy of primary photon is below the threshold of ${}^4\text{He}$ destruction.

Constraints from the present mass density of the universe may give another information on exotic particles. Especially in the SUSY models, the present mass density of the relic LSP is calculated in detail, and constraints on SUSY parameters are derived. Furthermore, particles with lifetime longer than $\sim 10^{10}\text{sec}$ may distort the cosmic microwave background.

These arguments have been applied to the LSP in SUSY models, the Polonyi field which is responsible for SUSY breaking [30], the massive neutrino [80, 81], the axion [82, 83, 84] and so on as well as the gravitino. Thus, cosmological considerations provide us with a great insight into exotic particles which we cannot investigate by any collider experiments because of the weakness of their interactions.

Acknowledgement

The author wishes to express his sincere gratitude to T. Yanagida for various suggestions, stimulating discussions and careful reading of this manuscript, and to M. Kawasaki, H. Murayama and M. Yamaguchi, who are collaborators in various parts of this thesis, for fruitful discussions. He is also grateful to M. Yoshimura for helpful comments. All of them helped the author greatly completing this thesis through valuable discussions and by making useful comments. Without their hearty encouragement, this work would not be completed.

He would like to thank Y. Shimizu for useful comments and careful reading of this manuscript. He is also grateful to T. Ataku, and also to Y. Shimizu for taking part in the maintenance of the computers he used for numerical calculations. Finally, he expresses his gratitude for all the members of the high energy theory group of Tohoku University for their hospitality.

Appendix A

Notations

A.1 Conventions

We use the metric (in flat space-time)

$$g_{\mu\nu} = \text{diag}(1, -1, -1, -1), \quad (\text{A.1})$$

and for totally anti-symmetric tensor (in flat space-time), we use the convention $\epsilon_{0123} = -1$.

A.2 Two component notation

For two component spinor, we essentially follow the notation used in ref.[26], except for the convention of the metric.

σ -matrices are defined as

$$\begin{aligned} \sigma_0 = \bar{\sigma}_0 &= \begin{pmatrix} 1 & 0 \\ 0 & 1 \end{pmatrix}, & \sigma_1 = -\bar{\sigma}_1 &= \begin{pmatrix} 0 & 1 \\ 1 & 0 \end{pmatrix}, \\ \sigma_2 = -\bar{\sigma}_2 &= \begin{pmatrix} 0 & -i \\ i & 0 \end{pmatrix}, & \sigma_3 = -\bar{\sigma}_3 &= \begin{pmatrix} 1 & 0 \\ 0 & -1 \end{pmatrix}. \end{aligned} \quad (\text{A.2})$$

For the anti-symmetric symbols $\epsilon_{\alpha\beta}$ and $\epsilon^{\alpha\beta}$, we use the following conventions;

$$\epsilon^{12} = -\epsilon^{21} = \epsilon_{21} = -\epsilon_{12} = 1, \quad (\text{A.3})$$

$$\epsilon^{11} = \epsilon^{22} = \epsilon_{11} = \epsilon_{22} = 0. \quad (\text{A.4})$$

Notice that $\epsilon_{\alpha\beta}$ and $\epsilon^{\alpha\beta}$ are related as $\epsilon_{\alpha\beta}\epsilon^{\beta\gamma} = \delta_\alpha^\gamma$. By using $\epsilon^{\alpha\beta}$, σ_μ and $\bar{\sigma}_\mu$ are related as

$$\bar{\sigma}_\mu^{\dot{\alpha}\alpha} = \epsilon^{\dot{\alpha}\dot{\beta}}\epsilon^{\alpha\beta}\sigma_{\mu\beta\dot{\beta}}. \quad (\text{A.5})$$

From these σ -matrices, the generators of the Lorentz group is the spinor representation

are obtained

$$\sigma_{\mu\nu} = \frac{1}{4}(\sigma_\mu \bar{\sigma}_\nu - \sigma_\nu \bar{\sigma}_\mu), \quad \bar{\sigma}_{\mu\nu} = \frac{1}{4}(\bar{\sigma}_\mu \sigma_\nu - \bar{\sigma}_\nu \sigma_\mu). \quad (\text{A.6})$$

A.3 Four component notation

γ -matrices obey the following commutation relation;

$$[\gamma_\mu, \gamma_\nu] = 2g_{\mu\nu}. \quad (\text{A.7})$$

From $\gamma^0 - \gamma^3$, γ_5 matrix is defined as

$$\gamma_5 = i\gamma^0\gamma^1\gamma^2\gamma^3. \quad (\text{A.8})$$

γ -matrices are transposed by a charge conjugation matrix C ;

$$C^{-1}\gamma_\mu C = -\gamma_\mu^T. \quad (\text{A.9})$$

Charge conjugation matrix C satisfies the following identities;

$$C^\dagger C = 1, \quad (\text{A.10})$$

$$C^T = -C. \quad (\text{A.11})$$

By using C , charge conjugation of four component spinor ψ is defined as

$$\psi^C \equiv C\bar{\psi}^T. \quad (\text{A.12})$$

Chiral representation

Four component spinor (in chiral representation) is constructed from two component spinor ξ_α and $\eta_{\dot{\alpha}}$ as

$$\psi \sim \begin{pmatrix} \xi_\alpha \\ \bar{\eta}^{\dot{\alpha}} \end{pmatrix}, \quad \bar{\psi} \sim (\eta^\alpha, \bar{\xi}_{\dot{\alpha}}). \quad (\text{A.13})$$

In this representation, γ -matrices are given by

$$\gamma_\mu = \begin{pmatrix} 0 & \bar{\sigma}_\mu \\ \sigma_\mu & 0 \end{pmatrix}, \quad \gamma_5 = \begin{pmatrix} 1 & 0 \\ 0 & -1 \end{pmatrix}, \quad (\text{A.14})$$

and charge conjugation matrix C is given by

$$C = i\gamma^2\gamma^0 = C^*. \quad (\text{A.15})$$

Dirac representation

γ -matrices in Dirac representation are related to those in chiral representation through unitary transformation;

$$\gamma_\mu^{(\text{chiral})} = U \gamma_\mu^{(\text{Dirac})} U^\dagger, \quad (\text{A.16})$$

with

$$U = \frac{1}{\sqrt{2}} \begin{pmatrix} 1 & 1 \\ -1 & 1 \end{pmatrix}. \quad (\text{A.17})$$

Explicit form of the γ -matrices in Dirac representation are given by

$$\gamma^0 = \begin{pmatrix} 1 & 0 \\ 0 & -1 \end{pmatrix}, \quad \gamma^i = \begin{pmatrix} 0 & \sigma_i \\ -\sigma_i & 0 \end{pmatrix}, \quad \gamma_5 = \begin{pmatrix} 0 & 1 \\ 1 & 0 \end{pmatrix}, \quad (\text{A.18})$$

and charge conjugation matrix C is obtained as

$$C = i\gamma^2\gamma^0 = C^*. \quad (\text{A.19})$$

In Dirac representation, solution to the Dirac equation (in momentum space);

$$(\not{p} - m) u(\mathbf{p}, s) = 0, \quad (\text{A.20})$$

with $p^\mu = (p_0, |\mathbf{p}| \sin \theta \cos \phi, |\mathbf{p}| \sin \theta \sin \phi, |\mathbf{p}| \cos \theta)$ takes the following form;

$$u(\mathbf{p}, s) = \begin{pmatrix} \sqrt{p_0 + m} \chi^{(s)} \\ \sqrt{p_0 - m} n_i \sigma_i \chi^{(s)} \end{pmatrix}, \quad (\text{A.21})$$

where $p_\mu p^\mu = m^2$, $\mathbf{n} \equiv \mathbf{p}/|\mathbf{p}|$, and

$$\chi^{(s=+1)} \equiv \begin{pmatrix} e^{-i\phi/2} \cos \theta/2 \\ e^{i\phi/2} \sin \theta/2 \end{pmatrix}, \quad \chi^{(s=-1)} \equiv \begin{pmatrix} -e^{-i\phi/2} \sin \theta/2 \\ e^{i\phi/2} \cos \theta/2 \end{pmatrix}. \quad (\text{A.22})$$

The above spinor $u(\mathbf{p}, s)$ is a eigenstate of helicity $\mathbf{n}\Sigma$;

$$(\mathbf{n}\Sigma) u(\mathbf{p}, s) = s u(\mathbf{p}, s), \quad (\text{A.23})$$

where Σ is given by

$$\Sigma^i \equiv \begin{pmatrix} \sigma_i & 0 \\ 0 & \sigma_i \end{pmatrix}. \quad (\text{A.24})$$

Appendix B

Photon spectrum

In order to investigate photo-dissociation processes, we have to calculate a photon spectrum induced by decay of gravitino. In this appendix, we will write down Boltzmann equations which determine the high energy photon spectrum with the case of high energy photon injection, and that of high energy neutrino injection. We will also solve them numerically and show the shape of the spectrum.

B.1 Boltzmann equations

In calculating photon spectrum (with high energy photon injection), we take the following processes into account;

- double photon pair creation,
- photon-photon scattering,
- pair creation in nuclei,
- Compton scattering off thermal electron,
- inverse Compton scattering off background photon,
- radiative decay of the gravitinos.

The Boltzmann equations for these cascade processes are formally given by

$$\begin{aligned} \frac{\partial f_\gamma(\epsilon_\gamma)}{\partial t} = & \left. \frac{\partial f_\gamma(\epsilon_\gamma)}{\partial t} \right|_{\text{DP}} + \left. \frac{\partial f_\gamma(\epsilon_\gamma)}{\partial t} \right|_{\text{PP}} + \left. \frac{\partial f_\gamma(\epsilon_\gamma)}{\partial t} \right|_{\text{PC}} + \left. \frac{\partial f_\gamma(\epsilon_\gamma)}{\partial t} \right|_{\text{CS}} \\ & + \left. \frac{\partial f_\gamma(\epsilon_\gamma)}{\partial t} \right|_{\text{IC}} + \left. \frac{\partial f_\gamma(\epsilon_\gamma)}{\partial t} \right|_{\text{DE}} + \left. \frac{\partial f_\gamma(\epsilon_\gamma)}{\partial t} \right|_{\text{EXP}}, \end{aligned} \quad (\text{B.1})$$

$$\begin{aligned} \frac{\partial f_e(E_e)}{\partial t} = & \left. \frac{\partial f_e(E_e)}{\partial t} \right|_{\text{DP}} + \left. \frac{\partial f_e(E_e)}{\partial t} \right|_{\text{PC}} + \left. \frac{\partial f_e(E_e)}{\partial t} \right|_{\text{CS}} + \left. \frac{\partial f_e(E_e)}{\partial t} \right|_{\text{IC}} \\ & + \left. \frac{\partial f_e(E_e)}{\partial t} \right|_{\text{DE}} + \left. \frac{\partial f_e(E_e)}{\partial t} \right|_{\text{EXP}}, \end{aligned} \quad (\text{B.2})$$

where terms with the index DP (PP, PC, CS, IC, DE, and EXP) represents the contribution from the double photon pair creation process (photon-photon scattering, pair creation in nuclei, Compton scattering, inverse Compton scattering, contribution from the gravitino decay, and the effects of the expansion of the universe). Notice that in the main part of this thesis, the expansion terms and the decay term in the Boltzmann equation for the electron distribution function are ignored. Below, we will see contributions from each processes in detail.

Double photon pair creation [$\gamma + \gamma \rightarrow e^+ + e^-$]

For high energy photon whose energy is larger than $\sim m_e^2/22T$, double photon pair creation is the most dominant process.

The total cross section σ_{DP} for the double photon pair creation process is given by

$$\sigma_{\text{DP}}(\beta) = \frac{1}{2}\pi r_e^2 (1 - \beta^2) \left\{ (3 - \beta^4) \ln \frac{1 + \beta}{1 - \beta} - 2\beta (2 - \beta^2) \right\}, \quad (\text{B.3})$$

where r_e is the classical radius of electron which is given by

$$r_e = \frac{\alpha}{m_e}, \quad (\text{B.4})$$

with $\alpha \simeq 1/137$ being the fine structure constant, and β is the electron (or positron) velocity in the center of mass frame. Using this formula, one can write down $(\partial f_\gamma / \partial t)|_{\text{DP}}$ as

$$\left. \frac{\partial f_\gamma(\epsilon_\gamma)}{\partial t} \right|_{\text{DP}} = -\frac{1}{8} \frac{1}{\epsilon_\gamma^2} f_\gamma(\epsilon_\gamma) \int_{m_e/\epsilon_\gamma}^{\infty} d\bar{\epsilon}_\gamma \frac{1}{\bar{\epsilon}_\gamma^2} \bar{f}_\gamma(\bar{\epsilon}_\gamma) \int_{4m_e^2}^{4\epsilon_\gamma \bar{\epsilon}_\gamma} ds s \sigma_{\text{DP}}(\beta) \Big|_{\beta=\sqrt{1-(4m_e^2/s)}}. \quad (\text{B.5})$$

The spectrum of final state electron and positron is obtained in ref.[85], and $(\partial f_e / \partial t)|_{\text{DP}}$ is given by

$$\left. \frac{\partial f_e(E_e)}{\partial t} \right|_{\text{DP}} = \frac{1}{4} \pi r_e^2 m_e^4 \int_{E_e}^{\infty} d\epsilon_\gamma \frac{f_\gamma(\epsilon_\gamma)}{\epsilon_\gamma^3} \int_0^{\infty} d\bar{\epsilon}_\gamma \frac{\bar{f}_\gamma(\bar{\epsilon}_\gamma)}{\bar{\epsilon}_\gamma^2} G(E_e, \epsilon_\gamma, \bar{\epsilon}_\gamma), \quad (\text{B.6})$$

where function $G(E_e, \epsilon_\gamma, \bar{\epsilon}_\gamma)$ is given by

$$\begin{aligned} G(E_e, \epsilon_\gamma, \bar{\epsilon}_\gamma) &= \frac{4(E_e + E_e')^2}{E_e E_e'} \ln \frac{4\bar{\epsilon}_\gamma E_e E_e'}{m_e^2 (E_e + E_e')} - \left\{ 1 - \frac{m_e^2}{\bar{\epsilon}_\gamma (E_e + E_e')} \right\} \frac{(E_e + E_e')^4}{E_e^2 E_e'^2} \\ &\quad + \frac{2 \{ 2\bar{\epsilon}_\gamma (E_e + E_e') - m_e^2 \} (E_e + E_e')^2}{m_e^2 E_e E_e'} - 8 \frac{\bar{\epsilon}_\gamma \epsilon_\gamma}{m_e^2}, \end{aligned} \quad (\text{B.7})$$

with $E_e' = \epsilon_\gamma + \bar{\epsilon}_\gamma - E_e$, and \bar{f}_γ represents the distribution function of the background photon

at temperature T ,

$$\bar{f}_\gamma(\bar{\epsilon}_\gamma) = \frac{\bar{\epsilon}_\gamma^2}{\pi^2} \times \frac{1}{\exp(\bar{\epsilon}_\gamma/T) - 1}. \quad (\text{B.8})$$

Photon-photon scattering [$\gamma + \gamma \rightarrow \gamma + \gamma$]

If the photon energy is below the effective threshold of the double photon pair creation, photon-photon scattering process becomes significant. This process is analyzed in ref.[76] and for $\epsilon'_\gamma \lesssim O(m_e^2/T)$, $(\partial f_\gamma/\partial t)|_{\text{PP}}$ is given by

$$\begin{aligned} \left. \frac{\partial f_\gamma(\epsilon'_\gamma)}{\partial t} \right|_{\text{PP}} &= \frac{35584}{10125\pi} \alpha^2 r_e^2 m_e^{-6} \int_{\epsilon'_\gamma}^{\infty} d\epsilon_\gamma f_\gamma(\epsilon_\gamma) \epsilon_\gamma^2 \left\{ 1 - \frac{\epsilon'_\gamma}{\epsilon_\gamma} + \left(\frac{\epsilon'_\gamma}{\epsilon_\gamma} \right)^2 \right\}^2 \int_0^\infty d\bar{\epsilon}_\gamma \bar{\epsilon}_\gamma^3 \bar{f}_\gamma(\bar{\epsilon}_\gamma) \\ &\quad - \frac{1946}{50625\pi} f_\gamma(\epsilon'_\gamma) \alpha^2 r_e^2 m_e^{-6} \epsilon_\gamma'^3 \int_0^\infty d\bar{\epsilon}_\gamma \bar{\epsilon}_\gamma^3 \bar{f}_\gamma(\bar{\epsilon}_\gamma). \end{aligned} \quad (\text{B.9})$$

For a larger value of ϵ'_γ , we cannot use this formula. But for high energy photons, photon-photon scattering is not significant because double photon pair creation determines the shape of the photon spectrum. Therefore, instead of using the exact formula, we take m_e^2/T as a cutoff scale of $(\partial f_\gamma/\partial t)|_{\text{PP}}$, *i.e.* for $\epsilon'_\gamma \leq m_e^2/T$ we use eq.(B.9) and for $\epsilon'_\gamma > m_e^2/T$ we take

$$\left. \frac{\partial f_\gamma(\epsilon'_\gamma > m_e^2/T)}{\partial t} \right|_{\text{PP}} = 0. \quad (\text{B.10})$$

Notice that we have checked the cutoff dependence of spectra is negligible.

Pair creation in nuclei [$\gamma + N \rightarrow e^+ + e^- + N$]

Scattering off the electric field around nucleon, high energy photon can produce electron positron pair if the photon energy is larger than $2m_e$. Denoting total cross section of this process σ_{PC} , $(\partial f_\gamma/\partial t)|_{\text{NP}}$ is given by

$$\left. \frac{\partial f_\gamma(\epsilon_\gamma)}{\partial t} \right|_{\text{NP}} = -\bar{n}_N \sigma_{\text{PC}}(\epsilon_\gamma) f_\gamma(\epsilon_\gamma), \quad (\text{B.11})$$

where \bar{n}_N is the nucleon number density. For σ_{PC} , we use the approximate formula derived by Maximon [86]. For ϵ_γ near the threshold ($\epsilon_\gamma < 4m_e$), the approximate formula is given by

$$\begin{aligned} \sigma_{\text{PC}}(\epsilon_\gamma)|_{k<4} &= \frac{2\pi}{3} Z^2 \alpha r_e^2 \left(\frac{k-2}{k} \right)^3 \\ &\quad \times \left(1 + \frac{1}{2}\rho + \frac{23}{40}\rho^2 + \frac{11}{60}\rho^3 + \frac{29}{960}\rho^4 + O(\rho^5) \right), \end{aligned} \quad (\text{B.12})$$

where

$$k \equiv \frac{\epsilon_\gamma}{m_e}, \quad \rho \equiv \frac{2k-4}{k+2+2\sqrt{2k}}, \quad (\text{B.13})$$

and Z is the charge of nuclei. For large ϵ_γ ($\epsilon_\gamma \geq 4m_e$), σ_{PC} are expanded in the parameter k^{-1} , which is given by

$$\begin{aligned} \sigma_{\text{PC}}(\epsilon_\gamma)|_{k \geq 4} = & Z^2 \alpha r_e^2 \left[\frac{28}{9} \ln 2k - \frac{218}{27} \right. \\ & + \left(\frac{2}{k} \right)^2 \left\{ \frac{2}{3} (\ln 2k)^3 - (\ln 2k)^2 + \left(6 - \frac{\pi^2}{3} \right) \ln 2k + 2\zeta(3) + \frac{\pi^2}{6} - \frac{7}{2} \right\} \\ & - \left(\frac{2}{k} \right)^4 \left\{ \frac{3}{16} \ln 2k + \frac{1}{8} \right\} \\ & \left. - \left(\frac{2}{k} \right)^6 \left\{ \frac{29}{2304} \ln 2k - \frac{77}{13824} \right\} + O(k^{-8}) \right]. \quad (\text{B.14}) \end{aligned}$$

Differential cross section for this process $d\sigma_{\text{PC}}/dE_+$ is given in ref.[87];

$$\begin{aligned} \frac{d\sigma_{\text{PC}}}{dE_+} = & Z^2 \alpha r_e^2 \left(\frac{p_+ p_-}{\epsilon_\gamma^3} \right) \left[-\frac{4}{3} - 2E_+ E_- \frac{p_+^2 + p_-^2}{p_+^2 p_-^2} \right. \\ & + m_e^2 \left\{ l_- \frac{E_+}{p_-^3} + l_+ \frac{E_-}{p_+^3} - l_+ l_- \frac{1}{p_+ p_-} \right\} \\ & + L \left\{ -\frac{8E_+ E_-}{3p_+ p_-} + \frac{\epsilon_\gamma^2}{p_+^3 p_-^3} (E_+^2 E_-^2 + p_+^2 p_-^2 - m_e^2 E_+ E_-) \right. \\ & \left. \left. - \frac{m_e^2 \epsilon_\gamma}{2p_+ p_-} \left(l_+ \frac{E_+ E_- - p_+^2}{p_+^3} + l_- \frac{E_+ E_- - p_-^2}{p_-^3} \right) \right\} \right], \quad (\text{B.15}) \end{aligned}$$

where

$$p_\pm \equiv \sqrt{E_\pm^2 - m_e^2}, \quad (\text{B.16})$$

$$L \equiv \ln \frac{E_+ E_- + p_+ p_- + m_e^2}{E_+ E_- - p_+ p_- + m_e^2}, \quad (\text{B.17})$$

$$l_\pm \equiv \ln \frac{E_\pm + p_\pm}{E_\pm - p_\pm}, \quad (\text{B.18})$$

with E_- (E_+) being the energy of electron (positron) in final state. By using this formula, $(\partial f_e / \partial t)|_{\text{NP}}$ is given by

$$\left. \frac{\partial f_e(E_e)}{\partial t} \right|_{\text{NP}} = \bar{n}_N \int_{E_e + m_e}^{\infty} d\epsilon_\gamma \frac{d\sigma_{\text{PC}}}{dE_e} f_\gamma(\epsilon_\gamma). \quad (\text{B.19})$$

Compton scattering [$\gamma + e^- \rightarrow \gamma + e^-$]

Compton scattering is one of the processes by which high energy photons lose their energy. Since the photo-dissociation of light elements occurs when the temperature drops below $\sim 0.1\text{MeV}$, we can consider the thermal electrons to be almost at rest. Using the total and differential cross sections at the electron rest frame σ_{CS} and $d\sigma_{\text{CS}}/dE_e$, one can derive

$$\left. \frac{\partial f_\gamma(\epsilon'_\gamma)}{\partial t} \right|_{\text{CS}} = \bar{n}_e \int_{\epsilon'_\gamma}^{\infty} d\epsilon_\gamma f_\gamma(\epsilon_\gamma) \frac{d\sigma_{\text{CS}}(\epsilon'_\gamma, \epsilon_\gamma)}{d\epsilon'_\gamma} - \bar{n}_e \sigma_{\text{CS}} f_\gamma(\epsilon'_\gamma), \quad (\text{B.20})$$

$$\left. \frac{\partial f_e(E'_e)}{\partial t} \right|_{\text{CS}} = \bar{n}_e \int_{E'_e}^{\infty} d\epsilon_\gamma f_\gamma(\epsilon_\gamma) \frac{d\sigma_{\text{CS}}(\epsilon_\gamma + m_e - E'_e, \epsilon_\gamma)}{d\epsilon'_\gamma}, \quad (\text{B.21})$$

where \bar{n}_e is the number density of background electron. Explicit forms of σ_{CS} and $d\sigma_{\text{CS}}/dE_e$ are given as

$$\sigma_{\text{CS}} = 2\pi r_e^2 \frac{1}{x} \left\{ \left(1 - \frac{4}{x} - \frac{8}{x^2} \right) \ln(1+x) + \frac{1}{2} + \frac{8}{x} - \frac{1}{2(1+x)^2} \right\}, \quad (\text{B.22})$$

$$\frac{d\sigma_{\text{CS}}(\epsilon'_\gamma, \epsilon_\gamma)}{d\epsilon'_\gamma} = \pi r_e^2 \frac{m_e}{\epsilon_\gamma^2} \left\{ \frac{\epsilon_\gamma}{\epsilon'_\gamma} + \frac{\epsilon'_\gamma}{\epsilon_\gamma} + \left(\frac{m_e}{\epsilon'_\gamma} - \frac{m_e}{\epsilon_\gamma} \right)^2 - 2m_e \left(\frac{1}{\epsilon'_\gamma} - \frac{1}{\epsilon_\gamma} \right) \right\}, \quad (\text{B.23})$$

with

$$x \equiv \frac{s - m_e^2}{m_e^2} = \frac{2\epsilon_\gamma}{m_e}. \quad (\text{B.24})$$

Inverse Compton scattering [$e^\pm + \gamma \rightarrow e^\pm + \gamma$]

Formula for the inverse Compton process is given by Jones [88], and $(\partial f / \partial t)|_{\text{IC}}$ is given by

$$\left. \frac{\partial f_\gamma(\epsilon_\gamma)}{\partial t} \right|_{\text{IC}} = 2\pi r_e^2 m_e^2 \int_{\epsilon_\gamma + m_e}^{\infty} dE_e \frac{2f_e(E_e)}{E_e^2} \int_0^{\infty} d\bar{\epsilon}_\gamma \frac{\bar{f}_\gamma(\bar{\epsilon}_\gamma)}{\bar{\epsilon}_\gamma} F(\epsilon_\gamma, E_e, \bar{\epsilon}_\gamma), \quad (\text{B.25})$$

$$\begin{aligned} \left. \frac{\partial f_e(E'_e)}{\partial t} \right|_{\text{IC}} &= 2\pi r_e^2 m_e^2 \int_{E'_e}^{\infty} dE_e \frac{f_e(E_e)}{E_e^2} \int_0^{\infty} d\bar{\epsilon}_\gamma \frac{\bar{f}_\gamma(\bar{\epsilon}_\gamma)}{\bar{\epsilon}_\gamma} F(E_e + \bar{\epsilon}_\gamma - E'_e, E_e, \bar{\epsilon}_\gamma) \\ &\quad - 2\pi r_e^2 m_e^2 \frac{f_e(E'_e)}{E_e'^2} \int_{E'_e}^{\infty} d\epsilon_\gamma \int_0^{\infty} d\bar{\epsilon}_\gamma \frac{\bar{f}_\gamma(\bar{\epsilon}_\gamma)}{\bar{\epsilon}_\gamma} F(\epsilon_\gamma, E'_e, \bar{\epsilon}_\gamma), \end{aligned} \quad (\text{B.26})$$

where function $F(\epsilon_\gamma, E_e, \bar{\epsilon}_\gamma)$ is given by

$$F(\epsilon_\gamma, E_e, \bar{\epsilon}_\gamma)|_{0 \leq q \leq 1} = 2q \ln q + (1 + 2q)(1 - q) + \frac{(\Gamma_\epsilon q)^2}{2(1 - \Gamma_\epsilon q)}(1 - q), \quad (\text{B.27})$$

$$F(\epsilon_\gamma, E_e, \bar{\epsilon}_\gamma)|_{\text{otherwise}} = 0, \quad (\text{B.28})$$

with

$$\Gamma_\epsilon = \frac{4\bar{\epsilon}_\gamma E_e}{m_e^2}, \quad q = \frac{\epsilon_\gamma}{\Gamma_\epsilon(E_e - \epsilon_\gamma)}.$$

Radiative decay of the gravitino [$\psi_\mu \rightarrow \gamma + \tilde{\gamma}$]

Source of the non-thermal photon and electron spectra is radiative decay of gravitino. Since gravitinos are almost at rest when they decay and we only consider two body decay process, incoming high energy photons have monochromatic energy $\epsilon_{\gamma 0}$, which is given by

$$\epsilon_{\gamma 0} = \frac{m_{3/2}^2 - m_{\tilde{\gamma}}^2}{2m_{3/2}}. \quad (\text{B.29})$$

In this case, $(\partial f_\gamma / \partial t)|_{\text{DE}}$ can be written as

$$\left. \frac{\partial f_\gamma(\epsilon_\gamma)}{\partial t} \right|_{\text{DE}} = B_\gamma \delta(\epsilon_\gamma - \epsilon_{\gamma 0}) \frac{n_{3/2}}{\tau_{3/2}}, \quad (\text{B.30})$$

where B_γ is the branching ratio for the process $\psi_\mu \rightarrow \gamma + \tilde{\gamma}$. If the gravitino decays into an electron and a selectron, $(\partial f_e / \partial t)|_{\text{DE}}$ cannot be ignored. Denoting the branching ratio for this decay process B_e , the formula for $(\partial f_e / \partial t)|_{\text{DE}}$ is given by

$$\left. \frac{\partial f_e(E_e)}{\partial t} \right|_{\text{DE}} = B_e \delta(E_e - E_{e0}) \frac{n_{3/2}}{\tau_{3/2}}, \quad (\text{B.31})$$

where E_{e0} is the energy of the injecting electron.

B.2 Spectrum with high energy photon injection

Having obtained the explicit forms for the Boltzmann equations, we solve them in this section. In deriving high energy photon and electron spectra, we have to use numerical method since the Boltzmann equations (B.1) and (B.2) are very much complicated. Before solving them numerically, we explain our approach to the Boltzmann equations [89].

At first, we classify the right-hand side of eq.(B.1) and eq.(B.2) into the “outgoing” parts and “incoming” ones. Below, we ignore the expansion terms $(\partial f_\gamma / \partial t)|_{\text{EXP}}$ and $(\partial f_e / \partial t)|_{\text{EXP}}$ in the Boltzmann equations (B.1) and (B.2) since the expansion rate of the universe is much smaller than the scattering rates of electro-magnetic processes. Then, eq.(B.1) and eq.(B.2) can be written as

$$\frac{\partial f_\gamma(\epsilon_\gamma)}{\partial t} = -\Gamma_\gamma(\epsilon_\gamma; T) f_\gamma(\epsilon_\gamma) + \dot{f}_{\gamma, \text{IN}}(\epsilon_\gamma), \quad (\text{B.32})$$

$$\frac{\partial f_e(E_e)}{\partial t} = -\Gamma_e(E_e; T) f_e(E_e) + \dot{f}_{e, \text{IN}}(E_e), \quad (\text{B.33})$$

where “incoming” terms $\dot{f}_{\gamma,\text{IN}}$ and $\dot{f}_{e,\text{IN}}$ can be obtained as the sums of the contributions from the decay terms and the functionals of the distribution functions of the photon and the electron;

$$\begin{aligned}\dot{f}_{\gamma,\text{IN}}(\epsilon_\gamma) &= \left. \frac{\partial f_\gamma(\epsilon_\gamma)}{\partial t} \right|_{\text{DE}} + \int_{\epsilon_\gamma}^{\infty} d\epsilon'_\gamma K_{\gamma,\gamma}(\epsilon_\gamma, \epsilon'_\gamma; T) f_\gamma(\epsilon'_\gamma) \\ &\quad + \int_{\epsilon_\gamma}^{\infty} dE'_e K_{\gamma,e}(\epsilon_\gamma, E'_e; T) f_e(E'_e),\end{aligned}\tag{B.34}$$

$$\begin{aligned}\dot{f}_{e,\text{IN}}(E_e) &= \left. \frac{\partial f_e(E_e)}{\partial t} \right|_{\text{DE}} + \int_{E_e}^{\infty} d\epsilon'_\gamma K_{e,\gamma}(E_e, \epsilon'_\gamma; T) f_\gamma(\epsilon'_\gamma) \\ &\quad + \int_{E_e}^{\infty} dE'_e K_{e,e}(E_e, E'_e; T) f_e(E'_e).\end{aligned}\tag{B.35}$$

The explicit forms of Γ_A and K_{AB} ($A, B = \gamma, e$) can be obtained from the full details of the Boltzmann equations given in the previous section.

As mentioned before, the strategy we use here is to calculate a stationary solution to the Boltzmann equations (B.1) and (B.2), which obey

$$\frac{\partial f_\gamma(\epsilon_\gamma)}{\partial t} = \frac{\partial f_e(E_e)}{\partial t} = 0.\tag{B.36}$$

In our approach, the distribution functions f_γ and f_e of the photon and the electron can be formally given as

$$f_\gamma(\epsilon_\gamma) = \frac{\dot{f}_{\gamma,\text{IN}}(\epsilon_\gamma)}{\Gamma_\gamma(\epsilon_\gamma; T)},\tag{B.37}$$

$$f_e(E_e) = \frac{\dot{f}_{e,\text{IN}}(E_e)}{\Gamma_e(E_e; T)}.\tag{B.38}$$

The important thing is that the “incoming” terms $\dot{f}_{\gamma,\text{IN}}(\epsilon_\gamma)$ and $\dot{f}_{e,\text{IN}}(E_e)$ depend only on $f_\gamma(\epsilon')$ and $f_e(\epsilon')$ with $\epsilon' > \epsilon_\gamma, E_e$. Therefore, if the distribution functions $f_\gamma(\epsilon_\gamma)$ and $f_e(E_e)$ with $\epsilon_\gamma, E_e > \epsilon$ (and the source terms) are known, we can obtain $f_\gamma(\epsilon)$ and $f_e(\epsilon)$ from eq.(B.37) and eq.(B.38). By using this fact, we solve the Boltzmann equations with monochromatic high energy photon injection. As one will see, extensions to the cases with non-monochromatic sources or the high energy electron source are trivial.

In our numerical calculations, we use the mesh points E_i ($0 \leq i \leq N_{\text{mesh}} + 1$) with $E_0 = \epsilon_{\text{min}}$ and $E_{N_{\text{mesh}}} = \epsilon_0$, where ϵ_{min} is some minimum energy we are concerning (which we take $\epsilon_{\text{min}} = 1\text{MeV}$) and ϵ_0 is the energy of the primary injecting photons. The energy range between ϵ_{min} and ϵ_0 is divided logarithmically, *i.e.* the i -th mesh point E_i is given by

$$E_i = \epsilon_{\text{min}} \left(\frac{\epsilon_0}{\epsilon_{\text{min}}} \right)^{i/N_{\text{mesh}}}.\tag{B.39}$$

By using the fact that the incoming photons into the mesh point $E_{N_{\text{mesh}}}$ are supplied only

by the photon source, incoming terms for $i = N_{\text{mesh}}$ is given by

$$\dot{f}_{\gamma, \text{IN}}(E_{N_{\text{mesh}}}) \simeq \dot{n}_{\gamma} \times \frac{1}{\Delta_{N_{\text{mesh}}}}, \quad (\text{B.40})$$

$$\dot{f}_{e, \text{IN}}(E_{N_{\text{mesh}}}) \simeq 0, \quad (\text{B.41})$$

where \dot{n}_{γ} is the production rate of monochromatic photons, and $\Delta_i \equiv (E_{i+1} - E_{i-1})/2$. Combining eq.(B.40) and eq.(B.41) with eq.(B.37) and eq.(B.38), we can obtain the distribution functions at the N_{mesh} -th mesh point $f_{\gamma}(E_{N_{\text{mesh}}})$ and $f_e(E_{N_{\text{mesh}}})$.

Next we determine the distribution functions for lower energy region. Essentially, “incoming” terms for the i -th mesh point are derived from the distribution functions $f_{\gamma}(E_j)$ and $f_e(E_j)$ with $j > i$. Discretizing eq.(B.34) and eq.(B.35), “incoming” terms are (approximately) given by

$$\dot{f}_{\gamma, \text{IN}}(E_i) \simeq \sum_{j>i} \Delta_j \{K_{\gamma\gamma}(E_i, E_j) f_{\gamma}(E_j) + K_{\gamma e}(E_i, E_j) f_e(E_j)\}, \quad (\text{B.42})$$

$$\dot{f}_{e, \text{IN}}(E_i) \simeq \sum_{j>i} \Delta_j \{K_{e\gamma}(E_i, E_j) f_{\gamma}(E_j) + K_{ee}(E_i, E_j) f_e(E_j)\}, \quad (\text{B.43})$$

from which we can obtain $f_{\gamma}(E_i)$ and $f_e(E_i)$ by using eq.(B.37) and eq.(B.38).¹ In a way explained above, we calculate the photon and electron distribution functions $f_{\gamma}(E_i)$ and $f_e(E_i)$ at each mesh points from $i = N_{\text{mesh}} - 1$ to $i = 0$ in order.

For each T and $\epsilon_{\gamma 0}$, we calculate the spectra $f_{\gamma}(\epsilon_{\gamma})$ and $f_e(E_e)$ by solving eq.(B.1) and eq.(B.2) numerically. Typical spectra are shown in Fig. B.1 in which we show the case with $\epsilon_{\gamma 0} = 100\text{GeV}$ and 10TeV , $T = 100\text{keV}$, 1keV , 10eV , and the incoming flux of the high energy photon is normalized to be

$$\epsilon_{\gamma 0} \times \left. \frac{\partial f_{\gamma}(\epsilon_{\gamma})}{\partial t} \right|_{\text{DE}} = \delta(\epsilon_{\gamma} - \epsilon_{\gamma 0}) \text{ GeV}^5. \quad (\text{B.44})$$

Notice that eq.(B.1) and eq.(B.2) are linear in f_{γ} and f_e . Therefore, once the solution $f_{\gamma, \text{ref}}$ is obtained with some reference value of the decay term $(\partial f_{\gamma}/\partial t)|_{\text{DE, ref}}$, we can reconstruct the photon spectrum for arbitrary value of $(\partial f_{\gamma}/\partial t)|_{\text{DE}}$ with temperature T and the incident photon energy $\epsilon_{\gamma 0}$ fixed;

$$f_{\gamma}(\epsilon_{\gamma}) = f_{\gamma, \text{ref}}(\epsilon_{\gamma}) \times \frac{(\partial f_{\gamma}/\partial t)|_{\text{DE}}}{(\partial f_{\gamma}/\partial t)|_{\text{DE, ref}}}. \quad (\text{B.45})$$

The behaviors of the photon spectrum can be understood in the following way. In the region $\epsilon_{\gamma} \gtrsim m_e^2/22T$, the photon number density is extremely suppressed since the rate of double photon pair creation process is very large. Just below this threshold value, the shape

¹In fact, eq.(B.40) – eq.(B.43) receive corrections of the order of Δ , which is due to the discretization of the energy range. In our numerical calculations, we take these corrections into account.

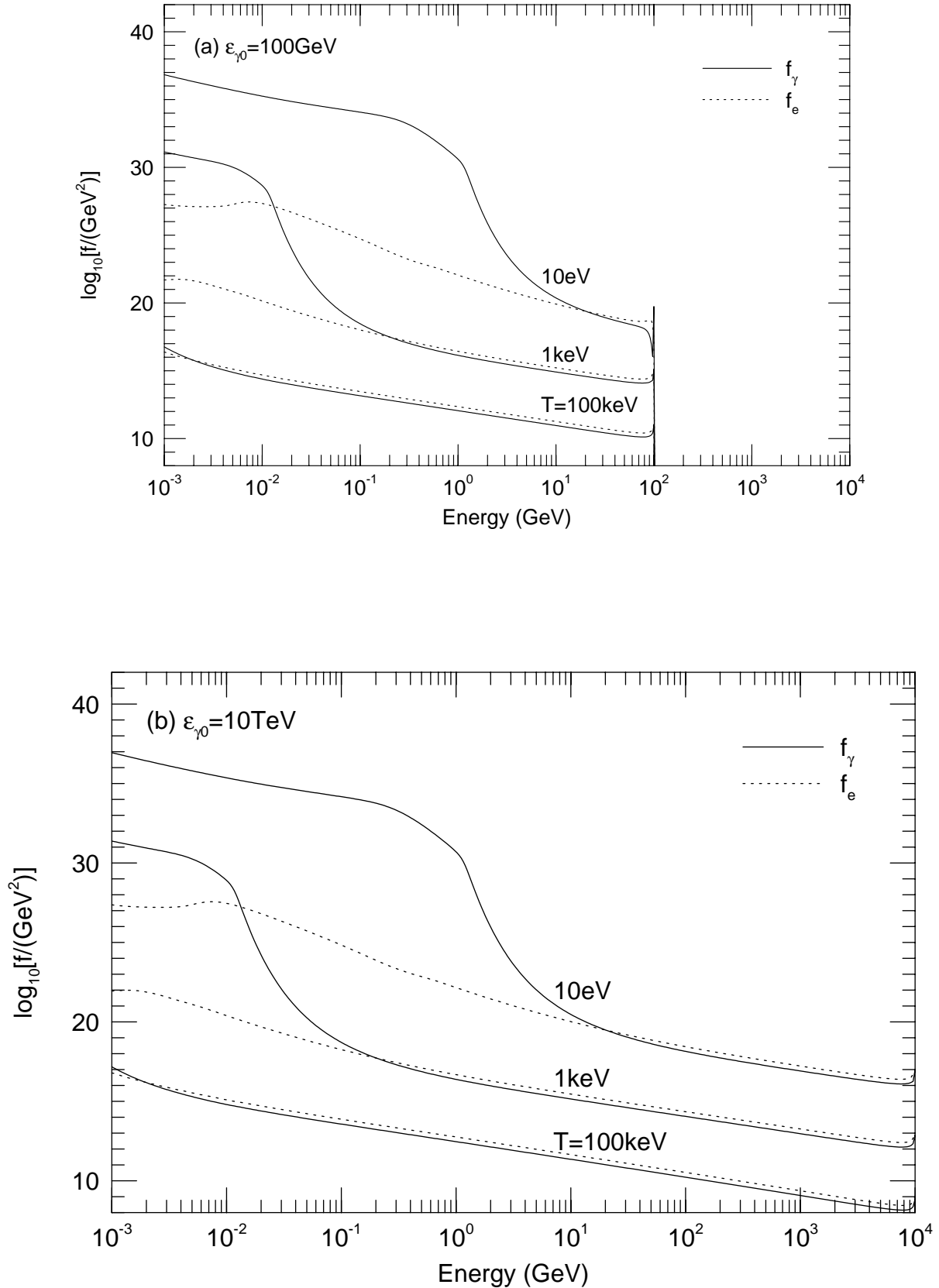


Figure B.1: Typical spectra of photon (the solid lines) and electron (the dotted lines). We take the temperature of the background photon to be $T = 100\text{keV}, 1\text{keV}, 10\text{eV}$, and the energy of the incoming high energy photon $\epsilon_{\gamma 0}$ is (a) 100GeV and (b) 10TeV . Normalization of the initial photon is given by $\epsilon_{\gamma 0} \times (\partial f(\epsilon_{\gamma 0}) / \partial t)|_{\text{EFT}} = \delta(\epsilon_{\gamma 0} - \epsilon_{\gamma 0}) \text{GeV}^5$

$\epsilon_{\gamma 0} = 10 \text{ TeV}$				
Temperature	P_{low}	$N_{\text{low}} \text{ GeV}^2$	P_{pp}	$N_{\text{pp}} \text{ GeV}^2$
1 eV	-1.57	1.6×10^8	-5.10	6.9×10^{-18}
10 eV	-1.34	5.4×10^8	-5.20	6.0×10^{-18}
100 eV	-1.22	1.7×10^9	-4.84	1.1×10^{-17}
$\epsilon_{\gamma 0} = 1 \text{ TeV}$				
Temperature	P_{low}	$N_{\text{low}} \text{ GeV}^2$	P_{pp}	$N_{\text{pp}} \text{ GeV}^2$
1 eV	-1.56	1.4×10^8	-5.07	6.2×10^{-18}
10 eV	-1.34	4.9×10^8	-5.17	5.5×10^{-18}
100 eV	-1.22	1.4×10^9	-4.79	1.0×10^{-17}
$\epsilon_{\gamma 0} = 100 \text{ GeV}$				
Temperature	P_{low}	$N_{\text{low}} \text{ GeV}^2$	P_{pp}	$N_{\text{pp}} \text{ GeV}^2$
1 eV	-1.56	1.4×10^8	-5.01	5.7×10^{-18}
10 eV	-1.33	4.7×10^8	-5.15	5.3×10^{-18}
100 eV	-1.22	1.3×10^9	-4.74	1.1×10^{-17}
$\epsilon_{\gamma 0} = 10 \text{ GeV}$				
Temperature	P_{low}	$N_{\text{low}} \text{ GeV}^2$	P_{pp}	$N_{\text{pp}} \text{ GeV}^2$
1 eV	—	—	—	—
10 eV	-1.33	4.5×10^8	-5.12	5.5×10^{-18}
100 eV	-1.22	1.3×10^9	-4.77	9.6×10^{-18}

Table B.1: P_{low} , N_{low} , P_{pp} and N_{pp} for the cases of $T = 1 \text{ eV}, 10 \text{ eV}, 100 \text{ eV}$, and $\epsilon_{\gamma 0} = 10 \text{ TeV}, 1 \text{ TeV}, 100 \text{ GeV}, 10 \text{ GeV}$. Here, we take $N_{\text{mesh}} = 401$.

of the photon spectrum is determined by the photon-photon scattering process, and if the photon energy is sufficiently small, the Compton scattering with the thermal electron is the dominant process for photons.

As one can see in Figs. B.1, both the photon spectrum for sufficiently low energy region and that for the photon-photon scattering region obey power-law spectrum; $f_{\gamma}(\epsilon_{\gamma}) \propto \epsilon_{\gamma}^P$. We fit the photon spectrum at the sufficiently low energy region as

$$f_{\gamma}(\epsilon_{\gamma}) \simeq N_{\text{low}} \left(\frac{\dot{\rho}_{\text{IN}}}{\text{GeV}^5} \right) \left(\frac{T}{\text{GeV}} \right)^{-3} \left(\frac{\epsilon_{\gamma}}{\text{GeV}} \right)^{P_{\text{low}}}, \quad (\text{B.46})$$

and that for the photon-photon scattering region as

$$f_{\gamma}(\epsilon_{\gamma}) \simeq N_{\text{pp}} \left(\frac{\dot{\rho}_{\text{IN}}}{\text{GeV}^5} \right) \left(\frac{T}{\text{GeV}} \right)^{-6} \left(\frac{\epsilon_{\gamma}}{\text{GeV}} \right)^{P_{\text{pp}}}, \quad (\text{B.47})$$

with $\dot{\rho}_{\text{IN}}$ being the total amount of the energy injection from the gravitino decay;

$$\dot{\rho}_{\text{IN}} = \int d\epsilon_\gamma \epsilon_\gamma \left. \frac{\partial f_\gamma(\epsilon_\gamma)}{\partial t} \right|_{\text{DE}}. \quad (\text{B.48})$$

Notice that the amplitude of the spectrum is proportional to the mean free time of the photon. In low energy region the mean free time is determined by Compton scattering and depends on the background temperature as $\sim T^{-3}$. For the photon-photon scattering region, the amplitude is proportional to $\sim T^{-6}$ since the cross section depends on $\sim T^3$. For the cases $T = 1\text{eV}, 10\text{eV}, 100\text{eV}$ and $\epsilon_0 = 10\text{TeV}, 1\text{TeV}, 100\text{GeV}, 10\text{GeV}$, we calculate the fitting parameters $P_{\text{low}}, P_{\text{pp}}, N_{\text{low}}$ and N_{pp} , and the results are shown in Table B.1.² These variables slightly depend on the background temperature, while their dependence on the initial photon energy $\epsilon_{\gamma 0}$ is insignificant.

In Fig. B.2, we compare our photon spectrum with the results of the simple fitting formula used in ref.[40], which is given by³

$$f_\gamma(\epsilon_\gamma) = \frac{1}{\bar{n}_e \sigma_{\text{CS}}(\epsilon_\gamma)} \times \frac{n_{3/2}}{\tau_{3/2}} \frac{dn_E(\epsilon_\gamma)}{d\epsilon_\gamma}, \quad (\text{B.49})$$

where

$$\left. \frac{dn_E(\epsilon_\gamma)}{d\epsilon_\gamma} \right|_{0 \leq \epsilon_\gamma \leq \epsilon_{\text{max}}/2} = \frac{24\sqrt{2}}{55} \frac{\epsilon_{\gamma 0}}{\sqrt{\epsilon_{\text{max}}}} \epsilon_\gamma^{-3/2}, \quad (\text{B.50})$$

$$\left. \frac{dn_E(\epsilon_\gamma)}{d\epsilon_\gamma} \right|_{\epsilon_{\text{max}}/2 \leq \epsilon_\gamma \leq \epsilon_{\text{max}}} = \frac{3}{55} \epsilon_{\gamma 0} \epsilon_{\text{max}}^3 \epsilon_\gamma^{-5}, \quad (\text{B.51})$$

$$\left. \frac{dn_E(\epsilon_\gamma)}{d\epsilon_\gamma} \right|_{\epsilon_\gamma \geq \epsilon_{\text{max}}} = 0, \quad (\text{B.52})$$

with

$$\epsilon_{\text{max}} \equiv \frac{m_e^2}{22T}. \quad (\text{B.53})$$

As one can see, not only the absolute value but also the form of the spectrum differs between them. The fitting formula in ref.[40] is derived from the numerical results given in refs.[75, 76] in which, however, the effect of the Compton scattering is not taken into account. Our results indicate that the number of Compton scattering events is comparable to that of the inverse Compton events for such low energy region, since the number density of the high energy electron is extremely smaller than that of high energy photon. Therefore, the

²Notice that the formulae (B.46) and (B.47) are relevant for the cases when the initial photon energy $\epsilon_{\gamma 0}$ is much larger than the effective threshold of the double photon pair creation process.

³Although the photon spectrum is not explicitly given in ref. [40], we obtain it from their photon production spectrum divided by the cross section for Compton scattering. Since the cross section has energy dependence, the resultant spectrum ($\propto \epsilon_\gamma^{-0.9}$) becomes softer than that for photon production ($\propto \epsilon_\gamma^{-1.5}$).

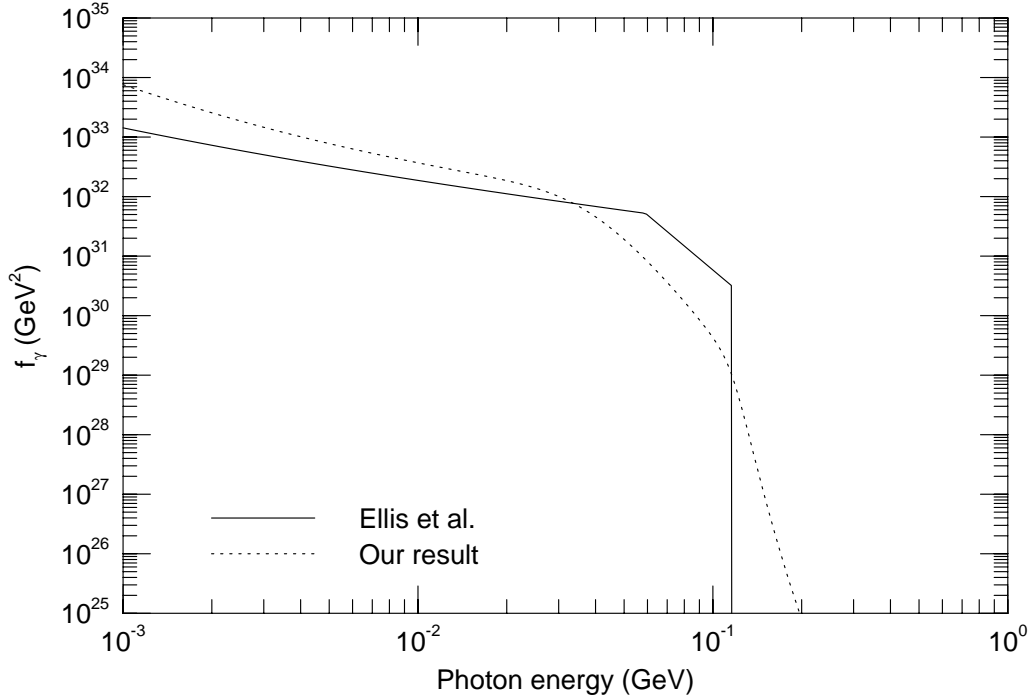


Figure B.2: Photon spectrum derived from the fitting formula used in Ellis et al. [40] (solid line) is compared with our result with $\epsilon_\gamma = 100\text{GeV}$ (dashed line). We take the temperature of the background photon to be 100eV and the normalization of the incoming flux is the same as Fig. B.1.

deformation of the photon spectrum by Compton scattering is expected below the threshold of the photon-photon scattering.

Before closing section, we should comment on the case with high energy electron sources. By numerical calculations, we have checked that the spectra in the case with high energy electron injection are almost the same as those with photon injection if the background temperature and the total amount of the energy injection are fixed. Numerically, their differences are at most $O(10\%)$. Therefore, the formulae given in eq.(B.46) and eq.(B.47) with Table B.1 are well approximated ones if one redefines the $\dot{\rho}_{\text{IN}}$ as

$$\dot{\rho}_{\text{IN}} = \int d\epsilon_\gamma \epsilon_\gamma \left. \frac{\partial f_\gamma(\epsilon_\gamma)}{\partial t} \right|_{\text{DE}} + \int dE_e E_e \left. \frac{\partial f_e(E_e)}{\partial t} \right|_{\text{DE}}. \quad (\text{B.54})$$

B.3 Spectrum with high energy neutrino injection

Next we will consider the case of high energy neutrino injection. In this case, the emitted high energy neutrinos may scatter off the background neutrinos and produce an e^+e^- (or $\mu^+\mu^-$) pairs, which then produces many soft photons through electro-magnetic interactions. Since the rates of neutrino-neutrino scattering processes are not large enough, we cannot ignore the effect of the expansion of the universe. Therefore we calculate high energy photon

Process	a	b	c	d
$\nu_i + \nu_{i,b} \rightarrow \nu_i + \nu_i$	2	0	0	0
$\nu_i + \bar{\nu}_{i,b} \rightarrow \nu_i + \bar{\nu}_i$	0	0	9	0
$\nu_i + \bar{\nu}_{i,b} \rightarrow \nu_j + \bar{\nu}_j$	0	0	1	0
$\nu_i + \nu_{j,b} \rightarrow \nu_i + \nu_j$	1	0	0	0
$\nu_i + \bar{\nu}_{j,b} \rightarrow \nu_i + \bar{\nu}_j$	0	0	1	0
$\nu_i + \bar{\nu}_{i,b} \rightarrow l_i^- + l_i^+$	0	$16 \sin^4 \theta_W$	$16 \sin^4 \theta_W$	$16 \sin^4 \theta_W$
$\nu_i + \bar{\nu}_{i,b} \rightarrow l_j^- + l_j^+$	0	$16 \sin^4 \theta_W$	$(4 \sin^2 \theta_W - 2)^2$	$(4 \sin^2 \theta_W - 2)^2 - 4$

Table B.2: Coefficients $a - d$ for each processes. Index i and j (with $i \neq j$) represent the generation, $\nu_{i,b}$ is the background neutrino of i -th generation, l_i^\pm is the charged lepton of i -th generation (in our case, e^\pm or μ^\pm), and θ_W is the Weinberg angle.

spectrum in two steps; first we determine the time evolution of the distribution function of high energy neutrinos, and then we calculate the photon (and the electron) spectrum by regarding the high energy neutrinos as sources of high energy e^+e^- (and $\mu^+\mu^-$) pairs. The procedures for the second step are essentially equal to those given in the previous section, and in this section, we will explain the first step.

Let us begin by deriving the Boltzmann equations which determines the high energy neutrino spectra. Injecting high energy neutrinos scatter off the thermal neutrinos in the following processes;

$$\nu_i + \nu_{i,b} \rightarrow \nu_i + \nu_i, \quad (\text{B.55})$$

$$\nu_i + \bar{\nu}_{i,b} \rightarrow \nu_i + \bar{\nu}_i, \quad (\text{B.56})$$

$$\nu_i + \bar{\nu}_{i,b} \rightarrow \nu_j + \bar{\nu}_j, \quad (\text{B.57})$$

$$\nu_i + \nu_{j,b} \rightarrow \nu_i + \nu_j, \quad (\text{B.58})$$

$$\nu_i + \bar{\nu}_{j,b} \rightarrow \nu_i + \bar{\nu}_j, \quad (\text{B.59})$$

$$\nu_i + \bar{\nu}_{i,b} \rightarrow e^- + e^+, \quad (\text{B.60})$$

$$\nu_i + \bar{\nu}_{i,b} \rightarrow \mu^- + \mu^+. \quad (\text{B.61})$$

where index i and j are the generation indices with $i \neq j$, and l^\pm represents e^\pm and μ^\pm . All the amplitude squared $|\mathcal{M}|^2$ in these reactions take the form given by

$$|\mathcal{M}|^2 = 32G_F^2 \left\{ a(pp')^2 + b(pq)^2 + c(pq')^2 + dm^2(pp') \right\}, \quad (\text{B.62})$$

where $G_F \equiv (1/\sqrt{2}v^2) \simeq 1.17 \times 10^{-5} \text{GeV}^{-2}$ is the Fermi constant (with $v \simeq 246 \text{GeV}$), p and p' the initial momenta of high energy neutrino and background neutrino, q and q' the final momenta, m the mass of the fermion in final state, and the coefficients $a - d$ depend on individual reaction. Coefficients for each processes are given in Table B.2.

First, we will consider the neutrino scattering processes (B.55) – (B.59). Let us derive

a formula for the energy distribution of scattered neutrino for the case where a high energy neutrino with energy E_ν runs through a region filled with neutrino gas with temperature T_ν . For this purpose, it is convenient to consider the momenta $p - q'$ in the center-of-mass frame. In the center-of-mass frame, we parametrize $p - q'$ by using parameters ξ, η, ζ ($0 \leq \xi, \eta \leq \pi$, and $0 \leq \zeta \leq 2\pi$) as

$$p_{\text{cm}}^\mu = \omega(1, 0, \sin \xi, \cos \xi), \quad (\text{B.63})$$

$$p'_{\text{cm}}^\mu = \omega(1, 0, -\sin \xi, -\cos \xi), \quad (\text{B.64})$$

$$q_{\text{cm}}^\mu = \omega(1, \sin \eta \cos \zeta, \sin \eta \sin \zeta, \cos \eta), \quad (\text{B.65})$$

$$q'_{\text{cm}}^\mu = \omega(1, -\sin \eta \cos \zeta, -\sin \eta \sin \zeta, -\cos \eta). \quad (\text{B.66})$$

Then the differential cross section is given by

$$\frac{d\sigma}{d\cos\eta d\zeta} = \frac{1}{2\pi^2 s} G_F^2 \left\{ a(pp')^2 + b(pq)^2 + c(pq')^2 + dm^2(pp') \right\}, \quad (\text{B.67})$$

with

$$s \equiv (p + p')^2 = 4\omega^2. \quad (\text{B.68})$$

Boosting this system to z -direction with velocity β , we obtain

$$p^\mu = \omega(\gamma(1 + \beta \cos \xi), 0, \sin \xi, \gamma(\cos \xi + \beta)), \quad (\text{B.69})$$

$$p'^\mu = \omega(\gamma(1 - \beta \cos \xi), 0, \sin \xi, \gamma(-\cos \xi + \beta)), \quad (\text{B.70})$$

with $\gamma^{-1} \equiv \sqrt{1 - \beta^2}$. We identify these momenta as those in the comoving frame. Then the energy of initial high energy neutrino E_ν and that of thermal neutrino \bar{E}_ν are given by

$$E_\nu = \omega\gamma(1 + \beta \cos \xi), \quad (\text{B.71})$$

$$\bar{E}_\nu = \omega\gamma(1 - \beta \cos \xi). \quad (\text{B.72})$$

Furthermore, the angle θ between \mathbf{p} and \mathbf{p}' (in the comoving frame) can be obtained from the following relation;

$$\cos \theta = 1 - \frac{2 - 2\beta^2}{1 - \beta^2 \cos \xi}, \quad (\text{B.73})$$

and the energy of the neutrino in final state E'_ν is given by

$$E'_\nu \equiv q^0 = \omega\gamma(1 + \beta \cos \eta). \quad (\text{B.74})$$

Using these identities and integrating with ζ , differential cross section (B.67) becomes

$$\begin{aligned} \frac{d\sigma}{dE'_\nu} &= \frac{s}{32\pi} G_F^2 (\beta\gamma\omega)^{-1} \\ &\times \left\{ 8a + b \left(3 - \cos^2 \xi - \cos^2 \eta - 4 \cos \xi \cos \eta + 3 \cos^2 \xi \cos^2 \eta \right) \right. \\ &\left. + c \left(3 - \cos^2 \xi - \cos^2 \eta + 4 \cos \xi \cos \eta + 3 \cos^2 \xi \cos^2 \eta \right) \right\}. \end{aligned} \quad (\text{B.75})$$

Now we are ready to calculate the number density of scattered neutrino with energy $E'_\nu - (E'_\nu + dE'_\nu)$ in unit time. For this purpose, let us consider the process in which incident high energy neutrino with energy $E_\nu - (E_\nu + dE_\nu)$ scatters off the thermal neutrino with energy $\bar{E}_\nu - (\bar{E}_\nu + d\bar{E}_\nu)$ and relative angle $\theta - (\theta + d\theta)$. For this process, number density of the target (thermal) neutrino is given by

$$(\text{target}) = \frac{1}{2} \bar{f}_\nu(\bar{E}_\nu) d\bar{E}_\nu \sin \theta d\theta.$$

where $\bar{f}_\nu(\bar{E}_\nu)$ is the distribution function of the background neutrino;

$$\bar{f}_\nu(\bar{E}_\nu) = \frac{\bar{E}_\nu^2}{2\pi^2} \frac{1}{e^{-\bar{E}_\nu/T_\nu} + 1}, \quad (\text{B.76})$$

with T_ν being the neutrino temperature. Furthermore, relative velocity of the two neutrino is $(1 - \cos \theta)$ and hence one can obtain the incident flux as

$$(\text{flux}) = (1 - \cos \theta) f_\nu(E_\nu) dE_\nu.$$

Then one can obtain the contribution to the time derivative of the neutrino distribution function as

$$\begin{aligned} \left. \frac{\partial f_\nu(E'_\nu)}{\partial E'_\nu} \right|_+ &= \int (\text{target}) \times (\text{flux}) \times \frac{d\sigma}{dE'_\nu} \\ &= \frac{1}{128\pi} G_F^2 \int_{E'_\nu}^\infty dE_\nu \int d\bar{E}_\nu \frac{1}{E_\nu \bar{E}_\nu} f_\nu(E_\nu) \bar{f}_\nu(\bar{E}_\nu) \int_0^{4E_\nu \bar{E}_\nu} ds s^2 (E_{\text{in}}^2 - s)^{-1/2} \\ &\times \left\{ (8a + 3b + 3c) - 4(b - c) \cos \xi \cos \eta \right. \\ &\left. + (b + c) \left(3 \cos^2 \xi \cos^2 \eta - \cos^2 \xi - \cos^2 \eta \right) \right\}, \end{aligned} \quad (\text{B.77})$$

with

$$E_{\text{in}} = E_\nu + \bar{E}_\nu. \quad (\text{B.78})$$

Notice that the angles ξ and η can be represented by the variables in the comoving frame

through the following relations;

$$\cos \xi = (E_\nu - \bar{E}_\nu) (E_{\text{in}}^2 - s)^{-1/2}, \quad (\text{B.79})$$

$$\cos \eta = (2E'_\nu - E_{\text{in}}) (E_{\text{in}}^2 - s)^{-1/2}. \quad (\text{B.80})$$

Define

$$H_p(E_\nu, \bar{E}_\nu) \equiv \int_0^{4E_\nu \bar{E}_\nu} ds s^2 (E_{\text{in}}^2 - s)^{-p/2}, \quad (\text{B.81})$$

then eq.(B.77) can be rewritten as

$$\begin{aligned} \left. \frac{\partial f_\nu(E'_\nu)}{\partial E'_\nu} \right|_+ &= \frac{1}{128\pi} G_F^2 \int dE_\nu d\bar{E}_\nu \frac{1}{E_\nu \bar{E}_\nu} f_\nu(E_\nu) \bar{f}_\nu(\bar{E}_\nu) \\ &\times \left\{ (8a + 3b + 3c) H_1(E_\nu, \bar{E}_\nu) \right. \\ &- (b + c) (E_\nu - \bar{E}_\nu)^2 H_3(E_\nu, \bar{E}_\nu) \\ &- (b + c) (2E'_\nu - E_{\text{in}})^2 H_3(E_\nu, \bar{E}_\nu) \\ &- 4(b - c) (E_\nu - \bar{E}_\nu) (2E'_\nu - E_{\text{in}}) H_3(E_\nu, \bar{E}_\nu) \\ &\left. + 3(b + c) (E_\nu - \bar{E}_\nu)^2 (2E'_\nu - E_{\text{in}})^2 H_5(E_\nu, \bar{E}_\nu) \right\}. \end{aligned} \quad (\text{B.82})$$

After some complicated calculations, the above equation becomes very simple form;

$$\begin{aligned} \left. \frac{\partial f_\nu(E'_\nu)}{\partial E'_\nu} \right|_+ &= \frac{4}{3\pi} G_F^2 \int_{E'_\nu}^\infty dE_\nu \int d\bar{E}_\nu \frac{\bar{E}_\nu}{E_\nu^2} f_\nu(E_\nu) \bar{f}_\nu(\bar{E}_\nu) \\ &\times \left\{ aE_\nu^2 + b(E_\nu - E'_\nu)^2 + cE_\nu'^2 \right. \\ &+ \frac{1}{2} aE_\nu \bar{E}_\nu + \frac{3}{2} b(E_\nu - E'_\nu) \bar{E}_\nu - \frac{1}{2} cE'_\nu \bar{E}_\nu \\ &\left. + \frac{1}{10} (a + 6b + c) \bar{E}_\nu^2 \right\}. \end{aligned} \quad (\text{B.83})$$

In the following analysis, we use the approximation $E_\nu, E'_\nu \gg \bar{E}_\nu$. With this approximation, the above equation becomes

$$\begin{aligned} \left. \frac{\partial f_\nu(E'_\nu)}{\partial E'_\nu} \right|_+ &= \frac{4}{3\pi} G_F^2 \int_{E'_\nu}^\infty dE_\nu \frac{1}{E_\nu^2} \left\{ aE_\nu^2 + b(E_\nu - E'_\nu) + cE_\nu'^2 \right\} f_\nu(E_\nu) \\ &\times \int_0^\infty d\bar{E}_\nu \bar{E}_\nu \bar{f}_\nu(\bar{E}_\nu). \end{aligned} \quad (\text{B.84})$$

Next we will calculate how many neutrinos scatter off the background neutrino in unit time. As is the similar method used above, contribution to the time derivative of the neutrino

distribution function from this effect can be obtained as

$$\begin{aligned} \left. \frac{\partial f_\nu(E_\nu)}{\partial E_\nu} \right|_- &= -\frac{1}{8} \frac{1}{E_\nu^2} f_\nu(E_\nu^2) \int_0^\infty d\bar{E}_\nu \frac{1}{\bar{E}_\nu^2} \bar{f}_\nu(\bar{E}_\nu) \int_0^{4E_\nu \bar{E}_\nu} ds \, s \sigma(s) \\ &= -\frac{4}{3\pi} G_F^2 \left(a + \frac{1}{3}b + \frac{1}{3}c \right) E_\nu f_\nu(E_\nu) \int_0^\infty d\bar{E}_\nu \bar{E}_\nu \bar{f}_\nu(\bar{E}_\nu), \end{aligned} \quad (\text{B.85})$$

where $\sigma(s)$ is the total cross section obtained from the amplitude (B.62). Notice that the condition for the neutrino number conservation is realized;

$$\int_0^\infty dE_\nu \left. \frac{\partial f_\nu(E_\nu)}{\partial E_\nu} \right|_+ = - \int_0^\infty dE_\nu \left. \frac{\partial f_\nu(E_\nu)}{\partial E_\nu} \right|_-, \quad (\text{B.86})$$

unless the effects of inelastic channels ($\nu + \bar{\nu} \rightarrow e^+ + e^-, \mu^+ + \mu^-$) are taken into account.

Effects of the charged lepton pair creation process can be taken into account in the same way, and the contribution to the time derivative of the neutrino distribution function is given by

$$\begin{aligned} \left. \frac{\partial f_\nu(E_\nu)}{\partial E'_\nu} \right|_{\nu+\bar{\nu} \rightarrow l^-+l^+} &= -\frac{1}{8} \frac{1}{E_\nu} f_\nu(E_\nu) \int_0^\infty d\bar{E}_\nu \frac{1}{\bar{E}_\nu^2} \bar{f}_\nu(\bar{E}_\nu) \int_{4m^2}^{4E_\nu \bar{E}_\nu} ds \, s \sigma(s) \\ &= -\frac{G_F^2}{16\pi} \frac{1}{E_\nu^2} f_{\nu_i}(E_\nu) \int_0^\infty d\bar{E}_\nu \bar{f}_\nu(\bar{E}_\nu) \\ &\quad \times \left\{ \left(a + \frac{1}{3}b + \frac{1}{3}c \right) I_2 + \left(2d - \frac{1}{3}b - \frac{1}{3}c \right) m^2 I_1 \right\}, \end{aligned} \quad (\text{B.87})$$

with

$$\begin{aligned} I_2 &= \frac{4}{3} \left\{ 4 - \frac{4m^2}{E_\nu \bar{E}_\nu} \right\}^{1/2} E_\nu \bar{E}_\nu \left(8E_\nu^2 \bar{E}_\nu^2 - 2m^2 E_\nu \bar{E}_\nu - 3m^4 \right) \\ &\quad - 4m^6 \ln \left[\frac{2 \left\{ 4 - (4m^2/E_\nu \bar{E}_\nu) \right\}^{1/2} E_\nu \bar{E}_\nu + 4E_\nu \bar{E}_\nu - 2m^2}{2m^2} \right], \end{aligned} \quad (\text{B.88})$$

$$\begin{aligned} I_1 &= 2 \left\{ 4 - \frac{4m^2}{E_\nu \bar{E}_\nu} \right\}^{1/2} E_\nu \bar{E}_\nu \left(2E_\nu \bar{E}_\nu - m^2 \right) \\ &\quad - 2m^4 \ln \left[\frac{2 \left\{ 4 - (4m^2/E_\nu \bar{E}_\nu) \right\}^{1/2} E_\nu \bar{E}_\nu + 4E_\nu \bar{E}_\nu - 2m^2}{2m^2} \right]. \end{aligned} \quad (\text{B.89})$$

Coefficients for the charged lepton production processes are given in Table B.2.

By using the above formulae, one can obtain the Boltzmann equation describing the evolution of the spectra for the high energy neutrinos;

$$\frac{\partial f_{\nu_i}(E'_\nu)}{\partial t} = \frac{4G_F^2}{3\pi} \int_{E'_\nu}^\infty \frac{dE_\nu}{E_\nu^2} f_{\nu_i}(E_\nu) \sum_j \left\{ a_{in,ij} E_\nu^2 + b_{in,ij} (E_\nu - E'_\nu)^2 + c_{in,ij} E_\nu'^2 \right\}$$

$$\begin{aligned}
& \times \int_0^\infty d\bar{E}_\nu \bar{E}_\nu \bar{f}_\nu(\bar{E}_\nu) \\
& - \frac{4G_F^2}{3\pi} E'_\nu f_{\nu_i}(E'_\nu) \left(a_{out} + \frac{1}{3} b_{out} + \frac{1}{3} c_{out} \right) \int_0^\infty d\bar{\epsilon}_\nu \bar{\epsilon}_\nu \bar{f}_\nu(\bar{\epsilon}_\nu) \\
& + \left. \frac{\partial f_{\nu_i}(E'_\nu)}{\partial t} \right|_{\nu_i + \bar{\nu}_i \rightarrow e^- + e^+} + \left. \frac{\partial f_{\nu_i}(E'_\nu)}{\partial t} \right|_{\nu_i + \bar{\nu}_i \rightarrow \mu^- + \mu^+} \\
& + \frac{1}{6\tau_{3/2}} n_{3/2} \delta(E'_\nu - m_{3/2}/2) \\
& + E'_\nu H \frac{\partial f_{\nu_i}(E'_\nu)}{\partial E'_\nu} - 2H f_{\nu_i}(E'_\nu) E'_\nu,
\end{aligned} \tag{B.90}$$

where H is the expansion rate of the universe, and the coefficients $a - c$ are given by

$$a_{out} = 4, \quad b_{out} = 0, \quad c_{out} = 13, \tag{B.91}$$

$$a_{in,ii} = 6, \quad b_{in,ii} = 9, \quad c_{in,ii} = 11, \tag{B.92}$$

$$a_{in,ij} = 1, \quad b_{in,ij} = 1, \quad c_{in,ij} = 2, \quad (i \neq j). \tag{B.93}$$

The formula for charged lepton pair creation are given in eq.(B.87).

We solve the Boltzmann equations for the distribution function of ν_e , ν_μ and ν_τ numerically. In Figs B.3 – B.5, we shown the time evolution of the distribution function of the electron neutrino for the cases of $m_{3/2} = 100\text{GeV}$, 1TeV , and 10TeV . We have also checked that the difference among three types of neutrinos are very small since the differences only comes from the charged lepton pair creation processes which are sub-dominant compared with the neutrino-neutrino scatterings. In Fig. B.6, the spectra of three types of neutrinos at $T = 1\text{eV}$ are shown for $m_{3/2} = 100\text{GeV}$, 1TeV , and 10TeV . (The time evolutions of the photon spectra are also shown in Fig. B.3 – Fig. B.5.)

By regarding these high energy neutrinos as sources of high energy charged leptons (*i.e.* e^+e^- and $\mu^+\mu^-$), we calculate the high energy photon spectrum induced by the gravitino decay into a neutrino and a sneutrino. The Boltzmann equations for the photon and the electron distribution function f_γ and f_e are given by

$$\begin{aligned}
\frac{\partial f_\gamma(\epsilon_\gamma)}{\partial t} = & \left. \frac{\partial f_\gamma(\epsilon_\gamma)}{\partial t} \right|_{\text{DP}} + \left. \frac{\partial f_\gamma(\epsilon_\gamma)}{\partial t} \right|_{\text{PP}} + \left. \frac{\partial f_\gamma(\epsilon_\gamma)}{\partial t} \right|_{\text{PC}} + \left. \frac{\partial f_\gamma(\epsilon_\gamma)}{\partial t} \right|_{\text{CS}} \\
& + \left. \frac{\partial f_\gamma(\epsilon_\gamma)}{\partial t} \right|_{\text{IC}} + \left. \frac{\partial f_\gamma(\epsilon_\gamma)}{\partial t} \right|_{\text{EXP}},
\end{aligned} \tag{B.94}$$

$$\begin{aligned}
\frac{\partial f_e(E_e)}{\partial t} = & \left. \frac{\partial f_e(E_e)}{\partial t} \right|_{\text{DP}} + \left. \frac{\partial f_e(E_e)}{\partial t} \right|_{\text{PC}} + \left. \frac{\partial f_e(E_e)}{\partial t} \right|_{\text{CS}} + \left. \frac{\partial f_e(E_e)}{\partial t} \right|_{\text{IC}} \\
& + \left. \frac{\partial f_e(E_e)}{\partial t} \right|_{\text{NEU}} + \left. \frac{\partial f_e(E_e)}{\partial t} \right|_{\text{EXP}},
\end{aligned} \tag{B.95}$$

where NEU represents the contribution from the $\nu - \nu$ scatterings. In our numerical calculations, we neglect the effects of the expansion of the universe as in the previous case. In

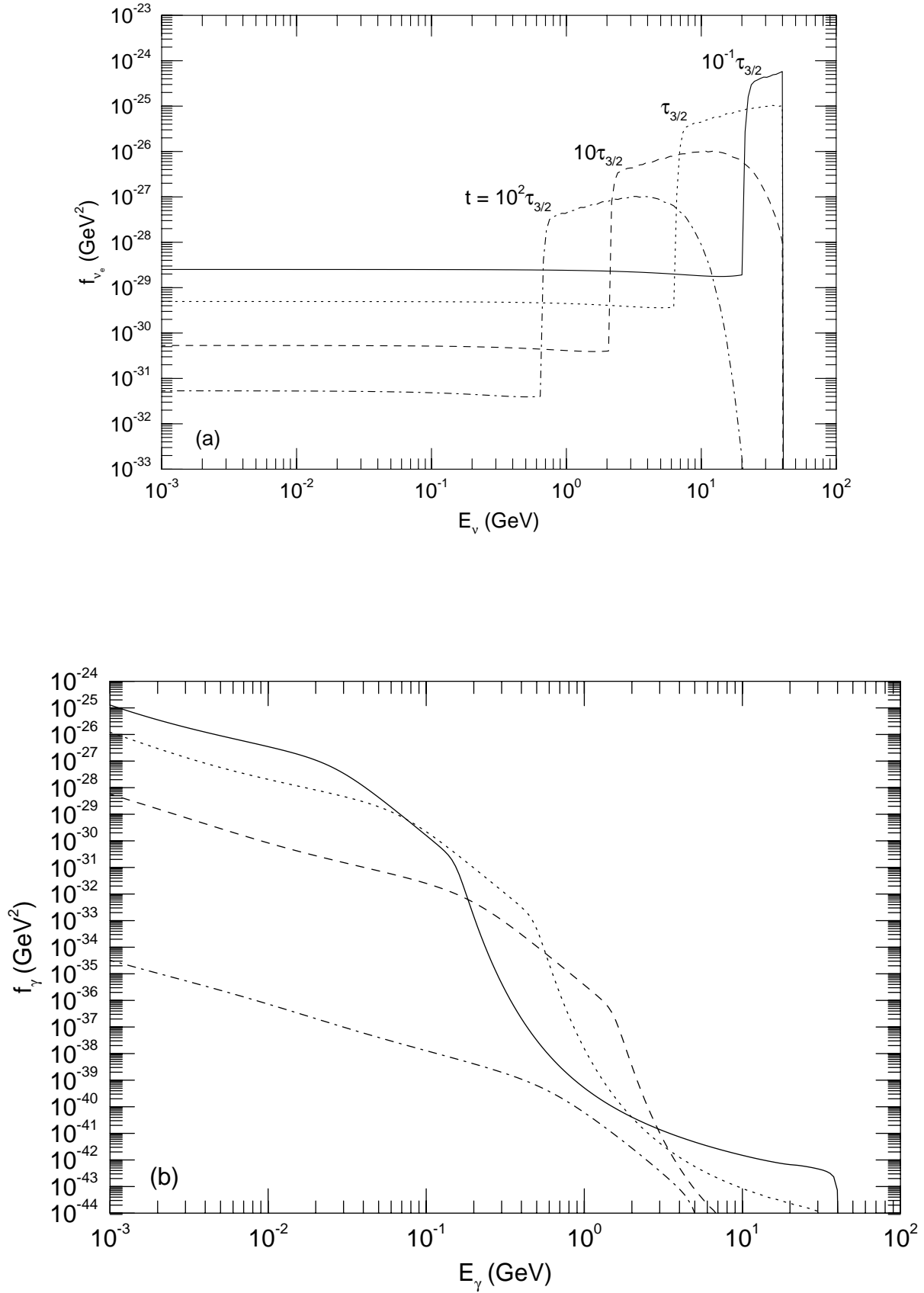


Figure B.3: Time evolution of the distribution function of (a) the electron neutrino, and (b) the photon for the case $m_{3/2} = 100 \text{ GeV}$. The solid curve (dotted curve, dashed curve, and dotted-dashed curve) represents the spectrum at the time $t = 10^{-1} \tau_{3/2}$ ($\tau_{3/2}$, $10 \tau_{3/2}$, and $10^2 \tau_{3/2}$).

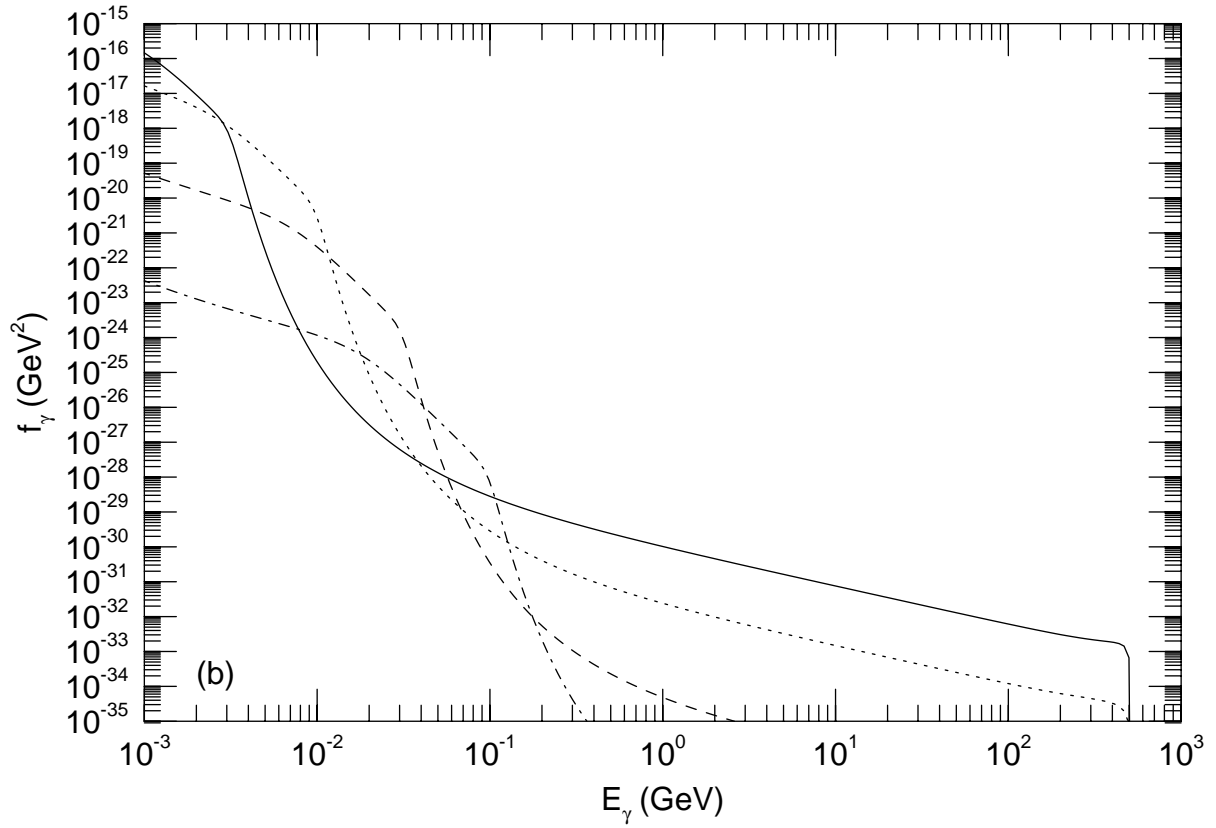
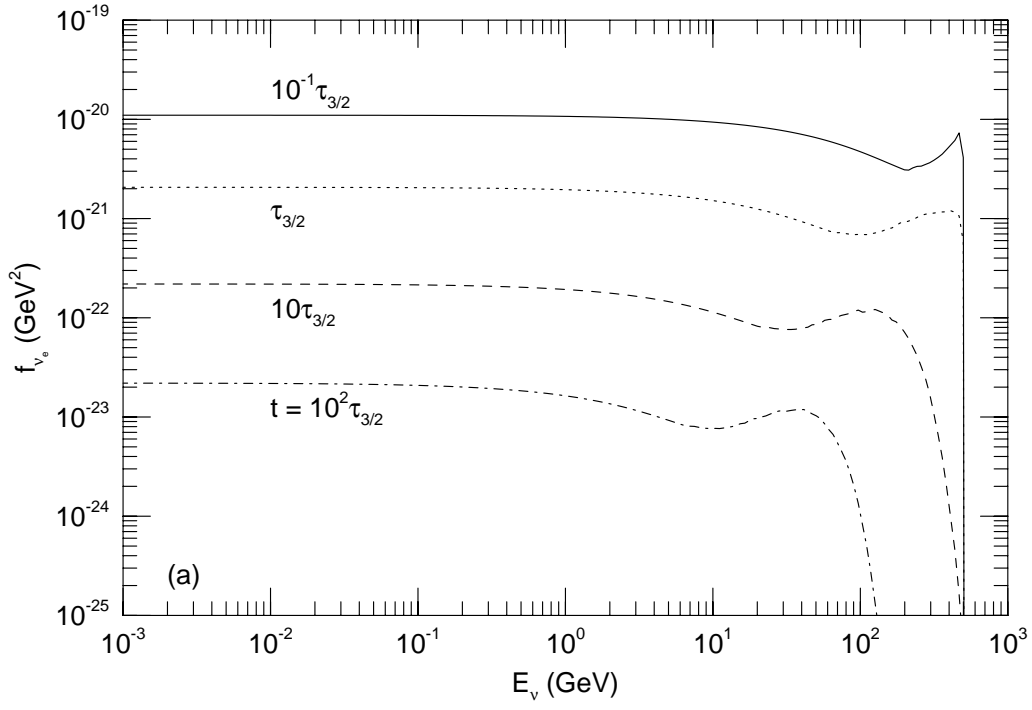


Figure B.4: Same as Fig. B.3 except for $m_{3/2} = 1\text{TeV}$.

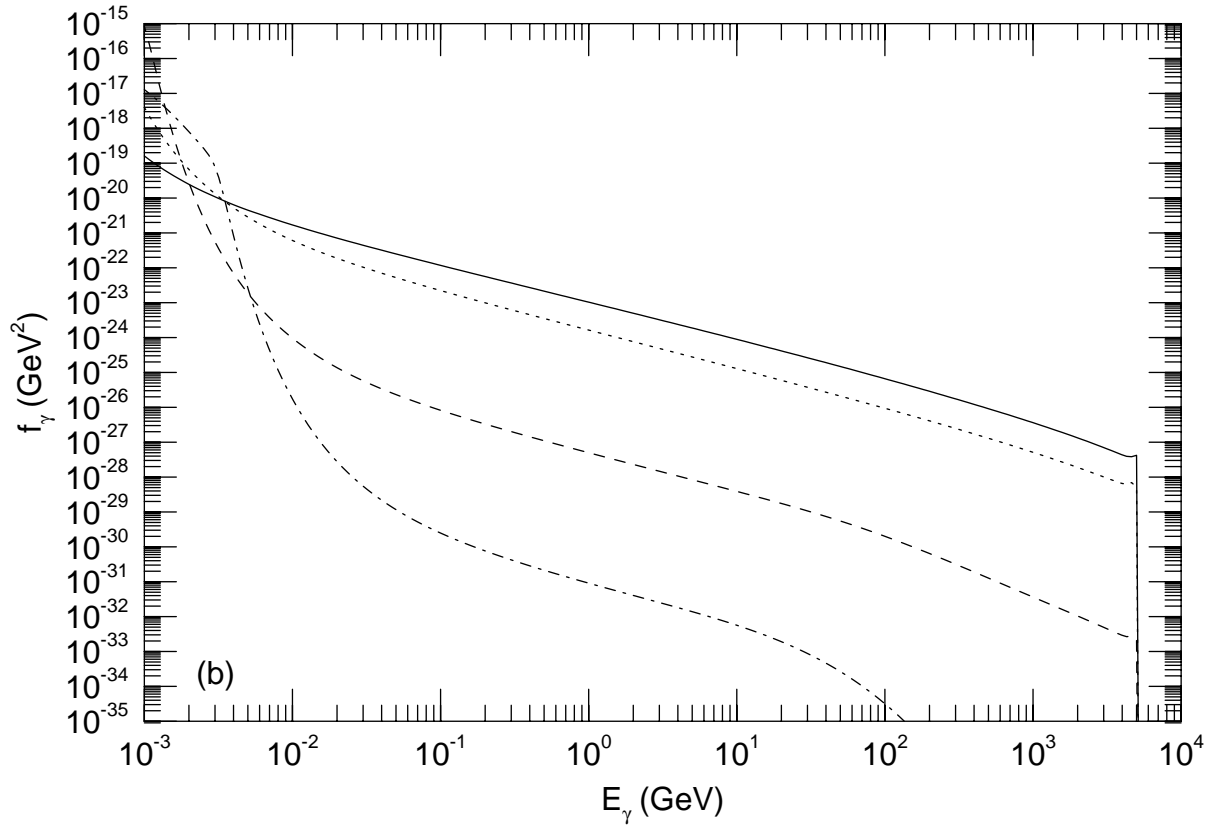
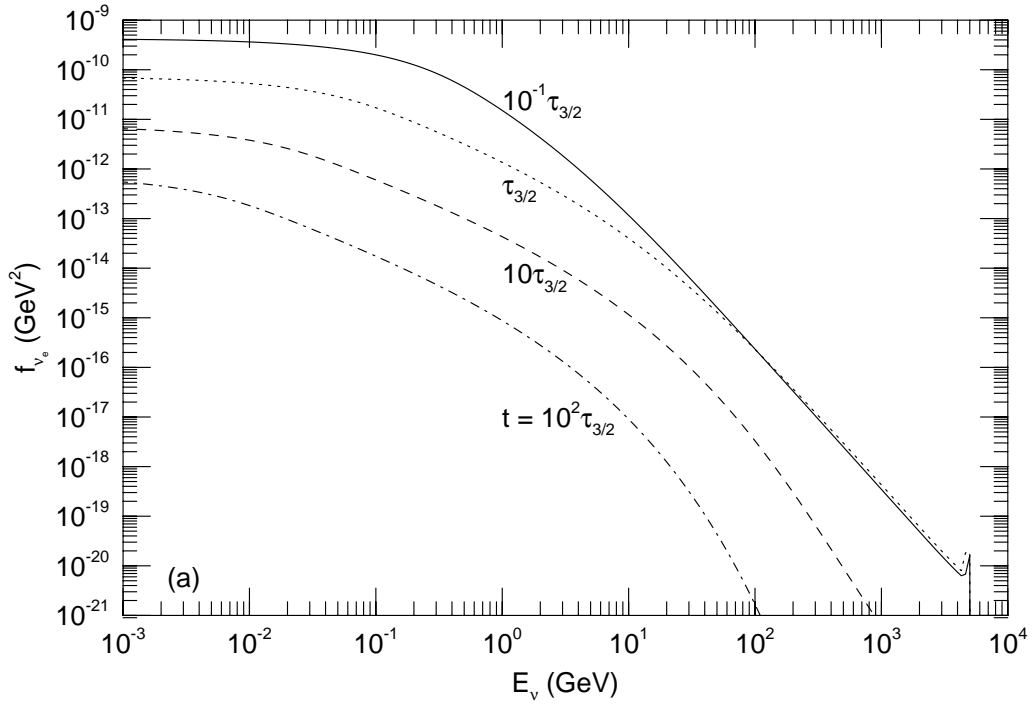


Figure B.5: Same as Fig. B.3 except for $m_{3/2} = 10\text{TeV}$.

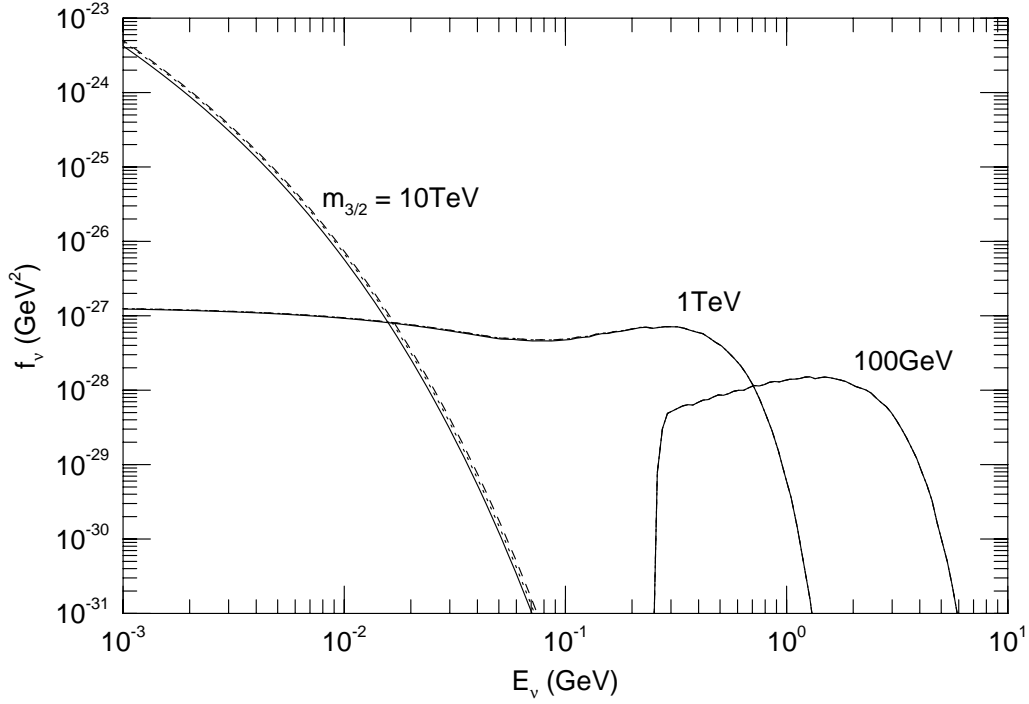


Figure B.6: Spectra of high energy electron-neutrino (solid curve), muon-neutrino (dotted curve) and tau-neutrino (dashed curve) at $T = 1\text{eV}$ for $m_{3/2} = 100\text{GeV}$, 1TeV and 10TeV . The gravitino abundance is normalized as $Y_{3/2} = e^{-t/\tau_{3/2}}$.

solving eq.(B.94) and eq.(B.95), we assume

$$\left. \frac{f_e(E)}{\partial t} \right|_{\text{NEU}} = - \sum_i \left(\left. \frac{f_{\nu_i}(E)}{\partial t} \right|_{\nu_i + \bar{\nu}_i \rightarrow e^- + e^+} + \left. \frac{f_{\nu_i}(E)}{\partial t} \right|_{\nu_i + \bar{\nu}_i \rightarrow \mu^- + \mu^+} \right), \quad (\text{B.96})$$

which respects the energy conservation although the actual energy distribution may be different. This assumption is adequate for our purpose since the photon (electron) spectrum is determined almost only by the total amount of the energy injection [41]. Furthermore we treat muons (and anti-muons) as electrons with the same energy and neglect the contribution from tau leptons whose creation rate is much smaller than the other charged leptons. Full details for other terms are shown in the previous section.

Appendix C

Big-bang nucleosynthesis

Along with the existence of the cosmic microwave background, big-bang nucleosynthesis (BBN) is one of the most important predictions of the big-bang cosmology. As we will see later, observations of the abundance of light nuclei with atomic number less than 7 are in good agreements with theoretical predictions. In this appendix, we will briefly review the theoretical framework of BBN, and compare its results to the observations.

C.1 Theoretical framework

BBN occurs when the temperature of the universe drops below $\sim 1\text{MeV}$. In this section, we will briefly review the BBN scenario by following the thermal history of the universe of temperature about 1MeV . (More details, see ref.[79].)

$T \gg 1\text{MeV}$

When the temperature of the universe is much larger than 1MeV , nuclear statistical equilibrium (NSE) among the light nuclei is established. Especially, proton (p) and neutron (n) are converted to each other in the following weak interaction processes;

$$\begin{aligned} n &\leftrightarrow p + e^- + \bar{\nu}_e, \\ n + \nu_e &\leftrightarrow p + e^-, \\ n + e^+ &\leftrightarrow p + \bar{\nu}_e. \end{aligned}$$

Since the rate of $p \leftrightarrow n$ conversion is sufficiently large, chemical potential of e , ν_e , p and n are related as

$$\mu_n + \mu_\nu = \mu_p + \mu_e, \tag{C.1}$$

where μ_X represents the chemical potential of particle X .

Here, we comment on the magnitude of the chemical potentials of leptons. Since the universe is charge neutral, charge density of electron is equal to the number density of

proton if T is much smaller than the muon mass. If the temperature is high enough, electron can be regarded as a relativistic particle. In this case, charge density is $O(\mu_e T^2)$ and we obtain

$$\left. \frac{\mu_e}{T} \right|_{T \gtrsim 1\text{MeV}} \sim \frac{n_e}{n_\gamma} = \frac{n_p}{n_\gamma} \sim O(10^{-10}). \quad (\text{C.2})$$

In order to estimate the neutrino chemical potential, we must know the lepton number density of the universe. In the early universe when the temperature is higher than the electroweak scale, baryon number and lepton number are converted to each other through the sphaleron transition. If this is true, lepton number of the universe is as the same order as the baryon number. From this fact, we adopt $\mu_\nu/T \sim O(10^{-10})$.

In kinetic equilibrium, number density of nuclei with atomic number A and charge Z is given by

$$n_A = g_A \left(\frac{m_A T}{2\pi} \right)^{3/2} \exp \left(\frac{\mu_A - m_A}{T} \right), \quad (\text{C.3})$$

where g_A represents the internal degrees of freedom. Especially number density of p and n can be written as

$$n_p = 2 \left(\frac{m_p T}{2\pi} \right)^{3/2} \exp \left(\frac{\mu_p - m_p}{T} \right), \quad (\text{C.4})$$

$$n_n = 2 \left(\frac{m_n T}{2\pi} \right)^{3/2} \exp \left(\frac{\mu_n - m_n}{T} \right). \quad (\text{C.5})$$

If the nucleon with the atomic number A and charge Z can be made out of Z protons and $(A - Z)$ neutrons rapidly enough, μ_A is related to μ_p and μ_n in the following way;

$$\mu_A = Z\mu_p + (A - Z)\mu_n. \quad (\text{C.6})$$

Using eq.(C.3) – eq.(C.6), n_A can be expressed as

$$n_A = g_A A^{3/2} 2^{-A} \left(\frac{2\pi}{m_N T} \right)^{3(A-1)/2} n_p^Z n_n^{A-Z} \exp(B_A/T), \quad (\text{C.7})$$

where B_A is binding energy which is defined as

$$B_A = Zm_p + (A - Z)m_n - m_A, \quad (\text{C.8})$$

and for simplicity all the “nucleon masses” (m_p , m_n and m_A/A) in the prefactor are replaced by the common mass m_N since their differences are not important. Numerical values of B_A and g_A for some nuclei are shown in Table C.1.

AZ	$B_A(\text{MeV})$	g_A
D	2.22	3
${}^3\text{H}$	6.92	2
${}^3\text{He}$	7.72	2
${}^4\text{He}$	28.3	1
${}^{12}\text{C}$	92.2	1

Table C.1: The binding energy and internal degrees of freedom of light nuclei.

For a later convenience, we define the mass fraction of species A ;

$$X_A = \frac{An_A}{n_B}, \quad (\text{C.9})$$

with n_B being the baryon number density;

$$n_B = n_p + n_n + \sum_{A,Z} An_A. \quad (\text{C.10})$$

Then we can get

$$X_A = g_A \left\{ \zeta(3)^{A-1} \pi^{(1-A)/2} 2^{(3A-5)/2} \right\} A^{5/2} (T/m_N)^{3(A-1)/2} \\ \times \eta_B^{A-1} X_p^Z X_n^{A-Z} \exp(B_A/T), \quad (\text{C.11})$$

where $\eta_B \equiv n_B/n_\gamma$ is the baryon-to-photon ratio. Notice that η_B is related to the present baryonic density parameter Ω_B as

$$\eta_B = \frac{n_B}{n_\gamma} \simeq 2.68 \times 10^{-8} \Omega_B h^2. \quad (\text{C.12})$$

Since X_A is proportional to η_B^{A-1} , mass fraction of species with large atomic number is extremely small if they are in chemical equilibrium. For example, with $T = 10\text{MeV}$,

$$\begin{aligned} X_p &\simeq 0.5, \\ X_n &\simeq 0.5, \\ X_D &\simeq 10^{-11}, \\ X_{{}^3\text{He}} &\simeq 10^{-23}, \\ X_{{}^4\text{He}} &\simeq 10^{-34}. \end{aligned}$$

$0.3\text{MeV} \lesssim T \lesssim 1\text{MeV}$

Once the temperature of the universe drops below $\sim 1\text{MeV}$, situation changes. When the temperature becomes $T_F \simeq 0.8\text{MeV}$, $p \leftrightarrow n$ conversion rate becomes smaller than the

expansion rate of the universe. At this freeze out temperature T_F , ratio of n_p and n_n is given by

$$\left. \frac{n_n}{n_p} \right|_{T=T_F} = \exp \left(\frac{m_p - m_n}{T_F} \right) \simeq \frac{1}{6}. \quad (\text{C.13})$$

Below T_F , number density of neutron decreases mainly through the free neutron decay process. But the decay rate of neutron is smaller than the expansion rate and hence, mass fraction of neutron is almost unchanged. On the other hand, nucleon production rate is still sufficiently large, number density of light nuclei (like D, ^3He , ^4He , \dots) takes the NSE value. At this stage mass fractions of light nuclei are as follows;

$$\begin{aligned} X_p &\simeq 1/7, \\ X_n &\simeq 6/7, \\ X_D &\simeq 10^{-12}, \\ X_{^3\text{He}} &\simeq 10^{-23}, \\ X_{^4\text{He}} &\simeq 10^{-28}. \end{aligned}$$

$T \lesssim 0.3\text{MeV}$

When the temperature becomes $\sim 0.3\text{MeV}$, NSE value of $X_{^4\text{He}}$ approaches to 1. This fact suggests that ^4He can be synthesized effectively at $T \lesssim 0.3\text{MeV}$. But for $T \gtrsim 0.1\text{MeV}$, D, which is a source of ^4He , is easily destroyed through the scattering processes off the background photon.

Once the temperature drops below $\sim 0.1\text{MeV}$, D's are effectively produced and they are rapidly translated into ^4He through the following processes;

$$\begin{aligned} &\text{D}(\text{D}, n)^3\text{He}(\text{D}, p)^4\text{He}, \\ &\text{D}(\text{D}, p)^3\text{H}(\text{D}, n)^4\text{He}, \\ &\text{D}(\text{D}, \gamma)^4\text{He}. \end{aligned}$$

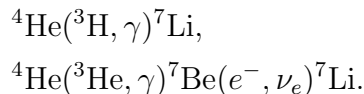
Through these processes, almost all of neutrons in the universe are trapped in ^4He and primordial abundance of D and ^3He becomes much less than that of ^4He . Order of the primordial mass fraction of ^4He , Y_p , can be estimated to be

$$Y_p = \left. \frac{4n_{^4\text{He}}}{n_B} \right|_p \sim \left. \frac{2n_n}{n_B} \right|_{T \sim 0.1\text{MeV}} \sim 0.25, \quad (\text{C.14})$$

where we have used $X_n|_{T \sim 0.1\text{MeV}} \sim 0.125$. (Notice that Y_P given in eq.(C.14) is overestimated and the result of numerical calculation shows that $Y_p \sim 0.24$.)

Finally, we will comment on the nucleosynthesis beyond ^4He . Since there is no tightly

bounded isotope with $A=5$ and 8, nucleus which is heavier than ^4He is scarcely synthesized. One important exception is ^7Li which can be synthesized in the following two processes;



C.2 Numerical results

In order to calculate the primordial abundance of light elements, we use numerical method. The following results are obtained by using the FORTRAN code written by Kawano [57].

Before looking at the numerical results, let us consider about the basic parameters of BBN. Essentially, primordial abundances of light elements depend only on one cosmological parameter, η_B , however predicted abundances of light nuclei are also affected by uncertainties come from the uncertainties of the fundamental theory (especially, by those of weak interaction).

Neutron lifetime τ_n is the significant parameter of BBN. In order to calculate the primordial abundance of ^4He , we must accurately determine neutron freeze out temperature T_F , which depends on weak interaction rates. These rates are calculated from only one matrix element which is also related to neutron lifetime τ_n , and hence experimental data of neutron lifetime is very important for calculating the primordial abundances. We will see that the predicted abundance of ^4He decreases as neutron lifetime τ_n increases. This can be understood in the following way. A larger value of τ_n implies smaller weak interaction rates, and this leads to a lower freeze out temperature T_F . Therefore, neutron lifetime increases, ratio of n_n to n_p at T_F decreases and hence a smaller value of ^4He abundance is expected.

In Fig. C.1, we show the results of the numerical calculations of BBN. For a neutron lifetime τ_n , we use $\tau_n = 891.2\text{sec}$ and $\tau_n = 887.0\text{sec}$. As mentioned before, for a larger value of τ_n , a smaller value of the primordial ^4He abundance is obtained. Primordial abundances also depend on the baryon-to-photon ratio η_B . As one can see, predicted abundance of ^4He is a increasing function of η_B while those of D and ^3He decreases as η_B increases, and ^7Li abundance takes its minimum value at $\eta_B \sim 3 \times 10^{-10}$.

In Fig. C.1, we also plot the predicted abundance of ^4He in a model with four neutrino species. As one can see, if we add extra neutrino species, predicted abundance of ^4He increases. This can be understood in the following way. If the extra neutrino exists, the expansion rate of the universe at $T \sim 1\text{MeV}$ gets higher due to the energy density of extra neutrino, and hence the neutron freeze out temperature T_F gets higher. In general, if there exists some exotic particle whose energy density at $T \sim 1\text{MeV}$ is not negligible, it speeds up the cosmic expansion rate and raise the neutron freeze out temperature. In this case more ^4He is synthesized since larger amount of relic neutron is expected. this argument constrains the properties of exotic particles. For example, existence if additional light neutrino species

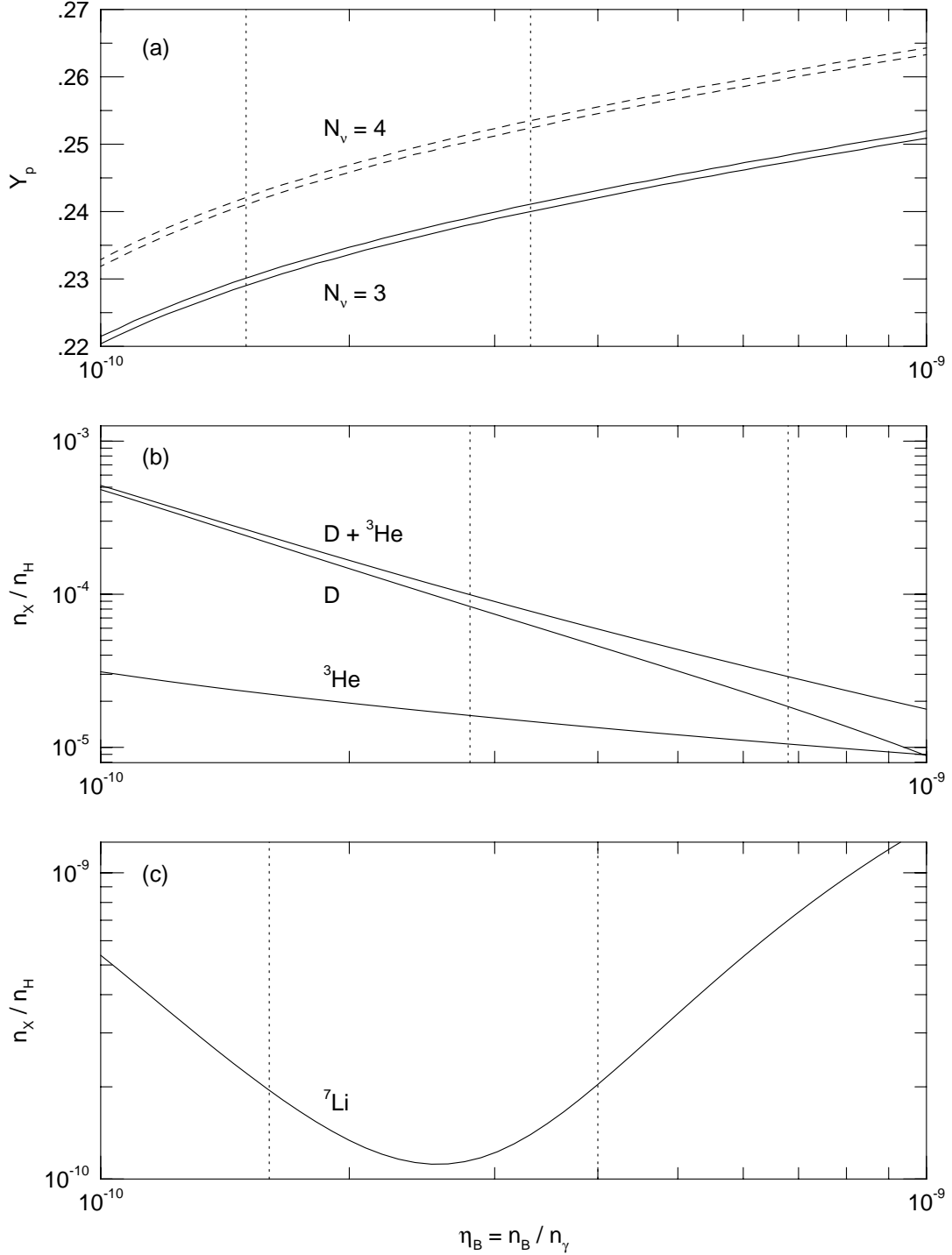


Figure C.1: Predicted abundances of (a) ${}^4\text{He}$, (b) D and ${}^3\text{He}$, and (c) ${}^7\text{Li}$. For a neutron lifetime τ_n , we use $\tau_n = 891.2\text{sec}$ (upper line) and $\tau_n = 887.0\text{sec}$ (lower line). Solid lines corresponds to the results with three neutrino species, and for ${}^4\text{He}$, predicted abundance with four neutrino species are also shown in dashed lines. Dotted lines represent bounds on η_B obtained from observations.

conflicts with observational data of ^4He abundance.

C.3 Observations

In order to see the validity of the theoretical predictions of big-bang nucleosynthesis, we must know the actual values of the *primordial* abundances of light elements. But it is not a simple task because the abundances of light elements evolve with time. Especially some nuclei are produced or destroyed in stars, which changes the abundances of light elements. Therefore we must reconstruct primordial abundances from the observational data. In this section, we will derive the constraints on the primordial abundances of D, ^3He , ^4He and ^7Li , and compare them with the theoretical predictions. The arguments and observational data used in this section mainly follows ref.[49].

D and ^3He

We start with discussing the primordial abundance of D. Since the binding energy of D is very small ($\sim 2.23\text{MeV}$), D is easily destroyed by (γ, p) reaction at $T \gtrsim 6.0 \times 10^5\text{K}$, and it is hard to produce D after BBN. Therefore most of D's in the present (or pre-solar) universe are expected to be produced by the big-bang nucleosynthesis. In the following we regard the observed pre-solar D abundance as a lowerbound on the primordial abundance of D.

Let us reconstruct pre-solar D abundance from the observational data. Pre-solar value of $(\text{D}+^3\text{He})$ abundance can be found in gas-rich meteorites;

$$3.84 \times 10^{-4} \leq \left[\frac{\text{D} + ^3\text{He}}{^4\text{He}} \right]_{pre\odot} \leq 4.22 \times 10^{-4}. \quad (\text{C.15})$$

On the other hand, carbonaceous chondrites, which is one of the most primitive solar system materials, provide us a pre-solar ^3He abundance;

$$1.48 \times 10^{-4} \leq \left[\frac{^3\text{He}}{^4\text{He}} \right]_{pre\odot} \leq 1.56 \times 10^{-4}. \quad (\text{C.16})$$

In order to normalize the abundance of the light elements by hydrogen abundance, we use the standard solar model prediction on ^4He abundance;

$$0.09 \leq \left[\frac{^4\text{He}}{\text{H}} \right]_{pre\odot} \leq 0.11, \quad (\text{C.17})$$

and we obtain

$$1.8 \times 10^{-5} \leq \left[\frac{\text{D}}{\text{H}} \right]_{pre\odot} \leq 3.3 \times 10^{-5}, \quad (\text{C.18})$$

$$1.3 \times 10^{-5} \leq \left[\frac{{}^3\text{He}}{\text{H}} \right]_{pre\odot} \leq 1.8 \times 10^{-5}, \quad (\text{C.19})$$

$$3.3 \times 10^{-5} \leq \left[\frac{\text{D} + {}^3\text{He}}{\text{H}} \right]_{pre\odot} \leq 4.9 \times 10^{-5}. \quad (\text{C.20})$$

As mentioned before, we expect the primordial abundance of D is larger than the pre-solar value since the abundance of D decreases with the galactic evolution. Therefore, pre-solar value of D abundance requires that

$$\left[\frac{\text{D}}{\text{H}} \right]_p \geq \left[\frac{\text{D}}{\text{H}} \right]_{pre\odot} \geq 1.8 \times 10^{-5}. \quad (\text{C.21})$$

Next we will consider the upperbound. Since some of D's are destroyed, it is hard to estimate the primordial D abundance without uncertainty. But D is burned to ${}^3\text{He}$, abundance of the sum (D+ ${}^3\text{He}$) is less uncertain. Therefore we will see the upperbound on this quantity below.

Once D is trapped in stars, it either survives or burns to ${}^3\text{He}$. Furthermore some ${}^3\text{He}$ in stars are destroyed. Therefore using the survival fraction of ${}^3\text{He}$ in stars, $g_{{}^3\text{He}}$, primordial abundance of (D+ ${}^3\text{He}$) can be written as

$$\begin{aligned} \left[\frac{\text{D} + {}^3\text{He}}{\text{H}} \right]_p &= \left[\frac{\text{D}}{\text{H}} \right]_{pre\odot} + g_{{}^3\text{He}}^{-1} \left[\frac{{}^3\text{He}}{\text{H}} \right]_{pre\odot} \\ &= \left[\frac{\text{D} + {}^3\text{He}}{\text{H}} \right]_{pre\odot} + (g_{{}^3\text{He}}^{-1} - 1) \left[\frac{{}^3\text{He}}{\text{H}} \right]_{pre\odot} \end{aligned} \quad (\text{C.22})$$

Combining eq.(C.22) with eq.(C.19) and eq.(C.20), and taking $g_{{}^3\text{He}} \geq 0.25$, we can get

$$\left[\frac{\text{D} + {}^3\text{He}}{\text{H}} \right]_p \leq 1 \times 10^{-4}. \quad (\text{C.23})$$

${}^4\text{He}$

In our universe, ${}^4\text{He}$ is the most abundant element next to hydrogen, but some of them have non-primordial origin, *i.e.* some ${}^4\text{He}$'s originate to stars. In order to see the uncontaminated primordial abundance of ${}^4\text{He}$, we shall use the observational data taken from the old environments which are not affected by galactic evolution. Here, the primordial ${}^4\text{He}$ abundance has been estimated from the observation in metal-poor extragalactic H_{II} region.

In Fig. C.2 – Fig. C.4, observational data of ${}^4\text{He}$ abundance, Y , obtained from metal-poor extragalactic H_{II} region are seen as a function of metallicity (O/H, N/H, C/H) [49]. Fitting these data linearly, one can get the following fitting formulae;

$$Y = 0.229 \pm 0.004 + (1.3 \pm 0.3) \times 10^2 (\text{O}/\text{H}), \quad (\text{C.24})$$

$$Y = 0.231 \pm 0.003 + (2.8 \pm 0.7) \times 10^3 (\text{N}/\text{H}), \quad (\text{C.25})$$

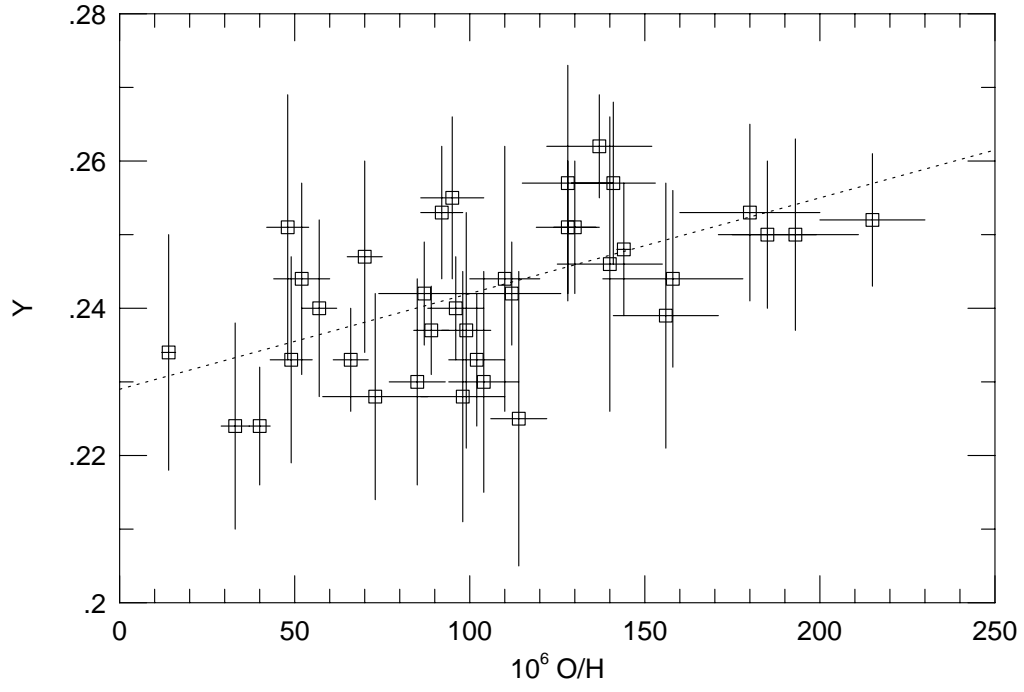


Figure C.2: ${}^4\text{He}$ mass fraction Y vs. observed oxygen abundance.

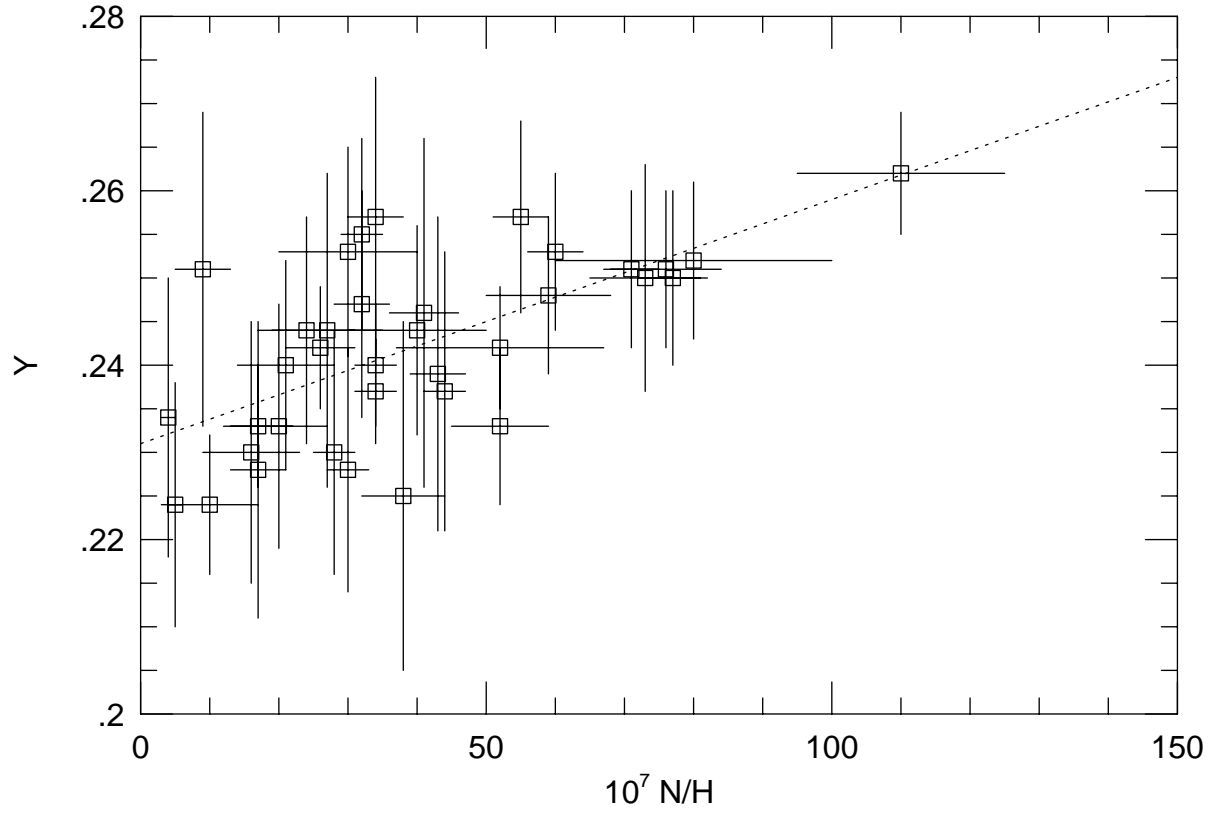


Figure C.3: ${}^4\text{He}$ mass fraction Y vs. observed nitrogen abundance.

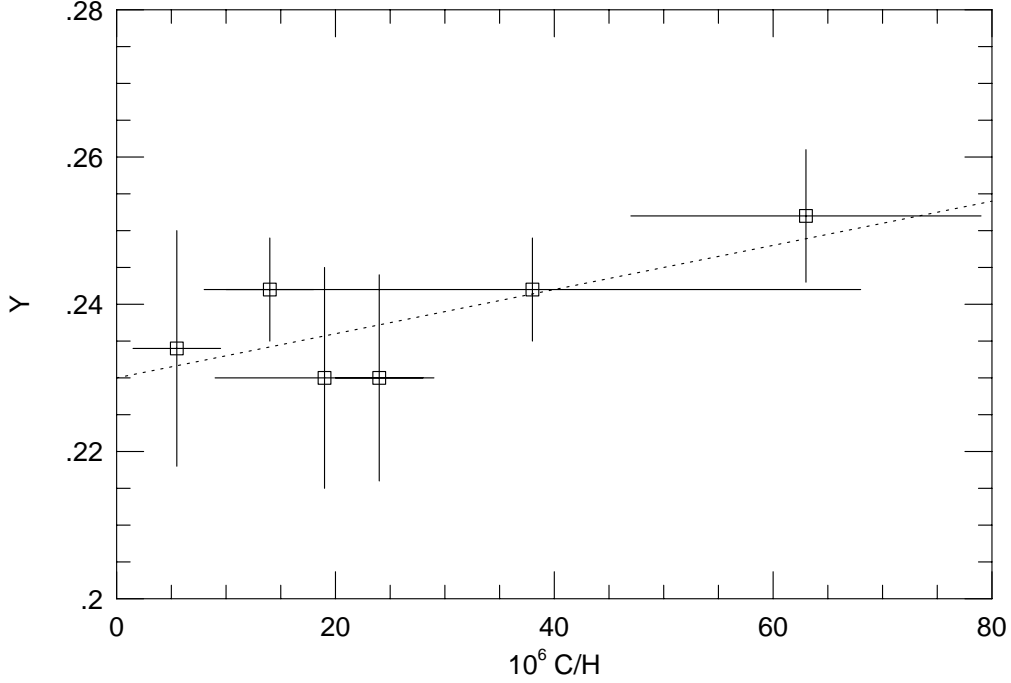


Figure C.4: ${}^4\text{He}$ mass fraction Y vs. observed carbon abundance.

$$Y = 0.230 \pm 0.007 + (3.1 \pm 2.2) \times 10^2 (\text{C/H}). \quad (\text{C.26})$$

From these data, primordial abundance of ${}^4\text{He}$ should be read off. Since the primordial ${}^4\text{He}$ in these metal-poor region is still contaminated by the one originating to stars, we take a limit that metallicity goes to zero. Then, the primordial abundance is estimated to be

$$\text{O} : Y_p = 0.229 \pm 0.004, \quad (\text{C.27})$$

$$\text{N} : Y_p = 0.231 \pm 0.003, \quad (\text{C.28})$$

$$\text{C} : Y_p = 0.230 \pm 0.007. \quad (\text{C.29})$$

Taking the observational uncertainty into account, we adopt the primordial ${}^4\text{He}$ abundance as $Y_p = 0.23 \pm 0.01$.

${}^7\text{Li}$

Next we will see the primordial abundance of ${}^7\text{Li}$. Since ${}^7\text{Li}$ can be produced after BBN by cosmic ray spallation or some stellar processes (like novae outbursts), and it is easily destroyed at $T \geq 2 \times 10^6 \text{K}$, we can not regard the present abundance of ${}^7\text{Li}$ as primordial one. This means that we have to observe the old environment so as to see the primordial ${}^7\text{Li}$ abundance. For this purpose, observational data of ${}^7\text{Li}$ abundance in metal-poor (and $T_{\text{surf}} \gtrsim 5500 \text{K}$, as will be explained below) population II stars are usually used since they are expected to reflect the uncontaminated ${}^7\text{Li}$ abundance.

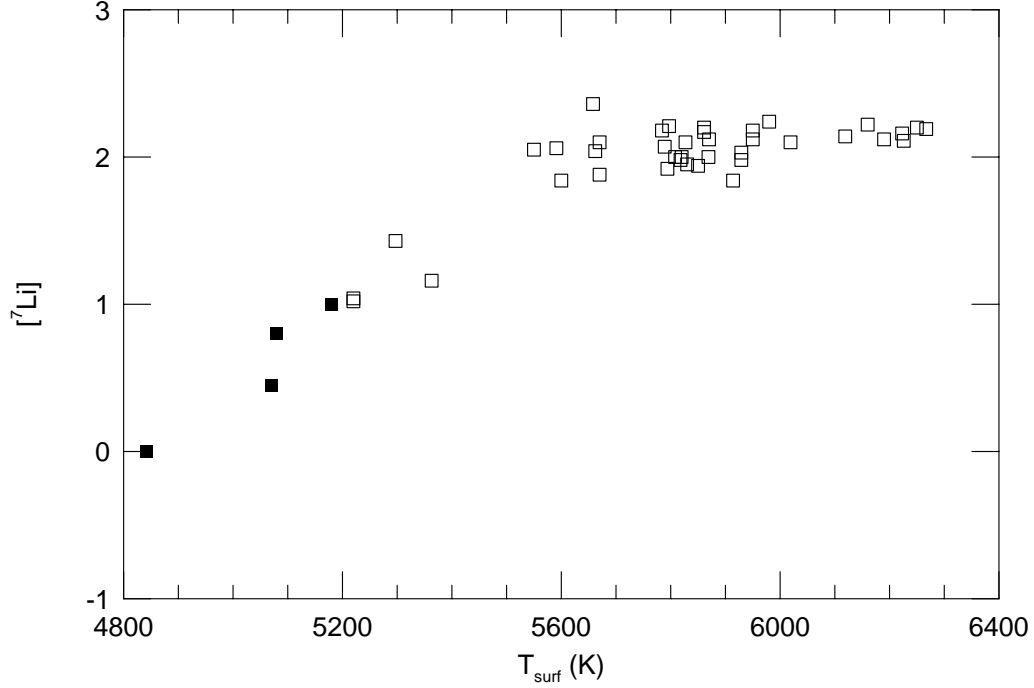


Figure C.5: ^7Li abundance $[^7\text{Li}] \equiv 12 + \log_{10}(^7\text{Li}/\text{H})$ in the metal-poor population II stars as a function of surface temperature T_{surf} . The filled marks represent upper limits to the ^7Li abundance.

In Fig. C.5, we plot the ^7Li abundance $[^7\text{Li}] \equiv 12 + \log_{10}(^7\text{Li}/\text{H})$ in the most metal-poor population II stars as a function of surface temperature T_{surf} . As one can see, “ ^7Li -plateau” appears at $T_{\text{surf}} \gtrsim 5500\text{K}$. Using the data with $T_{\text{surf}} \geq 5500\text{K}$, the “plateau” value of $[^7\text{Li}]$ is estimated to be

$$[^7\text{Li}]_{\text{plateau}} = 2.08 \pm 0.07. \quad (\text{C.30})$$

We identify this value as the primordial abundance of ^7Li . Notice that the data taken from stars with $T_{\text{surf}} \lesssim 5500\text{K}$ are not appropriate for our purpose, because cool stars have thick surface convective zones which carry ^7Li to deep region hot enough to burn it. Thus, we expect that ^7Li abundances at the low surface temperature stars are not primordial one. Using eq.(C.30), upperbound on the primordial ^7Li abundance is given by

$$[^7\text{Li}]_p \leq 2.15. \quad (\text{C.31})$$

Comparison with the theoretical predictions

Now we are at the position to compare the observational data of light nuclei with the theoretical predictions. At first, we will constrain baryon-to-photon ratio η_B from the data

of D, (D+³He) ⁴He, and ⁷Li.

Let us begin with D and ³He. Lowerbound on the primordial abundance of D is given in eq.(C.21) and using that, η_B is constrained to be

$$\text{D} : \eta_B \leq 6.8 \times 10^{-10}. \quad (\text{C.32})$$

On the other hand, upperbound on the primordial (D+³He) abundance, eq.(C.23), requires

$$\text{D} + {}^3\text{He} : \eta_B \geq 2.8 \times 10^{-10}. \quad (\text{C.33})$$

Theoretical prediction on the primordial abundance of ⁴He is considerably affected by an uncertainty of the neutron life time ($\tau_n = 889.1 \pm 2.1\text{sec}$). In order to get a conservative constraint on the baryon-to-photon ratio η_B , we use the value $\tau_n = 891.2\text{sec}$ in deriving the lowerbound on η_B , and $\tau_n = 887.0\text{sec}$ for upperbound. As a result, we obtain constraints on η_B from $Y_p = 0.23 \pm 0.01$ as

$${}^4\text{He} : 1.5 \times 10^{-10} \leq \eta_B \leq 3.3 \times 10^{-10}. \quad (\text{C.34})$$

Upperbound on the primordial ⁷Li abundance is given in eq.(C.31); $[{}^7\text{Li}]_p \leq 2.15$. If we naively use this value, η_B is constrained to be $1.9 \times 10^{-10} \leq \eta_B \leq 3.3 \times 10^{-10}$. But from the uncertainties in the nuclear reaction rate, the predicted ⁷Li abundance is expected to be uncertain by $\sim 40\%$. Assuming 40% residual uncertainty in the primordial abundance, bound on η_B is found to be

$${}^7\text{Li} : 1.6 \times 10^{-10} \leq \eta_B \leq 4.0 \times 10^{-10}. \quad (\text{C.35})$$

Combining eq.(C.32) – eq.(C.35), allowed range of baryon-to-photon ratio η_B is given by

$$\text{D}, {}^3\text{He}, {}^4\text{He}, {}^7\text{Li} : 2.8 \times 10^{-10} \leq \eta_B \leq 3.3 \times 10^{-10}, \quad (\text{C.36})$$

i.e. $\eta_B \sim 3 \times 10^{-10}$ is predicted from BBN.

Finally we will comment on the baryonic density of the present universe. By using eq.(C.12), constraints on η_B (C.36) becomes

$$1.0 \times 10^{-2} \leq \Omega_B h^2 \leq 1.2 \times 10^{-2}. \quad (\text{C.37})$$

Therefore, baryonic dark matter ($\Omega_B \sim 1$) conflicts with the theoretical predictions of BBN provided $0.5 \lesssim h \lesssim 1$.

Bibliography

- [1] J. Wess and B. Zumino, *Nucl. Phys.* **B70** (1974) 39.
- [2] L. Maiani, *Gif-sur-Yvette Summer School on Particle Physics*, (Natl. Inst. Nucl. Phys. Part. Phys., Paris, 1979).
- [3] M.J.G. Veltman, *Acta Phys. Pol.* **B12** (1981) 437.
- [4] P. Langacker and M. Luo, *Phys. Rev.* **D44** (1991) 817.
- [5] U. Amaldi, W. de Boer and H. Fürstenau, *Phys. Lett.* **B260** (1991) 447.
- [6] S. Dimopoulos and H. Georgi, *Nucl. Phys.* **B193** (1981) 150.
- [7] N. Sakai, *Z. Phys.* **C11** (1981) 153.
- [8] E. Cremmer, S. Ferrara, L. Grardello and A. van Proeyen, *Nucl. Phys.* **B212** (1983) 413.
- [9] J. Ellis, C. Kounnas and D.V. Nanopoulos, *Phys. Lett.* **B143** (1984) 410.
- [10] J. Ellis, K. Enqvist and D.V. Nanopoulos, *Phys. Lett.* **B147** (1984) 99.
- [11] S. Weinberg, *Phys. Rev. Lett.* **48** (1982) 1303.
- [12] L.M. Krauss, *Nucl. Phys.* **B277** (1983) 556.
- [13] H. Pagels and J.R. Primack, *Phys. Rev. Lett.* **48** (1982) 223.
- [14] A.H. Guth, *Phys. Rev.* **D23** (1981) 347.
- [15] J. Ellis, A.D. Linde and D.V. Nanopoulos, *Phys. Lett.* **B118** (1982) 59.
- [16] T. Yanagida, Talk given at Physical Society of Japan Symposium on JLC, (Yamagata, October 1994).
- [17] H. Murayama, preprint LBL-36175, (LBL, 1994, hep-ph/9410285).
- [18] M.T. Grisaru, W. Siegel and M. Roček, *Nucl. Phys.* **B159** (1979) 429.
- [19] B.A. Campbell, S. Davidson, J. Ellis and K.A. Olive, *Phys. Lett.* **B256** (1991) 457.

- [20] H. Georgi and S.L. Glashow, *Phys. Rev. Lett.* **25** (1974) 438.
- [21] S. Kelly, J. L. Lopez and D. V. Nanopoulos, *Phys. Lett.* **B247** (1992) 387.
- [22] V. Barger, M.S. Berger and P. Ohmann, *Phys. Rev.* **D47** (1993) 1093.
- [23] P. Langacker and N. Polonsky, *Phys. Rev.* **D49** (1994) 1454.
- [24] Particle Data Group, *Phys. Rev.* **D50** (1994) 1173.
- [25] J. Gasser and H. Leutwyler, *Phys. Rep.* **C87** (1982) 77.
- [26] J. Wess and J. Bagger, *Supersymmetry and Supergravity*, (Princeton University Press, 1992).
- [27] J. Polonyi, preprint KFK-1977-93 (Budapest, 1977).
- [28] T. Banks, D.B. Kaplan and A.E. Nelson, *Phys. Rev.* **D49** (1994) 779.
- [29] I. Joichi, Y. Kawamura and M. Yamaguchi, preprint TU-462, (Tohoku University, 1994, hep-ph/9407385).
- [30] G.D. Coughlan, W. Fischler, E.W. Kolb, S. Raby and G.G. Ross, *Phys. Lett.* **B131** (1983) 59.
- [31] P.R. Auvil and J.J. Brehm, *Phys. Rev.* **145** (1966) 1152.
- [32] P. Fayet, *Phys. Lett.* **B175** (1986) 471.
- [33] D.A. Dicus, S. Nandi and J. Woodside, *Phys. Lett.* **B258** (1991) 231.
- [34] D.V. Nanopoulos, K.A. Olive and M. Srednicki, *Phys. Lett.* **B127** (1983) 30.
- [35] M.Yu. Khlopov and A.D. Linde, *Phys. Lett.* **B138** (1984) 265.
- [36] J. Ellis, E. Kim and D.V. Nanopoulos, *Phys. Lett.* **B145** (1984) 181.
- [37] R. Juskiewicz, J. Silk and A. Stebbins, *Phys. Lett.* **B158** (1985) 463.
- [38] J. Ellis, D.V. Nanopoulos and S. Sarkar, *Nucl. Phys.* **B259** (1985) 175.
- [39] M. Kawasaki and K. Sato, *Phys. Lett.* **B189** (1987) 23.
- [40] J. Ellis, G.B. Gelmini, J.L. Lopez, D.V. Nanopoulos and S. Sarker, *Nucl. Phys.* **B373** (1992) 399.
- [41] M. Kawasaki and T. Moroi, preprint TU-457, (Tohoku University, 1994, hep-ph/9403364).

- [42] T. Moroi, H. Murayama and M. Yamaguchi, *Phys. Lett.* **B303** (1993) 289.
- [43] T. Moroi, M. Yamaguchi and T. Yanagida, *Phys. Lett.* **B342** (1995) 105.
- [44] I. Affleck and M. Dine, *Nucl. Phys.* **B249** (1985) 361.
- [45] H. Murayama, H. Suzuki, T. Yanagida and J. Yokoyama, *Phys. Rev.* **D50** (1994) 2356.
- [46] T. Moroi and T. Yanagida, *Prog. Theor. Phys.* **91** (1994) 1277.
- [47] M. Kawasaki and T. Moroi, preprint TU-463, (Tohoku University, 1994, hep-ph/9408321).
- [48] W. Fischler, *Phys. Lett.* **B332** (1994) 277.
- [49] T.P. Walker, G. Steigman, D.N. Schramm, K.A. Olive and H.-S. Kang, *Ap. J.* **376** (1991) 51.
- [50] R.D. Evans, *The Atomic Nucleus* (McGraw-Hill, New York, 1955).
- [51] R. Piffner, *Z. Phys.* **208** (1968) 129.
- [52] D.D. Faul, B.L. Berman, P. Mayer and D.L. Olson, *Phys. Rev. Lett.* **44** (1980) 44.
- [53] A.N. Gorbunov and A.T. Varfolomeev, *Phys. Lett.* **11** (1964) 137.
- [54] Yu.M. Arkatov, P.I. Vatset, V.I. Voloshchuk, V.A. Zolenko, I.M. Prokhorets and V.I. Chimil', *Sov. J. Nucl. Phys.* **19** (1974) 589.
- [55] J.D. Irish, R.G. Johnson, B.L. Berman, B.J. Thomas, K.G. McNeill and J.W. Jury, *Can. J. Phys.* **53** (1975) 802.
- [56] C.K. Malcolm, D.B. Webb, Y.M. Shin and D.M. Skopik, *Phys. Lett.* **B47** (1973) 433.
- [57] L. Kawano, preprint FERMILAB-Pub-92/04-A (Fermilab., 1992).
- [58] J. Gratsias, R.J. Scherrer and D.N. Spergel, *Phys. Lett.* **B262** (1991) 198.
- [59] M.H. Reno and D. Seckel, *Phys. Rev.* **D37** (1988) 3441.
- [60] S. Dimopoulos, R. Esmailzadeh, L.J. Hall and G.D. Starkman, *Ap. J.* **330** (1988) 545.
- [61] S. Dimopoulos, R. Esmailzadeh, L.J. Hall and G.D. Starkman, *Nucl. Phys.* **B311** (1989) 699.
- [62] K. Hidaka, *Phys. Rev.* **D44** (1991) 927.
- [63] J. McDonald, K.A. Olive and M. Srednicki, *Phys. Lett.* **B283** (1992) 80.

- [64] S. Mizuta and M. Yamaguchi, *Phys. Lett.* **B298** (1993) 120.
- [65] M. Drees and M.M. Nojiri, *Phys. Rev.* **D47** (1993) 376.
- [66] J. Ellis, C. Kounnas and D.V. Nanopoulos, *Nucl. Phys.* **B247** (1984) 373.
- [67] K. Inoue, M. Kawasaki, M. Yamaguchi and T. Yanagida, *Phys. Rev.* **D45** (1992) 328.
- [68] S. Kelley, J.L. Lopez, D.V. Nanopoulos, H. Pois and K. Yuan, *Nucl. Phys.* **B398** (1993) 3.
- [69] E. Witten, *Phys. Lett.* **B155** (1985) 151.
- [70] M. Matsumoto, J. Arafune, H. Tanaka and K. Shiraishi, *Phys. Rev.* **D46** (1992) 3966.
- [71] J.L. Lopez, D.V. Nanopoulos and A. Zichichi, *Phys. Lett.* **B291** (1992) 255.
- [72] J.L. Lopez, D.V. Nanopoulos and H. Pois, *Phys. Rev.* **D47** (1993) 2468.
- [73] P.J. Kernan and L.M. Krauss, *Phys. Rev. Lett.* **72** (1994) 3309.
- [74] M. Fukugita and N. Sakai, *Phys. Lett.* **B114** (1982) 23.
- [75] A.A. Zdziarski, *Ap. J.* **335** (1988) 786.
- [76] R. Svensson and A.A. Zdziarski, *Ap. J.* **349** (1990) 415.
- [77] A.D. Linde, *Phys. Lett.* **B129** (1983) 177.
- [78] D.S. Salopek, *Phys. Rev. Lett.* **69** (1992) 3602.
- [79] E.W. Kolb and M.S. Turner, *The Early Universe* (Addison-Wesley, 1990).
- [80] B.W. Lee and S. Weinberg, *Phys. Rev. Lett.* **39** (1977) 165.
- [81] N. Terasawa, M. Kawasaki and K. Sato, *Nucl. Phys.* **B302** (1988) 697.
- [82] J. Preskill, M.B. Wise and F. Wilczek, *Phys. Lett.* **B120** (1983) 127.
- [83] L.F. Abbott and P. Sikivie, *Phys. Lett.* **B120** (1983) 133.
- [84] M. Dine and W. Fischler, *Phys. Lett.* **B120** (1983) 137.
- [85] F.A. Agaryan, A.M. Atyan and A.N. Najapetyan, *Astrofizika* **19** (1983) 323.
- [86] L.C. Maximon, *J. Res. NBS* **72(B)** (1968) 79.
- [87] V.B. Berestetskii, E.M. Lifshitz and L.P. Pitaevskii, *Quantum Electrodynamics* (Pergamon press, Oxford, 1982).

- [88] F.C. Jones, *Phys. Rev.* **167** (1968) 1159.
- [89] M. Kawasaki and T. Moroi, preprint TU-474, (Tohoku University, 1994, astro-ph/9412055).